

Braid Index of Satellite Links

Thesis submitted in accordance
with the requirements of the
University of Liverpool
for the degree of
Doctor in Philosophy



by

Ian John Nutt

February 1995

Braid Index of Satellite Links

Ian John Nutt

ABSTRACT

This thesis is a study of the braid index of satellite links. Let $V \subset S^3$ be a solid, possibly knotted torus. Through the work of Birman and Menasco, the observation has been made that a satellite link $L \subset V$ (with companion C , pattern P and essential torus $T = \partial V$) falls into one of two broad categories: reverse string or non-reverse string. These are distinguished by the existence of, or lack of, a meridional disc $D \subset V$ with an orientation, whose intersections with the oriented satellite L are all similarly oriented. If no such D exists, then L is a reverse string satellite.

For non-reverse string satellites L it is shown that the braid index $b(L)$ is dependent only on $b(C)$ and certain specified properties of the pattern. Birman and Menasco conjectured that, for reverse string satellites L , the braid index $b(L)$ depends on the *arc index* $\alpha(C)$, and properties of the pattern. Here, we study this further via established upper and lower bounds for braid index. The upper bound comes from explicit closed braid diagrams of L , for which constructions are shown. The lower bound comes from the Homfly polynomial, via the Morton-Franks-Williams inequality. It is conjectured that for all reverse string satellites L , this lower bound grows linearly with framing, hence emulating the relationship between the upper bound and the framing.

The arc index of a link L is investigated in its own right, taking advantage of the work of Cromwell. Relationships are found between arc index and other standard link invariants. A computer algorithm is described, which is enough to identify all knots of low arc index, via computation of their Homfly polynomials.

The work of Rudolph on quasipositive annuli is employed to deduce the following inequality:

$$\alpha(K) \geq 2 + \text{spr}_a(G_K(a, x)),$$

where $G_K(a, x)$ is the Kauffman polynomial with coefficients reduced modulo 2. It is conjectured that this relation yields equality if, and only if, K is alternating.

For my parents
and grandparents

Acknowledgements

I am grateful to have been under the supervision of Dr. Hugh Morton during the period of my study. His encouragement and expert guidance have been of great value.

The Department of Pure Mathematics has been a very welcoming place to study, and I acknowledge the support of its staff and postgraduates. In particular I must mention Dr. Peter Cromwell, who has shown an interest in this work from the beginning, and Anna Aiston, Dr. Wendy Hawes and Dr. Farid Tari, who provided helpful criticism of the manuscript, and (among many others) gave useful discussion. Thanks are also due to Dr. Richard Morris for the loan of computer hardware, and to Dr. Neil Kirk and others for technical advice.

I thank SERC for financial support, and the Newton Institute, the University of Warwick, the London Mathematical Society and the MAP Project for supporting my visits to Cambridge, Warwick, Southampton and Pisa respectively.

To those musicians, house-mates, office-mates and others who provided distraction from the heady world of Knot Theory, I am equally grateful. A special mention must go to Sean, Joe, Rachel, Col, Stephen and Catherine. I am fortunate enough to have had the continued encouragement of my family.

Finally, thanks to Wendy for her friendship and phenomenally good cooking.

Contents

- Introduction iv

- 1 Basic definitions 1**
 - 1.1 Knots and links 1
 - 1.2 Equivalence of links 2
 - 1.3 Braids 4
 - 1.4 Some standard knot and link invariants 7
 - 1.5 Polynomial invariants 8
 - 1.5.I The Homfly polynomial 8
 - 1.5.II The Kauffman polynomial 10
 - 1.5.III Comments 11
 - 1.6 Composite links 11

- 2 Embeddings of links in a book of halfplanes 15**
 - 2.1 Basic definition and initial remarks 15
 - 2.2 The arc index, $\alpha(L)$ 17
 - 2.3 Equivalence of arc diagrams 19
 - 2.4 Behaviour of $\alpha(L)$ under knot operations 26
 - 2.5 Relating $\alpha(L)$ to other link invariants 28
 - 2.5.I Braid index 28

2.5.II	Crossing index	29
2.5.III	Homfly polynomial	40
3	Satellite links as closed braids	41
3.1	Motivation	41
3.2	Braid index of satellites: types 0 and 1	42
3.3	Reverse string satellites	59
3.4	Braid presentations of reverse string satellites	68
3.5	Concerning the framing of satellite links	76
3.6	A formal definition for framing	80
3.7	A linear relation between framing and Homfly polynomial	85
3.7.I	Development of the tools	86
3.7.II	Proof of theorems 3.7.1 and 3.7.2	92
3.8	Comparing upper and lower bounds for braid index of reverse string satellites	97
4	The modulus of quasipositivity	99
4.1	Introduction	99
4.2	Quasipositivity and arc index	99
4.3	The framed polynomial	106
4.4	A lower bound for arc index from the Kauffman polynomial	107
4.5	A conjecture for alternating knots	112
4.6	Proof of theorem 2.3.3	114
5	Extended computations for knots with small arc index	116
5.1	Introduction	116
5.2	Constructing the knot	117

5.3	Representing the knot	118
5.4	Preliminary sieves on the list of α -cycles	118
5.4.I	Base points and arc-reducing moves	119
5.4.II	Sieving mirror images	120
5.4.III	Rotating the grid diagram	123
5.4.IV	Initial discussion of the pseudocode	126
5.5	More sieves on the list of diagrams	127
5.5.I	The transpose of an arc-diagram	127
5.5.II	Further discussion of the pseudocode	130
5.6	Size of output	132
5.7	Results	132
5.8	Comments	133
A	Pseudocode	148
	References	152

Introduction

This thesis presents a study of satellite links, and in particular of a geometric invariant of links which is intrinsic in the presentation of certain satellites as closed braids.

As part of their comprehensive study of links via closed braids, Birman and Menasco studied the effect of the knot operations of distant union and connect sum on the braid index. Let $A \subset S^3$ denote the braid axis; the complement $S^3 - A$ admits an open book fibration, where the fibres are open halfplanes H_θ . Let L be a closed braid relative to A , so L intersects each of the H_θ transversely in the same number of points. Let S denote the 2-sphere which defines the distant union/connect sum; then S is foliated by the leaves $S \cap H_\theta$. Birman and Menasco examined the foliation of S , and showed that S could be placed in nice position relative to the open book fibration, so that the distant union/connect sum was apparent from the presenting braid.

The behaviour of braid index with respect to the more complicated satellite construction could be studied using this work as a foundation. Let T be a hollow torus in S^3 : it is known by a theorem of Alexander that T bounds a solid torus V on at least one side. Suppose a link L is completely contained in the interior of V . If V is knotted then L is called a *satellite link*. We assume that L is a proper satellite: that is, T is essential (incompressible in $S^3 - L$).

The methods of Birman and Menasco, described above, could be applied to the satellite construction to develop formulae for braid index of satellites; comparable (independent) results are found here and in a further paper of Birman and Menasco. It is established that satellites, broadly speaking, fall into one of two types: reverse string, and non-reverse string. Braid index of the latter is dependent on the braid index of the companion knot. Birman and Menasco conjectured that braid index of the former is dependent on the *arc index* of the companion knot. The apparent dependence is not trivial, and we discuss this here, giving examples and illustrations.

A special class of reverse string satellite was a subject of study in the work of Rudolph. The boundary of an oriented knotted annulus (with core knot C , say) is an oriented link: its two components are oppositely oriented copies of C , running parallel to each other. We call this satellite link an *antiparallel* of C .

Rudolph studied the *modulus of quasipositivity* $q(C)$ of a knot C (introduced in the knot theory of complex plane curves) as it applies to ordinary knot theory: $q(C)$ can be characterized in terms of the *framing* of the antiparallel of C . Rudolph found upper and lower bounds for $q(C)$, and gave a relationship between the Kauffman polynomial of C and the Homfly polynomial of the antiparallel of C . We bring together the theory of general satellites, and the work of Rudolph through quasipositive surfaces, to make a number of deductions.

The contents of this thesis can be summarized as follows.

Chapter 1 covers some of the definitions of classical and modern knot theory, which are relevant to this thesis. Further definitions appear throughout the thesis.

Chapter 2 is an introduction to the arc index: we describe the underlying construction, and a two-dimensional method of representing the construction, the *grid diagram*. We define the arc index. Cromwell formalized a set of combinatorial moves, similar to the Reidemeister moves or the Markov moves, which relate a pair of grid diagrams of a link; these moves are covered in some detail in section 2.3. We include observations on how arc index relates to other link invariants, and a discussion on the behaviour of arc index under the knot operations of distant union and connect sum.

Chapter 3 can be regarded in two parts. The first part (sections 3.1 and 3.2) introduces and proves a result concerning braid index of non-reverse string satellites. The second part (sections 3.3–3.7) begins by stating the more complete result of Birman and Menasco, which recognizes the reverse string pattern types. The work continues by employing this result to develop explicit closed braid diagrams (and hence explicit words in the braid group) for reverse string satellites; this algorithm provides an upper bound for braid index of a reverse string satellite. We see how the framing of the satellite is a factor in determining braid index of reverse string satellites, and in section 3.7 we prove a relationship between framing of the satellite, and the size of its Homfly polynomial. This leads directly to a lower bound for braid index of the reverse string satellite, via the well-known Morton-Franks-Williams inequality; it is observed that, at least in special cases, the upper and lower bounds developed here behave identically with respect to framing.

In chapter 4 we bring in the work of Rudolph on quasipositive annuli. We review some of the necessary definitions and observations of Rudolph, and add some new observations. Section 4.4 brings together the work on quasipositivity, and the work on satellites, with the result that a lower bound for arc index can be deduced from the Kauffman polynomial. Moreover, this lower bound is remarkably similar, on face value at least, to a result (proved, independently, by Murasugi and by Thistlethwaite) relating crossing index and the Jones polynomial: in particular, both inequalities seem to be strict if, and only if, the link is non-alternating.

Chapter 5 returns to the arc index itself. We include a discussion of a computer algorithm which is enough to identify all knots of small arc index, via calculation of their Homfly polynomials. The algorithm is illustrated by inclusion of a pseudocode, and a number of corollaries are deduced.

Finally, a note on the organization of this thesis. Titles and labels are abundant, and usually they are numbered. For example, 3.7 is the seventh section of chapter 3, and 3.7.II is the second subsection of section 3.7. Theorems, propositions, lemmas, corollaries and conjectures are all covered under the same indexing system: 3.7.2 is the second such to be included in section 3.7 (irrespective of which subsection it appears in). Figure 3.5 is the fifth figure of chapter 3: figures are numbered consecutively. References are included at the end of the thesis; in the main body of the thesis, they are referred to within square brackets, *e.g.* [Ro]. The symbol \square indicates the end of a proof or, if it appears immediately after a statement, that no proof is given.

Chapter 1

Basic definitions

Throughout the thesis, \mathbf{N} , \mathbf{Z} and \mathbf{R} denote the natural numbers, the integers and the reals, respectively.

1.1 Knots and links

A *knot* (usually denoted K) is an embedding of S^1 into S^3 , $i : S^1 \rightarrow S^3$. A *link*, L , of $|L|$ components is an embedding of $|L|$ copies of S^1 into S^3 , $i : S^1 \cup \dots \cup S^1 \rightarrow S^3$.

In this work, we refer to smooth or piecewise linear knots and links. Also, we make the distinction between knots and links, since, in some circumstances, terminology for a 1-component link is valuable. Where the number of components is immaterial we refer to a link.

A link is said to be *oriented* if it comes with a choice of orientation for each component.

Let L be a link. A *diagram* of L is the image $D(L)$ of a projection map, $D : S^3 \rightarrow S^2$ or \mathbf{R}^2 , such that there are finitely many singular points, and each singular point is a transverse double point with its under- and over-crossings distinguished.

The *unknot*, denoted U_1 , is the only knot (1-component link) which can be represented by a non-singular diagram. Figure 1.1 shows some examples of diagrams of knots.

In a link diagram D , suppose we have p parallel, similarly oriented strings, running alongside each other without intertwining. We can replace this with



Figure 1.1: Diagrams of unknot, trefoil and figure-eight

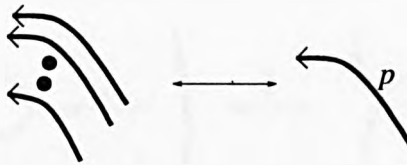


Figure 1.2: Weighted string represents p parallel strings in link diagram D

a *weighted* string of *weight* p , as illustrated in figure 1.2. This diagrammatic shorthand will be of use in later chapters.

Given a link L , its *obverse* \bar{L} is given by reflecting L in some mirror plane in S^3 .

1.2 Equivalence of links

Let D, D' be diagrams of links L, L' . By a theorem of Reidemeister [Re], the links L and L' are *equivalent up to ambient isotopy* if, and only if, D and D' are related by a sequence

$$D = D_0 \rightarrow D_1 \rightarrow \dots \rightarrow D_r = D',$$

where each D_i is related to D_{i-1} by one of the Reidemeister moves (illustrated in figure 1.3).

Two link diagrams are said to be *equivalent up to regular isotopy* if they are related by a sequence $D = D_0 \rightarrow \dots \rightarrow D_r = D'$ where each D_i is related to D_{i-1} by either the second or third Reidemeister moves.

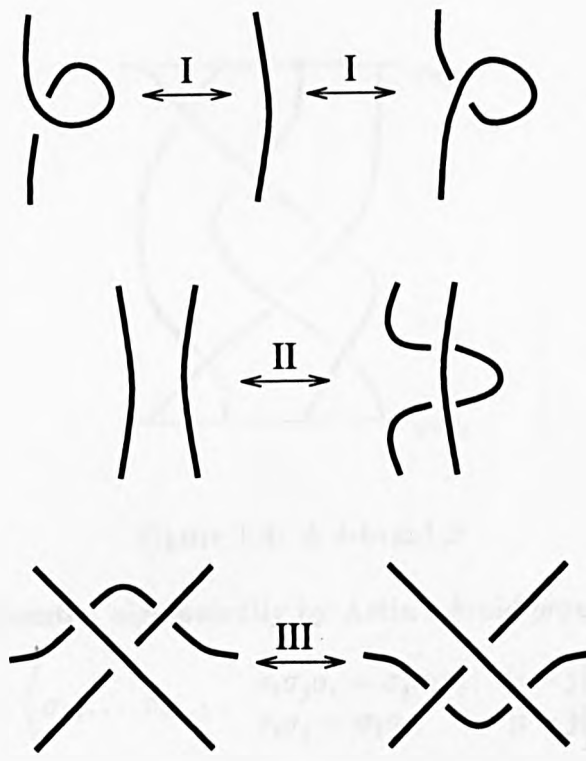


Figure 1.3: The Reidemeister moves

1.3 Braids

Let $\{(x, y, z) : z = z_0\}$, $\{(x, y, z) : z = z_1\}$ (with $z_0 < z_1$) be parallel planes in \mathbf{R}^3 . Choose m pairs of points (x_i, y_i, z_0) , (x_i, y_i, z_1) , $i = 1, \dots, m$ on the planes. An m -braid is a collection of m disjoint strings, each of which joins one of the points on $\{(x, y, z) : z = z_0\}$ to one on $\{(x, y, z) : z = z_1\}$ such that (a) each point is at the end of exactly one string, and (b) each string has transverse intersection with every plane $\{(x, y, z) : z = z'\}$, for $z_0 < z' < z_1$. An example is shown in figure 1.4. We study braids, as we study links, via diagrams with finitely many double points and no higher singularities.

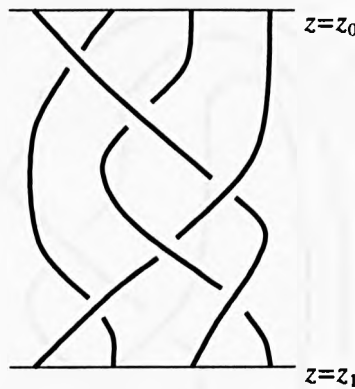


Figure 1.4: A 4-braid β

Braids are represented algebraically by Artin's *braid group* [Ar], B_m :

$$B_m = \left\langle \sigma_1, \dots, \sigma_{m-1} : \begin{array}{l} \sigma_i \sigma_j \sigma_i = \sigma_j \sigma_i \sigma_j, \quad |i - j| = 1; \\ \sigma_i \sigma_j = \sigma_j \sigma_i, \quad |i - j| \geq 2. \end{array} \right\rangle,$$

where the generator σ_i represents the crossing of the i th braidstring and $(i + 1)$ th braidstring, in the sense of figure 1.5.

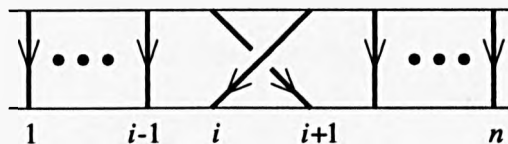


Figure 1.5: Elementary braid $\sigma_i \in B_n$

A *closed m -braid* $\hat{\beta}$ is a union of closed curves in S^3 , given by joining the points (x_i, y_i, z_0) , (x_i, y_i, z_1) , $\forall i$ of an m -braid β , as shown in figure 1.6.

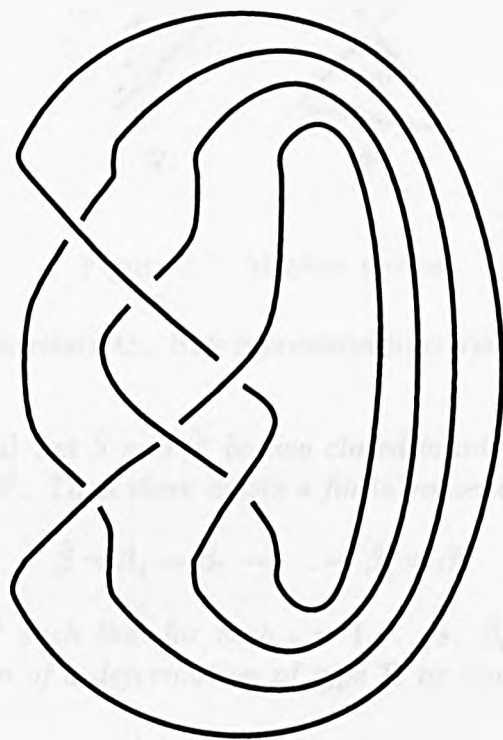


Figure 1.6: Closed 4-braid $\hat{\beta}$

Theorem 1.3.1 [Al] *Every link can be presented as a closed braid, and every closed braid is a link.* \square

Markov [Ma] described deformations which relate any pair of closed braid representations of the same link L . The *Markov moves* are illustrated in figure 1.7, where links are assumed to be piecewise linear. The dotted component is replaced by the full component, or *vice versa*.

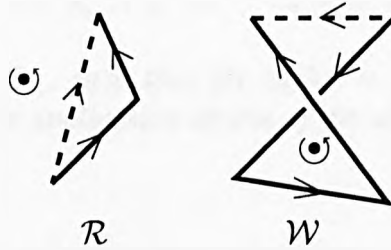


Figure 1.7: Markov moves

The Markov moves relate the link representations via the following theorem.

Theorem 1.3.2 [Ma] *Let $\hat{\beta}$ and $\hat{\beta}'$ be two closed braids in S^3 , which are combinatorially equivalent¹. Then there exists a finite sequence*

$$\hat{\beta} = \hat{\beta}_0 \rightarrow \hat{\beta}_1 \rightarrow \dots \rightarrow \hat{\beta}_s = \hat{\beta}'$$

of closed braids in S^3 such that for each $i = 1, \dots, s$, $\hat{\beta}_i$ is obtained from $\hat{\beta}_{i-1}$ by a single application of a deformation of type \mathcal{R} or type \mathcal{W} . (The converse is trivially true.) \square

In algebraic terms, this is equivalent to the following. A Markov move replaces a braid $\beta \in B_n$ by

(\mathcal{R}) $\beta' \in B_n$, where β' is conjugate to β in B_n ; or

(\mathcal{W}) $\beta\sigma_n^{\pm 1} \in B_{n+1}$; or

¹The *combinatorial equivalence class* of a link is its link isotopy type ([Bi] p.39). Two piecewise linear links L and L' are said to be *combinatorially equivalent* if they are related by a finite sequence of links, such that each link is obtained from its predecessor by a deformation of type \mathcal{R} . Since the Reidemeister moves can easily be generated from repeated application of move \mathcal{R} , then Reidemeister equivalence implies combinatorial equivalence. More trivially, combinatorial equivalence is just ambient isotopy, and so implies Reidemeister equivalence.

$(\mathcal{W}^{-1}) \beta' \in B_{n-1}$, where $\beta = \beta' \sigma_{n-1}^{\pm 1} \in B_n$.

Then the algebraic version of theorem 1.3.2 is as follows.

Theorem 1.3.3 [Ma] *Let $\hat{\beta}$ and $\hat{\beta}'$ be two closed braids in S^3 , with braid representations β and β' . Then $\hat{\beta}$ is combinatorially equivalent to $\hat{\beta}'$ if, and only if, there exists a finite sequence*

$$\beta = \beta_0 \rightarrow \beta_1 \rightarrow \dots \rightarrow \beta_s = \beta'$$

of braids, with each $\beta_i \in B_{n_i}$, such that for each $i = 1, \dots, s$, the braid β_i is obtained from β_{i-1} by a single application of one of the algebraic moves \mathcal{R} , \mathcal{W} , \mathcal{W}^{-1} described above. \square

Detailed proofs of Markov's theorem can be found in [Bi, Mo3, Tr], and outlined proofs in [Ma, Ha].

Finally in this section, we define a special braid. We let $\Delta_n \in B_n$ denote a positive half-twist of n strings, defined inductively by

$$\begin{aligned} \Delta_2 &= \sigma_1; \\ \Delta_n &= \Delta_{n-1} \cdot (\sigma_{n-1} \sigma_{n-2} \dots \sigma_1), \quad n > 2. \end{aligned}$$

1.4 Some standard knot and link invariants

There are many invariants of links. Here are some of the standard invariants used in this thesis.

Let L be a link, and D a diagram of L . Define $c(D)$ to be the number of (double point) singularities of D . The (*geometric*) *crossing index* of L , denoted $c(L)$, is defined as

$$c(L) = \min_{D=D(L)} \{c(D)\}.$$

Choose an orientation for L . Then the *sign* of a crossing p of D , denoted $\varepsilon(p)$ is defined as being ± 1 , according to the convention in figure 1.8. The convention comes from the right-hand twist rule. The sign of a crossing coincides with the sign of an elementary braid generator and is preserved by reversal of orientation of *all* the components of L .

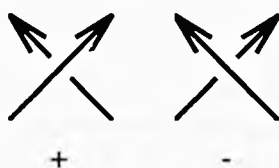


Figure 1.8: Sign of a crossing

The *algebraic crossing number* (or *writhe*) of D is the sum of the signs of the crossings:

$$w(D) = \sum_{p \subset D} \varepsilon(p).$$

Let β be a braid whose closure is the link L . Write $m(\beta)$ for the number of braidstrings of β , so that β lives naturally in B_m . The *braid index* $b(L)$ of L is the least number of braidstrings over all such braids β :

$$b(L) = \min_{\beta \text{ s.t. } \beta=L} \{m(\beta)\}.$$

There are finitely many inequivalent links of a given (geometric) crossing index; they are listed, for small $c(L)$, in [Ro, Th1], and elsewhere. There are infinitely many inequivalent links of a given braid index. Note that algebraic crossing number is defined on the diagram of a link, not the link itself.

1.5 Polynomial invariants

In this section we define a number of polynomial invariants of links. The *Jones polynomial* was discovered in the mid-1980s, and was soon found to generalize in two different ways, giving the *Homfly* and *Kauffman polynomials*. All of these generalize the older invariants of Conway and Alexander, and also provide more information about links.

1.5.I The Homfly polynomial

For each oriented link L there is a Laurent polynomial $\mathcal{P}_L(v, z)$ in two variables v, z . The polynomial is uniquely determined by the linear skein rule

$$v^{-1}\mathcal{P}_{D_+} - v\mathcal{P}_{D_-} = z\mathcal{P}_{D_0},$$

where D_+ , D_- , D_0 are diagrams of links, which are identical except in the neighbourhood of a single crossing of D_+ , where they appear as in figure 1.9. A normalization is required: the original versions of \mathcal{P} use the normalization $\mathcal{P}_{U_1}(v, z) = 1$, where U_1 is the unknot. For the purposes of this thesis, we use this normalization.² These relations ensure that $\mathcal{P}_L(v, z)$ is invariant under the three Reidemeister moves.



Figure 1.9: D_+ , D_- , D_0 differ as shown

The polynomial $\mathcal{P}_L(v, z)$ is commonly referred to as the *Homfly* or *two-variable Jones* polynomial. There exist several slightly different versions of it, involving different variables and normalization. The version used here follows [Mo2] and [Ru4]. The Lickorish-Millett version is obtained by the substitution $v = -il$, $z = im$, where $i = \sqrt{-1}$. The Thistlethwaite tabulations [Th4] of the Homfly polynomial, for knots of up to 13 crossings, require the substitution $v = a$, $z = x^{\frac{1}{2}} - x^{-\frac{1}{2}}$.

The polynomial \mathcal{P}_L is unchanged by reversal of the orientation of *all* the components of L . There are specializations of the two-variable polynomial. The *Jones polynomial* $V_L(t)$ is given by

$$V_L(t) = \mathcal{P}_L(t, t^{\frac{1}{2}} - t^{-\frac{1}{2}}),$$

and was the inspiration for the two-variable version [F-Y-H-L-M-O, P-T]. The *Alexander polynomial* $\Delta_L(t)$ is retrieved by the substitution

$$\Delta_L(t) = \mathcal{P}_L(1, t^{\frac{1}{2}} - t^{-\frac{1}{2}}),$$

and in Conway's version by

$$\nabla_L(z) = \mathcal{P}_L(1, z).$$

²In some contexts, it is more convenient to use $\mathcal{P}_\emptyset(v, z) = 1$, $\mathcal{P}_{U_1}(v, z) = \delta (= \frac{v^{-1}-v}{z})$, where \emptyset denotes the 'empty link' – the link with zero components.

1.5.II The Kauffman polynomial

A polynomial invariant for unoriented links was discovered by Kauffman [Kau1]. (This definition follows [Th2], and coincides with the version given in [Oc].) First define the regular isotopy invariant $\Lambda(a, x) \in \mathbf{Z}[a^{\pm 1}, x^{\pm 1}]$ by the relations

$$\begin{aligned}\Lambda_{D_+} + \Lambda_{D_-} &= x(\Lambda_{D_0} + \Lambda_{D_\infty}), \\ \Lambda_{D_s} &= a\Lambda_{D_t}\end{aligned}$$

where Λ_{D_+} , Λ_{D_-} , Λ_{D_0} , Λ_{D_∞} are polynomials of links with diagrams D_+ , D_- , D_0 , D_∞ which are identical except in the neighbourhood of a double point, where they appear as in figure 1.10, and Λ_{D_s} , Λ_{D_t} are polynomials of links with diagrams D_s , D_t , which are identical except as described in figure 1.11.

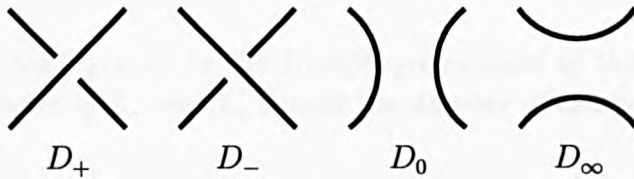


Figure 1.10: D_+ , D_- , D_0 , D_∞ differ as shown

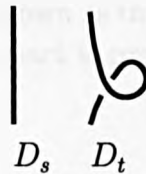


Figure 1.11: D_s , D_t differ as shown

Now write $F_L(a, x) = a^{-k}\Lambda(a, x)$, where $k = w(D)$ is the writhe (algebraic crossing number) of the oriented diagram D . The invariant F_L is an invariant of links up to ambient isotopy; Λ is an invariant up to regular isotopy. The polynomial invariant F_L is known as the *Kauffman polynomial*.

The Kauffman polynomial also specializes to the Jones polynomial, by the substitution

$$F_L\left(t^{-\frac{3}{4}}, -(t^{\frac{1}{4}} + t^{-\frac{1}{4}})\right) = V_L(t).$$

1.5.III Comments

Observation of extreme powers of these polynomials is sometimes useful, and so an appropriate notation is required. Let $H(x)$ be a Laurent polynomial in $R[x^{\pm 1}]$, for some ring R . Then write

$$\begin{aligned}\min\deg_x H(x) &= \sup\{n \in \mathbf{Z} : x^{-n}H(x) \in R[x] \subset R[x^{\pm 1}]\}, \\ \max\deg_x H(x) &= \inf\{n \in \mathbf{Z} : x^n H(x) \in R[x^{-1}] \subset R[x^{\pm 1}]\}.\end{aligned}$$

These formal definitions follow those of Rudolph, [Ru4], where they are called ord_x and deg_x respectively. Less formally, $\min\deg_x H(x)$ and $\max\deg_x H(x)$ are respectively the least and greatest powers of x with non-zero R -coefficient in $H(x)$.

These polynomials are known to predict geometrical properties of knots. The following theorem will be useful to us.

Theorem 1.5.1 *Let $\mathcal{P}_L(v, z)$ be the Homfly polynomial of the link L . Let $b(L)$ denote the braid index of L , and $|L|$ denote the number of components of L . Then*

(i) $b(L) \geq 1 + \frac{1}{2}(\max\deg_v \mathcal{P}_L - \min\deg_v \mathcal{P}_L)$;

(ii) $|L| = 1 - \min\deg_z \mathcal{P}_L$. □

The first part of this theorem is known as the Morton-Franks-Williams (MFW) inequality [Mo2, F-W]. The second part is proposition 22 of [L-M].

1.6 Composite links

There are natural ways to construct more complicated links from simpler ones. Some definitions and examples follow.

Some general topological definitions: if space Y is a subspace of space Z , and Y is homotopic to a point $z \in Z$, then Y is called *contractible* in Z .

Let F be a surface embedded into some 3-manifold M . Then F is *compressible* if either

- (i) there exists a 2-disc $D \subset M$ such that $D \cap F = \partial D$ and ∂D is non-contractible in F ;

(ii) F is a 2-sphere in M and F bounds a 3-cell in M .

Let L be a link, and S be a 2-dimensional sphere, embedded smoothly or piecewise linearly, in $S^3 - L$. Then S bounds two 3-balls B_1, B_2 in S^3 . The sphere S is incompressible in $S^3 - L$ if, and only if, each of the 3-balls has non-empty intersection with L . In this case we say that L is a *distant union* of the sub-links $L_1 = L \cap B_1$ and $L_2 = L \cap B_2$. We write $L = L_1 \sqcup L_2$. Sometimes, $L_1 \sqcup L_2$ is also said to be *split*. See the example in figure 1.12.

In particular, we define the *unlink* of n components, denoted U_n , to be the union of n mutually distant unknots.

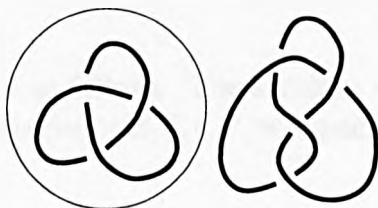


Figure 1.12: Distant union of trefoil and figure-eight, with separating 2-sphere

Suppose that L is not a distant union. Let S be a 2-sphere, embedded smoothly or piecewise linearly in S^3 , such that $S \cap L$ consists of exactly two transverse intersections, at the points p_1, p_2 . Join p_1 to p_2 by an arc $\gamma \subset S$. Again S bounds two 3-balls B_1, B_2 in S^3 . If, for $i = 1, 2$, the link $L_i = (L \cap B_i) \cup \gamma$ is not ambient isotopic to the unknot then we say that L is a *connected sum* with summands L_1 and L_2 . We write $L = L_1 \# L_2$. If no such S exists then L is called a *prime link*, otherwise it is *composite*. The terminology is based on the fact that there exists a prime decomposition theorem for links: this was first proved by Schubert, and a good account is given in [B-Z]. Figure 1.13 gives an example of a connected sum.

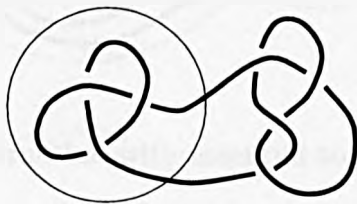


Figure 1.13: Connected sum of trefoil and figure-eight, with decomposing 2-sphere

Let T be a smooth or piecewise linear hollow torus in S^3 . It is known, by a theorem of Alexander (cited in [B-M7]), that T bounds a solid torus V on at least one side. Suppose a link L is completely contained in the interior of V . Say that T is *essential* if it is incompressible in $S^3 - L$. (Then, there does not exist any meridional disc D of V with $D \cap L = \emptyset$; also, V is a knotted torus, with its core ambient isotopic to the knot C , say.) Say that T is *peripheral* if it is parallel to the boundary of a tubular neighbourhood of L . If T is essential and non-peripheral then L is called a *satellite link*; C is its *companion*. A homeomorphism $h : V \rightarrow V_P$ maps V to an unknotted torus V_P ; the *decoration* (or *pattern*) P is the inclusion of $h(L)$ in V_P . Figure 1.14 clarifies this definition.

It should be noted that this is not well-defined: one is also required to control meridional twisting of $V_C = V$ by specifying a *framing* f . This is discussed in chapters 3 and 4.

Notation for satellites is as follows. The satellite with companion C , pattern P and unspecified framing is denoted $C * P$; we specify a framing f by using the notation $C *_f P$.

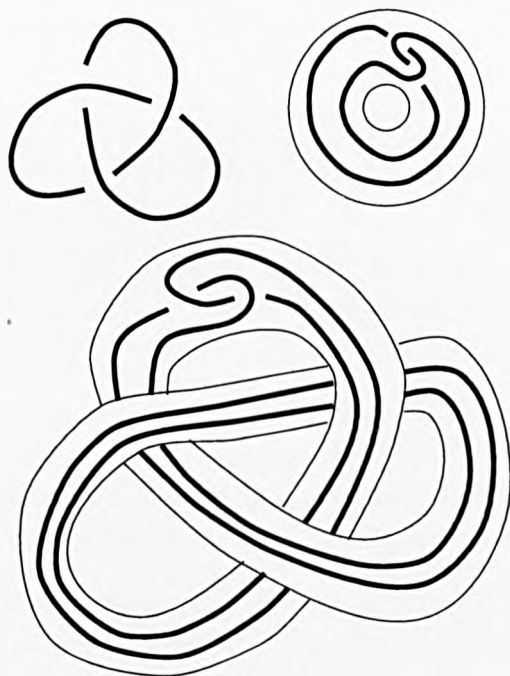


Figure 1.14: Satellite construction with essential torus, companion and pattern

As a final remark, we say that the pattern $P \subset V_P$ is *not proper* if, and only if, there exists some meridional disc $D \subset V_P$ which has empty intersection with P . If no such disc exists then we say that P is a *proper* pattern. Note that a ‘non-proper satellite’ $C * P$ constructed from a non-proper pattern P is independent of the choice of companion and framing; in this case the torus T is inessential in $S^3 - (C * P)$.

Chapter 2

Embeddings of links in a book of halfplanes

This chapter begins with the definition of a presentation of links which we find central to the study of certain satellites as closed braids. We go on to investigate some of the properties of this new presentation.

2.1 Basic definition and initial remarks

Our medium is the space S^3 . Let the *axis* $A \cong S^1$ be an (unknotted) loop in S^3 . The complement of A in S^3 admits a *fibration* H , whose fibres are open discs $\{H_\theta : 0 \leq \theta \leq 2\pi\}$.

If we consider S^3 with cylindrical polar coordinate system (r, θ, z) then we may take A to be the axis $r = 0$, and the fibres H_θ to be the half-planes $\theta = \text{constant}$. We call H the *open-book decomposition* of $S^3 - A$; the fibres are called *pages*. The axis A is also called the *binding circle* of H .

Let $\alpha \geq 2$ be a natural number. Choose an orientation for A and α points $p_0, p_1, \dots, p_{\alpha-1}$ which appear in order with the orientation of A . Choose also pages $\{H_\theta : \theta = \frac{2(\alpha-k)\pi}{\alpha}, k = 0, \dots, \alpha - 1\}$, and label these $\{h_0, \dots, h_{\alpha-1}\}$.

Now join pairs of points (p_m, p_n) by simple arcs a_j in the h_j such that

- (i) each h_j contains exactly one arc a_j ;
- (ii) each p_i is incident to exactly two arcs a_j .

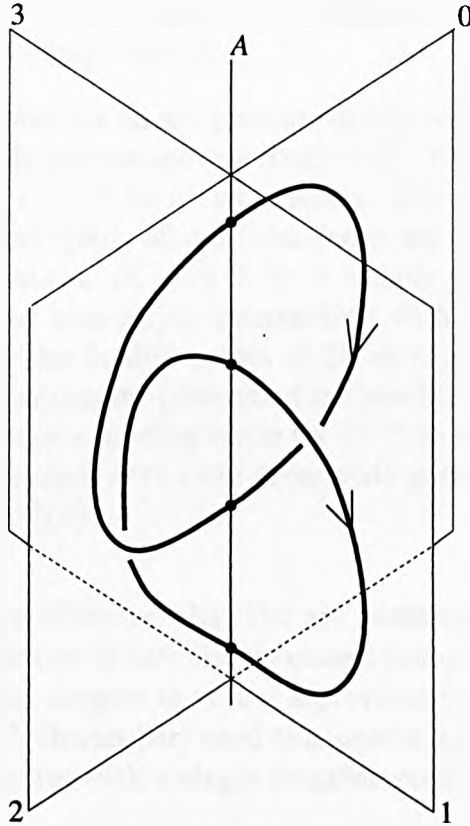


Figure 2.1: 4-arc presentation of a Hopf link

The union $\bigcup_{j=0}^{\alpha-1} a_j$ is called an *arc presentation*. An arc presentation with α arcs is called an α -*arc presentation*. Figure 2.1 gives an example of a 4-arc presentation.

It should be noted that an arc presentation of a link is itself a link, and lies in S^3 .

Proposition 2.1.1 *Every arc presentation is a link, and every link has an arc presentation.*

Proof. Let L be an arc presentation. Choose an arc a_{j_1} , say. Follow a_{j_1} to one of its end points, p_{m_1} . By hypothesis, p_{m_1} is incident to exactly one other arc, a_{j_2} , say. Continue by following a_{j_2} to its conclusion, at p_{m_2} , say, and so on. Since there are finitely many arcs, then one must eventually return to a_{j_1} . Since there are exactly two points incident to each arc, it is impossible to return to any of the a_{j_i} , $i \geq 2$, before we return to a_{j_1} . Hence the arcs traversed in this path form a loop, which is a one-component link (*i.e.* a knot).

If there are arcs which were not reached in this loop then choose one of them and repeat the process. If the process needs to be repeated $|L|$ times then the arc presentation is a $|L|$ -component link.

To show that every link has an arc presentation it suffices to give an algorithm to generate one. Methods for this are described in [Cr, C-N]. For example, given a link $L \subset S^3$, let $\pi(L) = D \subset S^2$ be a link diagram. Then D decomposes S^2 into a number of disjoint regions $\{R_i\}$, whose boundaries are sections of D , and whose vertices are double points of D . Let λ be a simple closed curve, superposed onto D , such that λ has non-empty intersection with each R_i , intersecting D transversely, away from the double points of D , at every point of $D \cap \lambda$. Then one can use a colouring argument (described in detail in the proof of proposition 2.5.2) to show that λ forms a binding circle for D . The inverse image $\pi^{-1}(D \cup \lambda)$ (where the intersection points $D \cap \lambda$ are preserved) gives an arc-presentation for L , with binding circle $\pi^{-1}(\lambda)$. \square

Birman and Menasco observed that the arc presentation of a link is central to the study of certain types of satellite as closed braids. They introduce it into their work in [B-M7], and suggest that it is a previously unnoticed manifestation of links. In fact, in 1897, Brunn [Br] used this presentation of a link to establish that any link has a diagram with a single singular point of high multiplicity.³

2.2 The arc index, $\alpha(L)$

From this presentation of a link comes a link invariant: the *arc index* $\alpha(L)$ of a link L is the least number of arcs over all arc presentations of L .

There is an easy way to translate the arc presentation to a special diagrammatic form for a link L , which has a number of applications. The diagram is called a *grid diagram*⁴, because it is constructed on an $\alpha \times \alpha$ grid, and made up of parts of loops and lines from the arc presentation. Its construction is described below.

Given an arc-presentation L , the first step is to isotop the link L away from A slightly. Choose a solid torus neighbourhood $N(A)$ of A such that each component of $L \cap N(A)$ is a small arc β_j containing exactly one point of $L \cap A$. So $L \cap N(A) = \{\beta_j : 1 \leq j \leq \alpha\}$. Apply an isotopy of L by projecting the β_j radially onto $\partial N(A)$: denote the image of this projection by β_j' . There are two ways to do this; they are demonstrated in figure 2.2. The β_j' are referred to as *semi-loops*.

³I am grateful to Józef Przytycki for introducing me to this work.

⁴In [Cr], Cromwell calls this a *loops & lines* diagram.

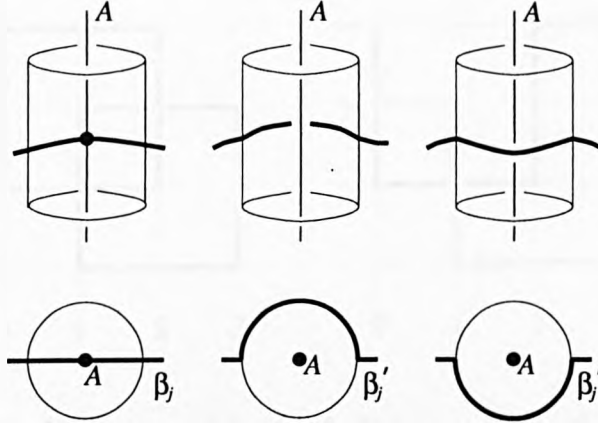


Figure 2.2: Isotopy $\beta_j \rightarrow \beta'_j \subset \partial N(A)$

Now another isotopy takes each of the (slightly trimmed) arcs onto the boundary $\partial N(A)$: there will be a number of double point singularities. If we now cut along the length of $\partial N(A)$, we can lay the hollow tube out on a plane, hence giving a 2-dimensional presentation for the 3-dimensional embedding of L . The semi-loops appear as horizontal lines on the grid, and the (trimmed) arcs appear as vertical lines. The double point singularities on $\partial N(A)$ are resolved as crossings in the usual way, with one strand under-crossing the other. In fact, to preserve the link we must have the vertical line *over*-crossing the horizontal line at each double point.

The choice of semi-loops gives us different possible diagrams for L . For example, it is always possible to choose them to give an ordinary knot diagram of L , or a braid presentation of L . See figure 2.3.

Remark. Recall theorem 1.3.1 (Alexander's theorem), which states that every link can be represented as a closed braid. The existence of a braided format for each grid diagram really provides us with an alternative proof of theorem 1.3.1, since it gives us an alternative algorithm for constructing a braid representative for a given link L . The proof works as follows: given L , we know that L has an arc presentation (proposition 2.1.1). Then it is enough to take the grid diagram $G(L)$ corresponding to that arc presentation, with one of the two choices of semi-loops which present $G(L)$ as a braid.

We will also make use of the following notation. The set of links of arc index α is denoted $\mathcal{L}(\alpha)$. The set of knots of arc index α is denoted $\mathcal{K}(\alpha)$. Thus $\mathcal{K}(\alpha) \subset \mathcal{L}(\alpha)$. The set of $(\alpha \times \alpha)$ grid diagrams of links is denoted $\mathcal{D}_{\mathcal{L}}(\alpha)$; the

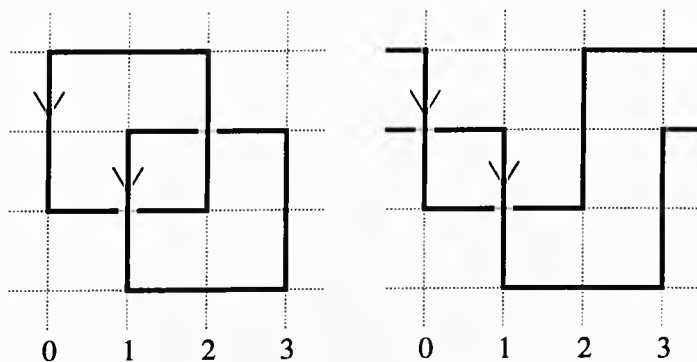


Figure 2.3: Closed diagram and braided diagram of Hopf link from the grid diagram (compare with figure 2.1)

set of $(\alpha \times \alpha)$ grid diagrams of knots is denoted $\mathcal{D}_{\mathcal{K}}(\alpha)$. (It is true that $\mathcal{D}_{\mathcal{L}}(\alpha)$ contains diagrams of every $L \in \mathcal{L}(i)$, for all $i \leq \alpha$. The corresponding fact is true regarding $\mathcal{D}_{\mathcal{K}}(\alpha)$.)

Finally in this section, let \mathcal{M}_{α} be the set of $\alpha \times \alpha$ matrices with exactly one 1 and one -1 in each row and column. It is sometimes helpful to view the (oriented) grid diagram G by a matrix, $M(G) \in \mathcal{M}_{\alpha}$. We define $M(G)$ by

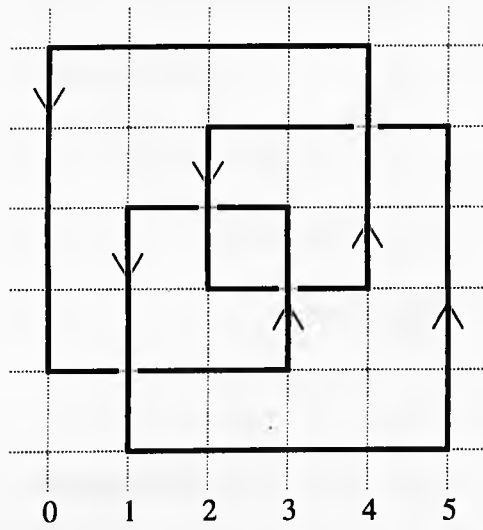
$$M_{ij}(G) = \begin{cases} 1 & \text{if arc } a_i \text{ begins at point } p_j; \\ -1 & \text{if arc } a_i \text{ ends at point } p_j; \\ 0 & \text{otherwise.} \end{cases}$$

This gives a bijection between the sets \mathcal{M}_{α} and $\mathcal{D}_{\mathcal{L}}(\alpha)$. The example in figure 2.4 should clarify the definition.

2.3 Equivalence of arc diagrams

A given link has infinitely many arc-presentations; even if we restrict to only those diagrams which use the minimum number of arcs, it is not clear whether there will be a unique presentation. An example is the $(2, 4)$ -torus link, cited in [Cr] and reproduced in figure 2.5.

When considering equivalence of link diagrams, we refer to the Reidemeister moves. Similarly, equivalence of closed braids is formulated by the Markov moves. In each case, two representations of a link are related by applying a finite sequence of combinatorial moves. Cromwell constructed a similar solution for the problem



$$\begin{pmatrix} 1 & 0 & 0 & 0 & -1 & 0 \\ 0 & 0 & 1 & 0 & 0 & -1 \\ 0 & 1 & 0 & -1 & 0 & 0 \\ 0 & 0 & -1 & 0 & 1 & 0 \\ -1 & 0 & 0 & 1 & 0 & 0 \\ 0 & -1 & 0 & 0 & 0 & 1 \end{pmatrix}$$

Figure 2.4: One possible G and $M(G)$ for the figure-eight knot

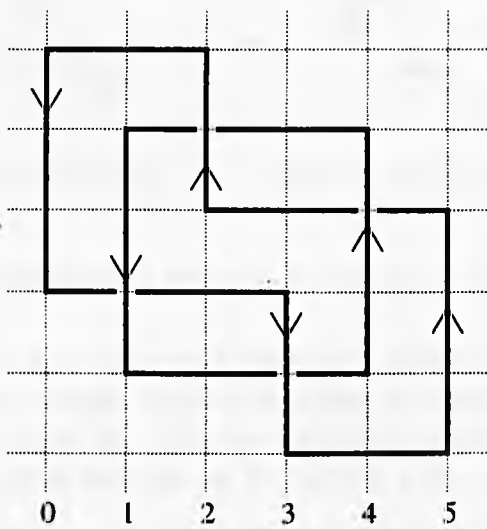
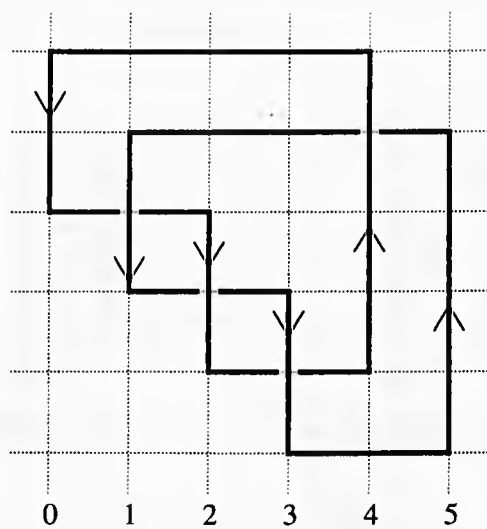


Figure 2.5: Two arc-diagrams of $T(2, 4)$

of equivalent arc-diagrams (*i.e.* arc-diagrams of the same link). First we need a number of definitions.

Let L be a link, and A be a binding circle. Say that two arcs *interleave* if the endpoints of one alternate with the endpoints of the other. Similarly, two points of $L \cap A$ *interleave* if the pages which contain the arcs incident to one of the points alternate with the pages which contain the arcs incident to the other. Figure 2.6 should clarify the definition.

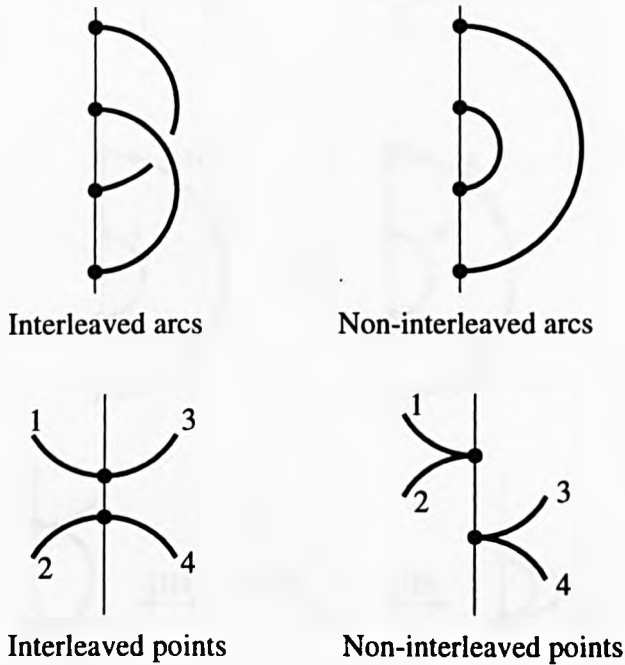


Figure 2.6: Interleaving and non-interleaving arcs and points

Two points of $L \cap A$ are *adjacent* if there is a section of A which is bounded by the two points, and whose interior contains no intersection with L . Two arcs, contained in the pages H_{θ_1} , H_{θ_2} are *adjacent* if there is an interval $I \subset S^1$, bounded by θ_1 and θ_2 , such that for all $\theta \in \text{int}(I)$, $(H_{\theta} - A) \cap L = \emptyset$.

Two points of $L \cap A$ are *consecutive* if they are at opposite ends of the same arc. Two arcs of L are *consecutive* if they are incident to the same point.

We are now in a position to describe the four moves on arc-diagrams. They are also illustrated in figure 2.7 and described as follows.

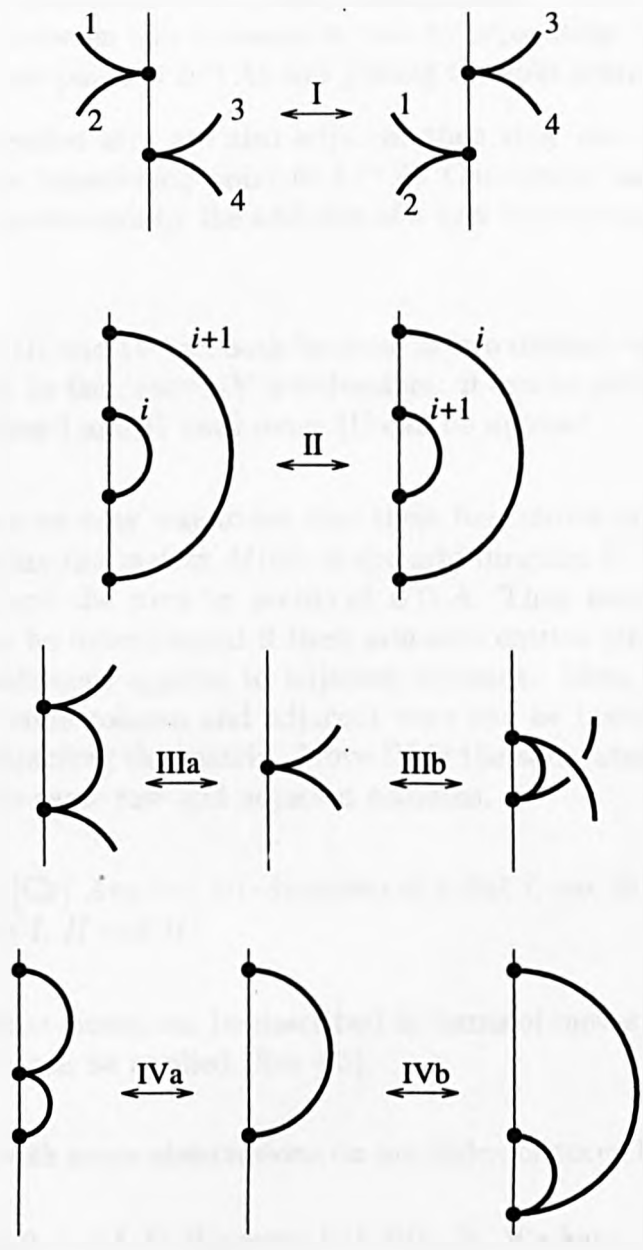


Figure 2.7: Moves I-IV relating equivalent arc-diagrams

- I. If two adjacent points of $L \cap A$ do not interleave then they may be interchanged.
- II. If two adjacent arcs do not interleave then they may be interchanged.
- III. If two consecutive points of $L \cap A$ are also adjacent then the intervening arc can be removed and the points amalgamated. Conversely, an arc can be inserted between two consecutive arcs by separating the two arcs (thus creating a new point of $L \cap A$) and joining the split point by a new arc.
- IV. If two consecutive arcs are also adjacent then they can be amalgamated, removing the intervening point of $L \cap A$. Conversely, an arc can be split into two adjacent arcs by the addition of a new intersection point of the arc with A .

Remark. Moves III and IV can both be done in two distinct ways, one of which preserves framing. In fact, move IV is redundant: it can be obtained by repeated application of moves I and II until move III can be applied.

Remark. There is an easy way to see that these four moves are in fact two dual pairs, by considering the matrix $M(G)$ of the grid diagram G . The columns are indexed by arcs, and the rows by points of $L \cap A$. Then move I says that two adjacent rows can be interchanged if their non-zero entries are separated. Move II is the same statement applied to adjacent columns. Move III says that a 1 and a -1 in the same column and adjacent rows can be inserted or deleted by expanding or contracting the matrix. Move IV is the same statement applied to a 1, -1 pair in the same row and adjacent columns.

Theorem 2.3.1 [Cr] *Any two arc-diagrams of a link L can be related by a finite sequence of moves I, II and III.*

Proof. The Markov moves can be described in terms of moves I, II and III; then Markov's theorem can be applied. See [Cr]. \square

We continue with some observations on arc index of torus links.

Proposition 2.3.2 *Let L be the torus link $T(p, q)$. We have $\alpha(L) \leq p + q$.*

Proof. A closed braid presentation for L is $L = \hat{\beta}$, where $\beta = (\sigma_{p-1} \dots \sigma_1)^q \in B_p$. The braid β can be generated by a grid diagram on $p + q$ arcs; the first q generate the crossings, and the remaining p provide a vertical 'shift' of the braidstrings, necessary in the grid diagram construction. The top picture in figure 2.5 illustrates this in the case $p = 2$, $q = 4$. \square

Theorem 2.3.3 *Let L be the torus link $T(2, q)$, $q \geq 2$. We have $\alpha(L) \geq 2 + q$.*

The proof of this is deferred until section 4.6. However, we can deduce the following.

Corollary 2.3.4 *Let L be the torus link $T(2, q)$, $q \geq 2$. We have $\alpha(L) = 2 + q$.*

Proof. Obvious from the statements of proposition 2.3.2 and theorem 2.3.3. \square

There is a natural comparison here to the stabilization index⁵, as discussed in [B-M5]. The question arises when relating two arc-presentations by moves I, II, III: can we relate them without increasing the arc number? The following theorem answers this question in the case of some torus links.

Theorem 2.3.5 *Let L be the torus link $T(2, q)$, $q \geq 4$. Then there exist arc-diagrams $G_0(L), G_s(L)$ of L with $\alpha(L)$ arcs, such that any sequence relating the two diagrams by moves I, II, III must contain at least one diagram with $\alpha(L) + 1$ arcs.*

Proof. By corollary 2.3.4, $\alpha(L) = 2 + q$. The diagrams can be constructed by choosing different binding circles as in the example in figure 2.8. The binding circle connects the ‘beads’ of the diagram in order in one case, and not in the other. The grid diagrams G_0, G_s are easily deduced from these. Notice that, by the definition of the moves, it is impossible to apply either move I or move II to G_0 . An arc-reducing type III move is also impossible, by definition of arc index, since G_0 has only $\alpha(L)$ arcs. \square

⁵This refers to two closed braid presentations $\hat{\beta}, \hat{\beta}'$ of a link L , where $\hat{\beta}'$ is a minimal closed braid presentation of L (i.e. on $b(L)$ braidstrings) and $\hat{\beta}$ is a closed braid presentation on $n \geq b(L)$ braidstrings. The closed braids $\hat{\beta}$ and $\hat{\beta}'$ are related by the sequence

$$\hat{\beta} = \hat{\beta}_0 \rightarrow \hat{\beta}_1 \rightarrow \dots \rightarrow \hat{\beta}_s = \hat{\beta}',$$

where each $\hat{\beta}_i$ is obtained from $\hat{\beta}_{i-1}$ by a Markov move. It may be necessary to increase the number of braid strings during the sequence. The *stabilization index* $s(L, n)$ is the minimum, over all possible sequences, of the number of braid strings added in the sequence. In [B-M5] it is shown that for all unlinks U_r , for $n > r$, we have $s(U_r, n) = 1$.

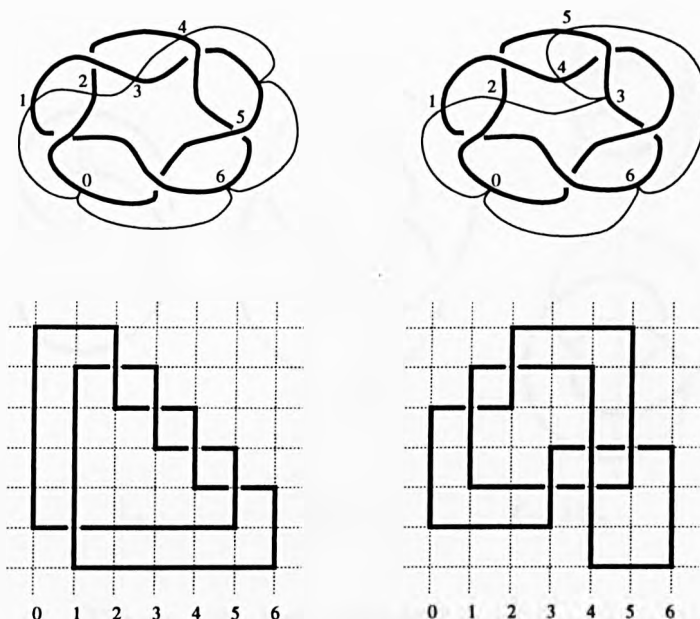


Figure 2.8: Different binding circles for the link $L = T(2, 5)$

2.4 Behaviour of $\alpha(L)$ under knot operations

The following results describe the behaviour of arc index under the operations of distant union and connect sum.

Theorem 2.4.1 *Let L_1, L_2 be links. Then*

$$\begin{aligned}\alpha(L_1 \sqcup L_2) &= \alpha(L_1) + \alpha(L_2); \\ \alpha(L_1 \# L_2) &= \alpha(L_1) + \alpha(L_2) - 2.\end{aligned}$$

These results are the conclusions of the following set of propositions.

Proposition 2.4.2 *Let $L = L_1 \sqcup L_2$. Then $\alpha(L) \leq \alpha(L_1) + \alpha(L_2)$.*

Proof. Construct an arc presentation for L by juxtaposing the presentations of L_1 and L_2 on the same axis A , as in figure 2.9.

This is an $(\alpha(L_1) + \alpha(L_2))$ -arc presentation for L , and by definition of arc index, $\alpha(L)$ is bounded above by $\alpha(L_1) + \alpha(L_2)$. \square

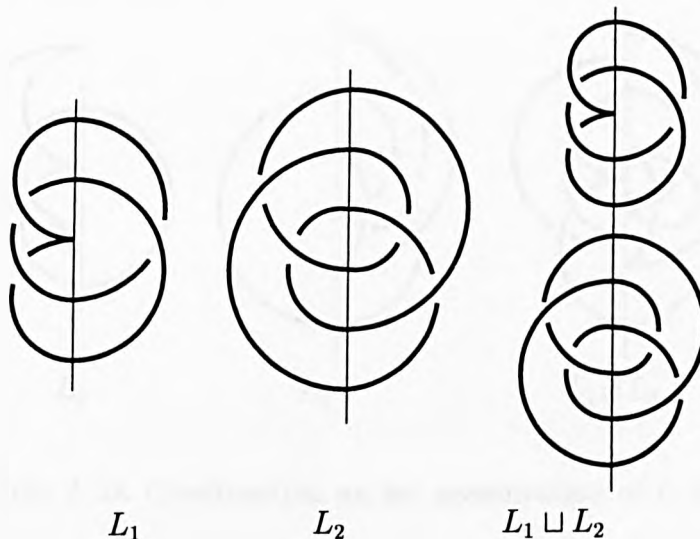


Figure 2.9: Arc presentation of $L_1 \# L_2$

Proposition 2.4.3 *Let $L = L_1 \# L_2$. Then $\alpha(L) \geq \alpha(L_1) + \alpha(L_2)$.*

Proof. We have an arc presentation of L on $\alpha(L)$ arcs. By a theorem of Birman and Menasco [B-M4], there exists a 2-sphere S which separates S^3 into two 3-balls B_1, B_2 , such that $L_i = L \cap B_i$. We reconstruct the arc presentation of L_1 by taking $((L \cup A) \cap B_1) \cup (A \cap B_2)$. By definition of arc index, this is a presentation of L_1 on at least $\alpha(L_1)$ arcs. Reconstruct L_2 in a similar way. Therefore the total number of arcs in the presentation is at least $\alpha(L_1) + \alpha(L_2)$. \square

Proposition 2.4.4 *Let $L = L_1 \# L_2$. Then $\alpha(L) \leq \alpha(L_1) + \alpha(L_2) - 2$.*

Proof. Start with arc presentations for L_1 and L_2 . With each presentation, swivel all the arcs but one, so that they lie in a half-space; delete the remaining arc. Then a presentation of L is obtained by identifying the axes of the two presentations, so that the loose ends of each link are identified and the other points of $(L_1 \cup L_2) \cap A$ remain distinct. See figure 2.10 for illustration.

The number of arcs of this presentation of L is

$$(\alpha(L_1) - 1) + (\alpha(L_2) - 1) = \alpha(L_1) + \alpha(L_2) - 2,$$

which is an upper bound for $\alpha(L)$. \square

Proposition 2.4.5 [Cr] *Let $L = L_1 \# L_2$. Then $\alpha(L) \geq \alpha(L_1) + \alpha(L_2) - 2$.*

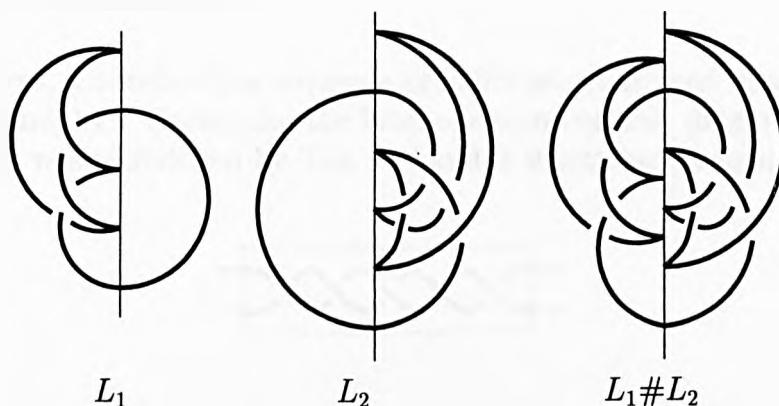


Figure 2.10: Constructing an arc presentation of $L_1 \# L_2$

Proof. The proof is adapted from a result of [B-M4] (part of theorem 3.1.1), and the reader is referred to that paper and to [Cr] for details. \square

2.5 Relating $\alpha(L)$ to other link invariants

It should be noted that there are finitely many links L with given arc index $\alpha(L)$. In this sense, arc index behaves like crossing index, but not like braid index.

The main results of this section concern the relationship between arc index $\alpha(L)$ and crossing index $c(L)$ of a link L : these are covered in subsection 2.5.II. We also include observations on how arc index relates to braid index (subsection 2.5.I) and Homfly polynomial (subsection 2.5.III).

2.5.I Braid index

The ‘braided’ grid diagram (figure 2.3) leads us to the following result.

Proposition 2.5.1 *Let L be a link, $\alpha(L)$ its arc index and $b(L)$ its braid index. Then $b(L) \leq \frac{1}{2}\alpha(L)$.*

Proof. Let $G(L)$ be a grid diagram of L with $\alpha = \alpha(L)$ arcs. There are precisely two choices of semi-loops which make $G(L)$ into a braid: they have b_1 and b_2 braidstrings respectively. Now $b_1 + b_2 = \alpha$, so necessarily one of the b_i (b_1 , say) is bounded above by $\frac{1}{2}\alpha$. Then we have $b(L) \leq b_1 \leq \frac{1}{2}\alpha(L)$, as required. \square

2.5.II Crossing index

In what follows, a *twistbox* is a sequence of half-twists contained in a rectangular box, as in figure 2.11. Recall also the local operation on link diagrams known as a *flype*, which was introduced by Tait [Ta] and is illustrated in figure 2.12.



Figure 2.11: A twistbox with 5 half-twists

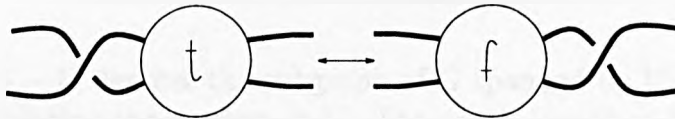


Figure 2.12: Tait's *flype* move

Proposition 2.5.2 [C-N] *Let L be a link, $\alpha(L)$ its arc index and $c(L)$ its (geometric) crossing index. Suppose that L has a diagram $D(L)$ which is drawn with minimal crossing number $c(L)$. Suppose further that D can be decomposed into a diagram with n twistboxes, and that this number cannot be reduced by application of flypes. Then the inequality $\alpha(L) \leq 2 + c(L)$ holds in the following cases:*

- (i) $n \leq 8$;
- (ii) $n \geq 9$ and $D(L)$ cannot be decomposed into the 4-tangle or 6-tangle structures of figure 2.13.

Proof. In order to establish this result we will need some graph theory, and so we begin by recapping some definitions, which also provide our notation.

All our graphs will be planar graphs embedded in \mathbf{R}^2 . Let V be the set of vertices of a graph G . An *edge* of G is a simple curve which joins a pair of vertices $[u, v]$. A *loop* is an edge $[v, v]$ which has the same vertex at both ends. An edge e such that $G - e$ is disconnected is called an *isthmus*. If $U \subset V$ then $\text{span}(U)$ is the subgraph of G whose edges connect vertices in U :

$$\text{span}(U) = \{[u_i, u_j] : \text{for all pairs } u_i, u_j \text{ in } U\}.$$

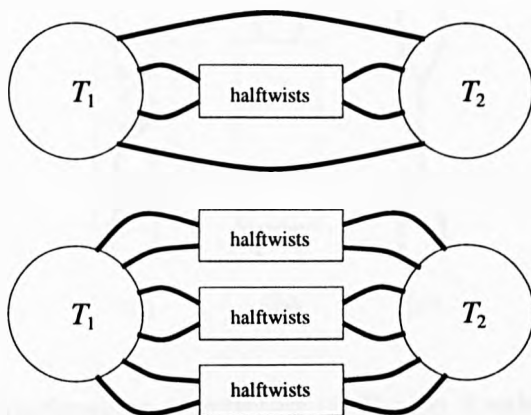


Figure 2.13: 4- and 6-tangle structures

If $U \subset V$ then $G - U$ denotes the subgraph of G spanned by $V - U$. Say $G - U$ is obtained by deleting the vertices in U . The graph is said to be r -connected if $r < |V|$ and at least r vertices must be deleted from G to disconnect it. A *cycle* is a simple closed curve which follows the edges of G . An n -cycle contains n edges. A *Hamiltonian circuit* of G is a simple closed curve which follows the edges of the graph and passes through every vertex in V exactly once.

Let D be a diagram of a prime link L . A sequence of half-twists in the diagram can be replaced by a rectangular twist-box as shown in figure 2.14(b). The diagram now consists of a collection of twist-boxes connected by a set of disjoint simple arcs. We form a graph G from this diagram as follows. If a twist-box contains only one crossing we replace it by a 4-valent vertex, otherwise we replace the twist-box by the graph shown in figure 2.14(c). Thus all vertices in G are 3-valent or 4-valent. The edges of G can be divided into two sets: D -type edges which contain part of the original diagram, and T -type edges which are contained in a twist-box.

To describe the embedding of L in an open book it suffices to indicate the path of the binding circle in the diagram. In order to find such a path we take a Hamiltonian circuit of the dual graph of G and then deform it so that it touches each twist-box once. The existence of such circuits is discussed later in the proof.

Let G^* denote the topological dual graph of G and let λ be a Hamiltonian circuit of G^* . This produces a simple closed curve which passes through every region of G exactly once. We convert λ into the desired binding circle as follows: if λ crosses a T -type edge of G then it passes through a twist-box. The circle λ and the m half-twists represented by the box can be arranged as shown in figures 2.15(a) and (b). Any twist-box that does not meet λ is treated as shown

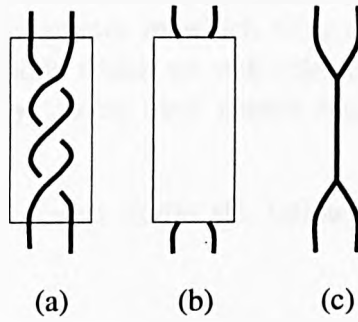


Figure 2.14: Transforming a twistbox of D into 3-valent vertices of G

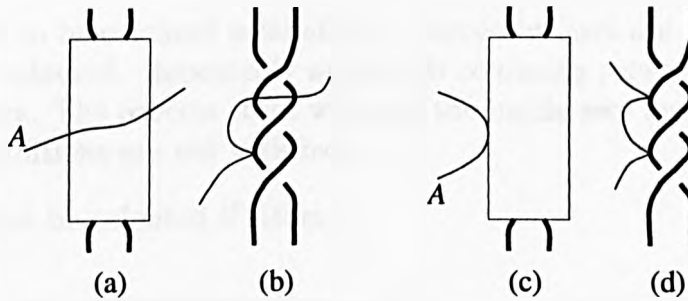


Figure 2.15: Placing the binding circle A on D

in figures 2.15(c) and (d). This is always possible since λ passes through every region of G and hence can be deformed to lie along one side of the twist-box.

The proof continues with a sequence of lemmas.

Lemma 2.5.3 *The loop λ just constructed represents a binding circle for L .*

Proof. We can isotop $D \cup \lambda$ in the plane so, without loss of generality, we can assume that λ is a circle. In particular we can take λ to be a straight line together with a point $\{\infty\}$. The link L can be embedded in \mathbf{R}^3 so that there is a projection π which carries L onto D . The faces of the 4-valent graph $\pi(L)$ are called the regions of D . Notice that all the regions of D have contact with λ : either λ passes through the region or λ has point-contact with its boundary.

Let $P = \{p_1, \dots, p_r\}$ be the set of points where λ meets D . The points $\pi^{-1}(p_i)$ divide L into a set of arcs $A = \{a_1, \dots, a_r\}$ each of which starts and ends at points in $\pi^{-1}(P)$ and contains no such points in its interior. Each of these arcs will be embedded in a half-plane. To each arc a_i in L there is a corresponding segment $\pi(a_i)$ of the diagram D which we will also refer to as an arc.

We will colour the arcs, and the order in which they are coloured will determine the position of the half-planes in which they are embedded. The plane is separated by λ into two regions which we will refer to as inside and outside. We will colour the arcs in D by taking each region separately. We start with the inside.

The colouring process proceeds under the following rules: an uncoloured arc can be coloured if

- (a) any arc crossing over it is coloured; and
- (b) any arc crossing under it is uncoloured.

The first arc to be coloured is labelled 1. Successive arcs are numbered in the order they are coloured. Repeatedly apply this colouring rule until it cannot be applied any more. The process stops when all the inside arcs have been coloured or when the conditions are not satisfied.

An arc cannot be coloured if either

- (c) some arc crossing over it is uncoloured; or
- (d) some arc crossing under it is coloured.

Because of the way the colouring is performed, the second case is impossible. Therefore, if the colouring is unfinished but cannot continue every uncoloured arc must fail on condition (c). Consequently, every uncoloured arc must cross under an uncoloured arc. This implies that some subset of arcs in D form a sequence in which each passes under the next making a pattern like that shown in figure 2.16. One could compare the loop formed by these arcs to the ‘ever-descending’ staircase in a sketch of M.C. Escher. This sketch has been reproduced in figure 2.17.

We now concentrate on the polygonal region formed from this ‘ever-descending’ set of arcs. Its corners are at crossings in D and its sides lie in arcs. There are regions of D which lie on both sides of the polygon and, by construction, λ has contact with every region of D . However, λ does not meet the sides of the polygon so it cannot touch regions on both sides. This contradiction shows that the colouring process stops only when all the arcs on the inside of λ are coloured.

The arcs on the outside of λ are coloured using the same process except that the first arc to be coloured is labelled τ , the next $\tau - 1$, and so on until every arc has been labelled.

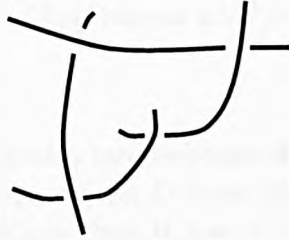


Figure 2.16: A region bounded by an 'ever-descending' set of arcs

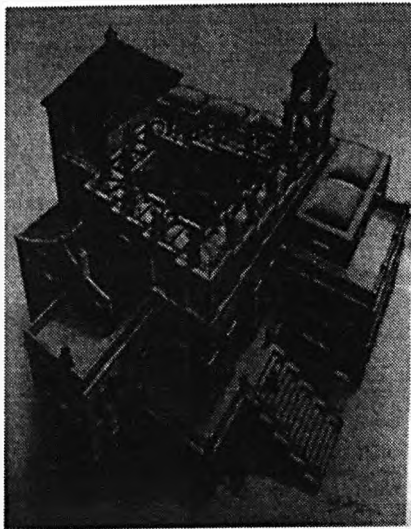


Figure 2.17: Reproduction of M.C. Escher's sketch, *Descending and Ascending*

If we now arrange r half-planes around λ at angles of $(360/r)^\circ$ and label them from 1 to r in order, the arc labelled i can be embedded in the corresponding half-plane. \square

Lemma 2.5.4 *The number of half-planes used in the construction is 2 plus the number of crossings in D .*

Proof. Suppose that D required n tangle-boxes of which r contain a single crossing. Then G has $(2n - r)$ vertices, $2n$ D-type edges and $(n - r)$ T-type edges. From Euler's formula we deduce that it has $n + 2$ regions (including the unbounded one). A Hamiltonian circuit of G^* passes through $n + 2$ vertices and therefore contains $n + 2$ edges. Thus λ crosses $n + 2$ edges of G . When a T-type edge is replaced by m half-twists as in figures 2.15(a)–(b), a single intersection of the axis and the diagram is increased to m intersections. (Recall that $m > 1$ for the existence of a T-type edge.) Running λ alongside a twist-box containing m twists as in figures 2.15(c)–(d) increases the number of intersections of λ with D by $m - 1$. Therefore the total number of intersections, and hence the number of half-planes required, is

$$\begin{aligned} n + 2 + \sum_{i=1}^n (m_i - 1) &= 2 + \sum_{i=1}^n m_i \\ &= 2 + \text{the number of crossings in } D. \end{aligned}$$

\square

We must now answer the question, when is the construction applicable? The existence of Hamiltonian circuits in planar graphs was studied by Barnette and Jukovič, and by Tutte. We make use of the following results.

Lemma 2.5.5 [Tu] *A 4-connected planar graph has a Hamiltonian circuit.* \square

Lemma 2.5.6 [B-J] *A 3-connected planar graph with at most 10 vertices has a Hamiltonian circuit.* \square

We now investigate how the connectedness of G^* is related to the diagram D .

1. Suppose that G^* is 1-connected. This means that there is a vertex $v \in V$ such that $G^* - v$ is disconnected. Every region of G^* is bounded by three or four edges, including the infinite region. This means that G^* has one of the

forms illustrated in figures 2.18(a)–(f). In the first five cases G^* contains a loop c and the corresponding edge e in G is an isthmus. If e were a D-type edge then the diagram D would cross the closed curve c once but this is not possible because any loop meeting D transversely must cross it an even number of times. So e must be a T-type edge giving D the form shown in figure 2.18(g). The twist-box is clearly redundant and the diagram does not have minimal crossing number. When G^* has the form shown in figure 2.18(f) the diagram D again has the form of figure 2.18(g); the infinite region of G^* corresponds to a (redundant) twist-box in D , containing a single crossing.

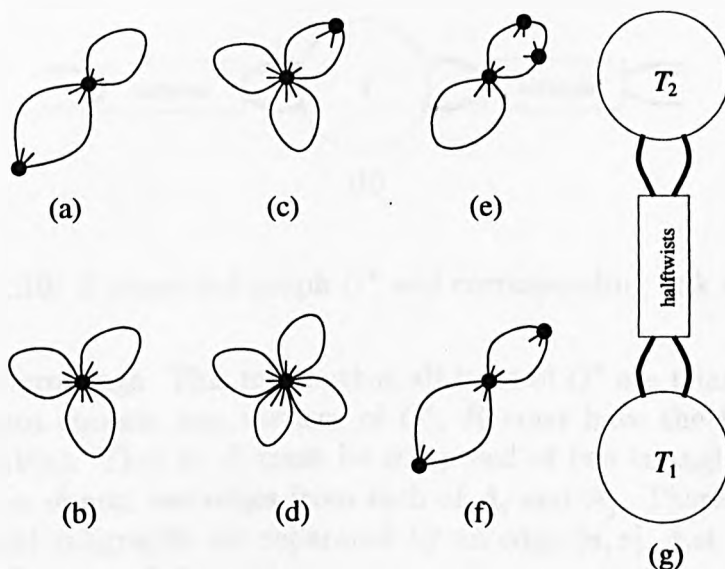


Figure 2.18: 1-connected graphs G^* with 3- or 4-sided infinite region

2. Suppose that G^* is 2-connected. Let u, v be two vertices such that $G^* - \{u, v\}$ is disconnected, and let U_i be the sets of vertices of the resulting components. Let A_i be the subgraph of G^* spanned by U_i, u and v defined as

$$A_i = \text{span}(U_i \cup u) \cup \text{span}(U_i \cup v).$$

Note that A_i and A_j have no edges in common when $i \neq j$, and that edges $\{u, v\}$ do not belong to any A_i .

Let F_i denote the interior of the infinite face of the graph A_i . We say that A_i and A_j are *adjacent* if one of the two regions of $F_i \cap F_j$ does not contain a vertex of G^* .

Now consider a pair of adjacent subgraphs A_i, A_j and let R be the region between them. Suppose for the moment that all the twist-boxes contain at

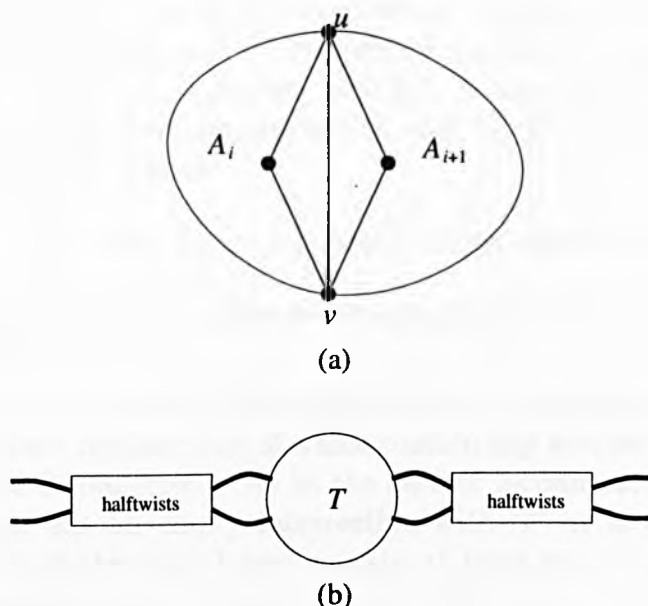


Figure 2.19: 2-connected graph G^* and corresponding link diagram

least two crossings. This means that all faces of G^* are triangles. Because R does not contain any vertices of G^* , R must have the form shown in figure 2.19(a). That is, R must be composed of two triangles bounded by an edge $[u, v]$ and two edges from each of A_i and A_j . Therefore, each pair of adjacent subgraphs are separated by an edge $[u, v]$. Let c be a 2-cycle composed of two of these edges.

The original graph G meets c in two points. Again, a parity argument shows that the 2-cycle crosses either two D-type edges or two T-type edges. In the first case, the diagram is decomposed into a connected sum of two factors. Since L is prime, one of the factors must be trivial but this contradicts the assumption that the number of crossings in D is minimal. In the second case the diagram D has the form shown in figure 2.19(b) and the number of twist-boxes can be reduced by a sequence of flypes.

We now consider what happens when some twist-boxes in D may contain only one crossing. In this case G^* can contain four-sided faces and it may be that R has empty intersection with G^* . This is equivalent to the previous case in which the edge $[u, v]$ is dual to a T-type edge except that the corresponding twist-box contains a single crossing; again the diagram admits a flype that reduces the number of twist-boxes.

3. Suppose that G^* is 3-connected. Let u, v and w be three vertices such that $G^* - \{u, v, w\}$ is disconnected, and let U_i be the sets of vertices of the

resulting components. Each U_i is joined by an edge to u , v and w , and vice versa, otherwise G^* would be 2-connected. Therefore the graph obtained from G^* by shrinking each U_i to a vertex contains the complete bipartite graph $K_{3,s}$. Since G^* is planar, and $K_{3,s}$ is non-planar for $s \geq 3$, then there must be only two components U_1 and U_2 . For $i = 1, 2$, let A_i be the subgraph of G^* defined as

$$A_i = \text{span}(U_i \cup u) \cup \text{span}(U_i \cup v) \cup \text{span}(U_i \cup w).$$

Again A_1 and A_2 have no edges in common, and do not contain edges $[u, v]$, $[v, w]$ or $[w, u]$.

Let F_i denote the interior of the infinite face of the graph A_i . Now $F_1 \cap F_2$ consists of three regions none of which contain any vertices of G^* (otherwise G^* would be 2-connected). As in the case of 2-connected graphs, each of these regions has an empty intersection with G^* or is composed of two triangles. If all the twist-boxes contain at least two crossings then there must be edges $[u, v]$, $[v, w]$ and $[w, u]$ which form a 3-cycle in G^* . The three edges in G crossed by this 3-cycle must be all T-type edges, or be one T-type and two D-type. The two possibilities for D are shown in figure 2.13. If some twist-boxes contain a single crossing it is possible that some of the edges in the 3-cycle may be missing. As in the 2-connected case, these missing edges are equivalent to T-type edges except that the corresponding twist-box contains a single crossing.

We are now in a position to complete the proof. If $n \leq 8$ then the dual graph has at most 10 vertices. The hypotheses on the diagram mean that it is 3-connected and hence a Hamiltonian circuit must exist [B-J]. When $n > 8$ we must exclude the diagrams which give rise to 3-connected graphs. These are precisely those in figure 2.13. \square

Corollary 2.5.7 [C-N] *Let $L = L_1 \# L_2 \# \dots \# L_r$ be a connected sum of prime alternating links L_1, L_2, \dots, L_r , each of which satisfies the inequality $\alpha(L_i) \leq 2 + c(L_i)$. Then $\alpha(L) \leq 2 + c(L)$.*

Remark. As an example, corollary 2.5.7 applies when each of the L_i satisfies the hypotheses of proposition 2.5.2.

Proof of corollary 2.5.7. For alternating links, $c(L_1 \# L_2) = c(L_1) + c(L_2)$ [Kau2, Mu, Th3]. Also, from theorem 2.4.1, we have that $\alpha(L_1 \# L_2) = \alpha(L_1) + \alpha(L_2) - 2$.

Hence

$$\begin{aligned} \alpha(L) - 2 &= \sum_{i=1}^r (\alpha(L_i) - 2) \\ &\leq \sum_{i=1}^r c(L_i) \\ &= c(L). \end{aligned}$$

□

Corollary 2.5.8 [C-N] (i) *Let K be a prime knot with $c(K) \leq 10$. Then $\alpha(K) \leq 2 + c(K)$.*

(ii) *Let L be a prime link with $c(L) \leq 9$. Then $\alpha(L) \leq 2 + c(L)$.*

Proof. The diagrams of these knots and links in [Ro] satisfy the hypotheses of proposition 2.5.2. □

Corollary 2.5.9 [C-N] *If L is a 2-bridge link then $\alpha(L) \leq 2 + c(L)$.*

Proof. The curve shown in figure 2.20 can be made into a binding circle. □

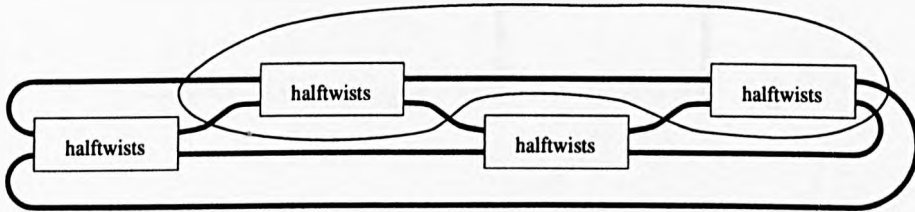


Figure 2.20: Schematic diagram of a 2-bridge link, with binding circle

The above discussion provides us with an upper bound for $\alpha(L)$ from $c(L)$, for ‘most’ links L . In section 4.5 we conjecture that this inequality holds for all knots K with equality if, and only if, K is an alternating knot. In the meantime we go on to explore a lower bound.

Proposition 2.5.10 [C-N] *Let L be a link; let $\alpha(L)$ be its arc index and $c(L)$ be its minimal crossing number. Then*

$$\alpha(L) \geq \begin{cases} 1 + \sqrt{1 + 4c(L)}, & \alpha(L) \text{ even} \\ 1 + \sqrt{4c(L)}, & \alpha(L) \text{ odd.} \end{cases}$$

Proof. Suppose that we have a minimal arc-presentation of L . Construct a grid diagram from this presentation.

We now consider how many times each of the horizontal lines can meet a vertical line. That is, how many arcs (vertical lines) cross over each loop. The topmost loop cannot cross any arcs but two arcs terminate here and these can cross other loops. The next loop down can be crossed by at most two arcs and is the source of at most two more. Continuing in this way we obtain the pattern shown in figure 2.21: the numbers by each loop indicate the maximum number of arcs which the loop can cross. The total is clearly a function of triangle numbers.

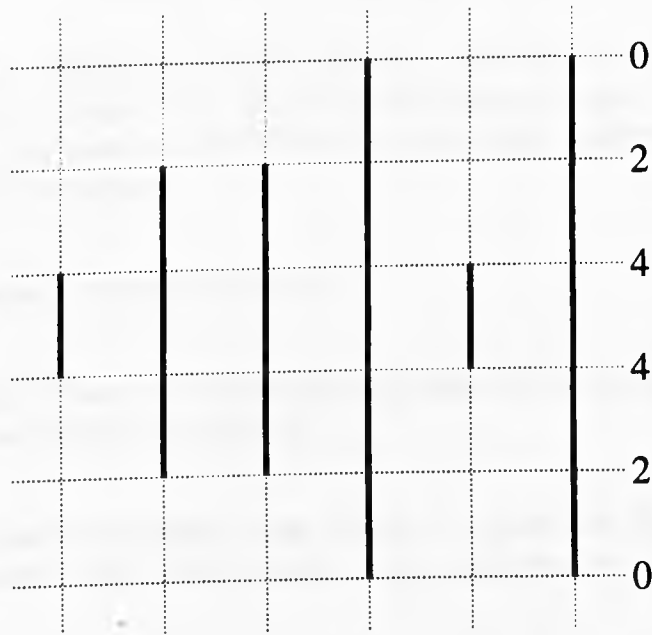


Figure 2.21: Counting the number of possible crossings in a grid diagram

The grid diagram is now converted into a conventional link diagram. To do this notice that each loop is divided naturally into two parts by the endpoints of two arcs. Choosing one part of each loop produces a diagram of L . We can choose the parts which minimise the number of crossings. So if a loop meets n arcs we can ensure that the loop contributes at most $\frac{n}{2}$ crossings to the diagram.

Let $\Delta(n) = \frac{1}{2}n(n + 1)$ denote the n th triangle number. If $\alpha(L)$ is even, let $m = \frac{1}{2}(\alpha(L) - 2)$. Then we see that $c(L)$ can be at most $2\Delta(m)$. If, on the other hand, $\alpha(L)$ is odd then let $m = \frac{1}{2}(\alpha(L) - 1)$: in this case we obtain $c(L) \leq \Delta(m) + \Delta(m - 1)$. Substituting for m in each case gives the desired inequalities. \square

Remark. This lower bound is achieved for the non-trivial $(p, p+1)$ -torus knots. For suppose we have $\alpha(L) \geq 2 + \sqrt{4c(L)}$, where $L = T(p, p+1)$, and hence $c(L) = p^2 - 1$ and $\alpha(L) \leq 2|p| + 1$. Then we can deduce $2|p| - 1 \geq 2\sqrt{p^2 - 1}$, and so after some computation, $|p| \leq \frac{5}{4}$. Hence $|p| \leq 1$, and L must be trivial.

2.5.III Homfly polynomial

Finally in this section, we make an observation on possible pairs of knots with identical Homfly polynomial. We employ the following result of Kanenobu.

Theorem 2.5.11 [Kan] *There exist infinitely many examples of infinitely many knots in S^3 (which are hyperbolic, fibred, ribbon, of genus 2 and 3-bridge), with the same Homfly polynomial and, therefore, the same Jones polynomial, but distinct Alexander module structures.*

Proof. The reader is referred to [Kan]. □

Corollary 2.5.12 *There exist infinitely many pairs of knots with the same Homfly polynomial and distinct arc indices.*

Proof. There exist only finitely many knots of a given arc index; therefore an infinite set of knots with a given Homfly polynomial cannot have a constant arc index. □

In chapter 5, we exhibit a pair of knots K_1, K_2 with $\mathcal{P}_{K_1} = \mathcal{P}_{K_2}$ and which can be distinguished by arc index; we also show that a famous pair of mutant knots, which necessarily have identical Homfly polynomial, also have identical arc index. The questions should then be posed of whether arc index is related to Alexander module structure, and whether there exist any pairs of mutant links with distinct arc index. As Kanenobu's result suggests, examination of the Alexander module structure may be a useful starting point in attacking this problem.

There is also a question of whether any similar result relating to the Kauffman polynomial is realistic.

Chapter 3

Satellite links as closed braids

3.1 Motivation

In their series of papers [B-M1, ..., B-M7], Birman and Menasco study links through the medium of closed braids. In particular in [B-M4], they consider the effects on braid index of the geometric operations of distant union and connect sum. They define a *split braid* and a *composite braid* to be one which is ‘obviously’ split or composite. Figure 3.1 illustrates what is meant.

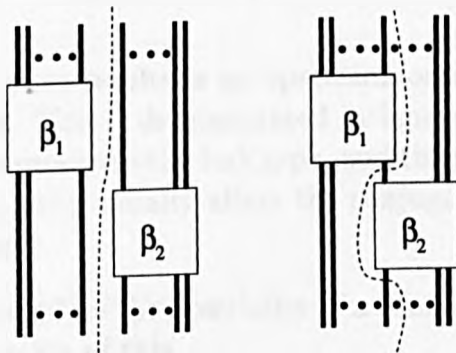


Figure 3.1: A split braid and a composite braid

Then Birman and Menasco's results from [B-M4] are summarized as follows.

Theorem 3.1.1 [B-M4] *Let L be a split (resp. composite) link, and let $\hat{\beta}$ be an arbitrary closed n -braid representative of L . Then there exists a split (resp. composite) n -braid $\hat{\beta}'$ which represents L and a finite sequence of closed n -braids*

$$\hat{\beta} = \hat{\beta}_0 \rightarrow \hat{\beta}_1 \rightarrow \dots \rightarrow \hat{\beta}_s = \hat{\beta}',$$

such that each $\hat{\beta}_{i+1}$ is obtained from $\hat{\beta}_i$ by either isotopy in the complement of the axis or an exchange move (figure 3.2). \square

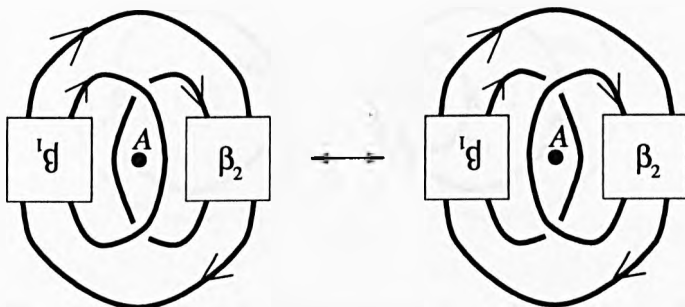


Figure 3.2: Exchange move

Corollary 3.1.2 [B-M4] *Braid index is additive (resp. additive minus one) under the operation of distant union (resp. connected sum). \square*

Central to proving these results is an operation on closed braids which they call the *exchange move*. This is demonstrated in figure 3.2. It should be noted that the exchange move preserves the link type, and the number of braidstrings of the braid presentation, but generally alters the conjugacy class of the presented braid in the braid group.

It is natural then to explore the possibility of a similar result for satellite links. What follows is a discussion of this.

3.2 Braid index of satellites: types 0 and 1

In [B-M7], Birman and Menasco attempted to find a formula for braid index of a general satellite L , from geometric features of the pattern and companion. Their approach, comparable with their work of [B-M4], is to examine the position of an essential torus $T = \partial V$ which lives in $S^3 - L$. Before stating this result we first

prove a lesser result, based on the same idea, which was proved independently of [B-M7].

It turns out that an important property of the pattern is the existence of, or lack of, a meridional disc D of V whose intersections with the oriented satellite are all identically oriented. If such a disc D exists then the pattern P fits into one of two types (illustrated in figure 3.3), according as to whether or not it winds monotonically around the longitude of V_P .

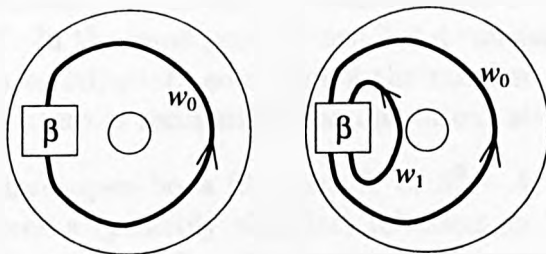


Figure 3.3: Standard patterns, type 0 and type 1

Type 0 has this ‘longitudinal braiding’ property, type 1 does not. The following theorem is a discussion of the position of the essential torus $T = \partial V_C$ in $S^3 - L$ when L is a satellite with a type 0 or type 1 pattern.

Theorem 3.2.1 *Let L be an oriented satellite link, and $\hat{\beta}$ be an n -braid presentation of L (relative to braid axis A). Suppose that $T = \partial V$ is an essential non-peripheral torus in $S^3 - \hat{\beta}$, such that $\hat{\beta}$ is contained in the solid torus V . Suppose also that there exists a meridional disc D of V such that each intersection point of $\hat{\beta} \cap D$ has the same sign, i.e. $\hat{\beta}$ intersects D transversely always from the same side of D . Then there exist*

(i) *a closed n -braid $\hat{\beta}^*$ which represents L ;*

(ii) *a finite sequence of closed n -braids*

$$\hat{\beta} = \hat{\beta}_0 \rightarrow \hat{\beta}_1 \rightarrow \dots \rightarrow \hat{\beta}_r = \hat{\beta}^*$$

such that each $\hat{\beta}_i$ is obtained from $\hat{\beta}_{i-1}$ by isotopy in $S^3 - A$, or by an exchange move; and

(iii) *an essential non-peripheral torus $T^* \subset S^3 - \hat{\beta}^*$ such that $|T^* \cap A| = 0$ or 2 . Further, the pattern of L is a type 0 or type 1 pattern, respectively.*

Proof. The proof is adapted from the proof of theorem 3.1.1, the main result of [B-M4]. The four lemmas that form part of this proof are analogous with the lemmas of the [B-M4] proof.

We have a satellite link L , which is the closure of a braid β , braided with respect to a braid axis A in S^3 . We are also given an essential torus T which realizes the satellite construction: T bounds a solid torus V on one side, with L completely contained in the interior of V . There is an orientation on L ; we assign an orientation to A so that L is oriented in the positive sense about A . We also assign an orientation to T , so that at each point of T there is a well-defined outward normal to T . In the most general case $T \cap A$ consists of many points; the aim, as in [B-M4], is to adjust L , so reducing the number of intersection points of $T \cap A$, until the pattern is recognizable as one of our standard forms.

We use the standard open-book fibration H of $S^3 - A$, with fibres $\{H_t : 0 \leq t < 2\pi\}$. This induces a (possibly singular) foliation on T : its leaves are the components of $T \cap H_t$, $0 \leq t < 2\pi$. Standard position arguments allow T to be placed in a nice position relative to H . Thus we may assume:

- (1) The intersections of A with T are finite in number, and transverse.
- (2) There is a solid torus neighbourhood $N(A)$ of A in $S^3 - L$ such that each component of $T \cap N(A)$ is a disc.
- (3) The foliation of each component of $T \cap N(A)$ is the standard radial foliation.
- (4) All but finitely many of the fibres H_t meet the torus T transversely, and those which do not (the *singular fibres*) are tangent to T at exactly one point in the interior of H_t .
- (5) The tangencies mentioned in (4) are local maxima or minima or saddle points.

A *singular leaf* in the foliation is one which contains a singular point; the other leaves are *non-singular*. The following observations can be made from (4) and (5):

- (i) Each non-singular leaf is either an arc with its endpoints on $A = \partial H_t$, or a simple closed curve (hereafter abbreviated to SCC).
- (ii) A singular fibre H_θ contains exactly one singularity.
- (iii) Each singularity p_θ is either a centre or a saddle.

As in [B-M1, B-M4], given a surface F , a complexity function on the pair (F, H) is defined as follows. Let $|F \cap A|$ be the number of point intersections of F with A . Let $|H \cdot F|$ be the number of singular points in the foliation of F . The complexity $c(F, H)$ is the pair $(|F \cap A|, |H \cdot F|)$, with a standard lexicographic ordering on the function. We follow [B-M4] by saying that (F, H) is *equivalent* to (F', H) if there is an isotopy taking F to F' which takes $(F \cap H_t, F \cap \partial H_t)$ to $(F' \cap H_t, F' \cap \partial H_t)$, for each $t \in [0, 2\pi]$. This definition of equivalence ensures that each representative of an equivalence class has the same complexity.

A non-singular leaf (a component of $T \cap H_t$) naturally splits the fibre H_t into two components Δ and Δ' . At least one of these components Δ , Δ' is a 2-disc. If Δ (or Δ') is a 2-disc component of H_t , and *also* has empty intersection with L , then we say that the leaf $T \cap H_t$ is *inessential*; otherwise we say that $T \cap H_t$ is *essential*. See figures 3.4 and 3.5. This definition is the first real departure from [B-M4].

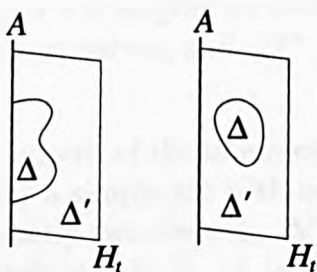


Figure 3.4: Possible occurrences of Δ and Δ' on H_t

Now we investigate the presence and nature of SCCs in $T \cap H$. Say that the pair $T \cap H$ has *SCCs* if there exists a non-singular fibre H_t such that a component of $T \cap H_t$ is a SCC.

Lemma 3.2.2 *Suppose that (T, H) satisfies the general position assumptions (1)–(5) and has inessential SCCs. Then there exists a torus T' such that (T', H) also satisfies (1)–(5) and has no inessential SCCs; moreover, $c(T', H) < c(T, H)$.*

Proof. The proof of this lemma is exactly the same as the proof given in [B-M4], and applies to a disc which is contained in the surface.

Suppose there is an inessential SCC $\gamma(t)$ in $T \cap H_t$, for some non-singular H_t . Follow $\gamma(t)$ as it evolves in the fibration; eventually we arrive at some closed curve $\gamma(\theta)$ which contains a singularity in the foliation. The curve $\gamma(\theta)$ lies on

the fibre H_θ , and bounds a disc Δ in H_θ . The loop $\gamma(\theta)$ is inessential, since $\gamma(t)$ is inessential and L is braided around $A = \partial H_t$.

If $\gamma(t)$ winds meridionally around T then $\gamma(t)$ is necessarily essential, since T is an essential torus. If $\gamma(t)$ winds longitudinally around T then H_t must split V longitudinally into two tori V_1 and V_2 ; since L is braided around A then L intersects H_t always from the same side, so any component of L is completely contained either in V_1 or V_2 . The link L is hence a distant union of the sublinks $L_1 = L \cap V_1$ and $L_2 = L \cap V_2$. By corollary 3.1.2 (braid index under distant union) we consider each of these sublinks separately. Therefore, we can assume that $\gamma(t)$ is null-homotopic on T , and hence $\partial\Delta$ is null-homotopic on T .

If $(\text{int}\Delta) \cap T = \emptyset$ then we can surger T along Δ , giving an essential torus T' and a 2-sphere S' . The sphere S' splits S^3 into two 3-balls B_1, B_2 : if $T' \subset B_1$ then $L \subset B_1$ so that $L \cap B_2 = \emptyset$. Therefore, we can remove S' without loss. Moreover, the complexity has not been increased. If $(\text{int}\Delta) \cap T \neq \emptyset$ then we find an innermost subdisc δ of Δ whose boundary is a component of $T \cap H_\theta$ and we surger T along δ . Ultimately we will acquire an essential torus T^* whose induced foliation has no inessential closed curves, and $c(T^*, H) < c(T, H)$. \square

By lemma 3.2.2, each component of the intersection of a non-singular H_t with T is either an essential SCC or a simple arc with both ends on $A = \partial H_t$. In the latter case, $T \cap H_t$ bounds exactly two discs Δ, Δ' on H_t . At most one of these discs, say Δ , is completely contained in V . If, in that case, $\Delta \cap L = \emptyset$ then we can push T inward along a 3-space neighbourhood of Δ to remove two points of $A \cap T$. (See figure 4 of [B-M4], reproduced in figure 3.5.) Any added SCCs are removed by lemma 3.2.2.

Our definition of essential leaves allows an adjustment in our general position assumptions, as follows:

(5a) The tangencies in (4) are saddle points.

(6) If H_t is non-singular then each component of $T \cap H_t$ is essential.

We continue to follow the proof of [B-M4]. The torus T is a closed surface, and A pierces T transversely each time, so $A \cap T$ must consist of an even number of pierce-points, say 2μ of them.

If $2\mu = 0$ then $A \cap T = \emptyset$. By hypothesis, there exists a meridional disc D of T whose intersections with L have identical sign. By a small isotopy we can assume that D lies in a fibre of H_t . This is enough to show that the core of T is braided around A ; for otherwise there exists a fibre H_t which is tangent to T yielding a

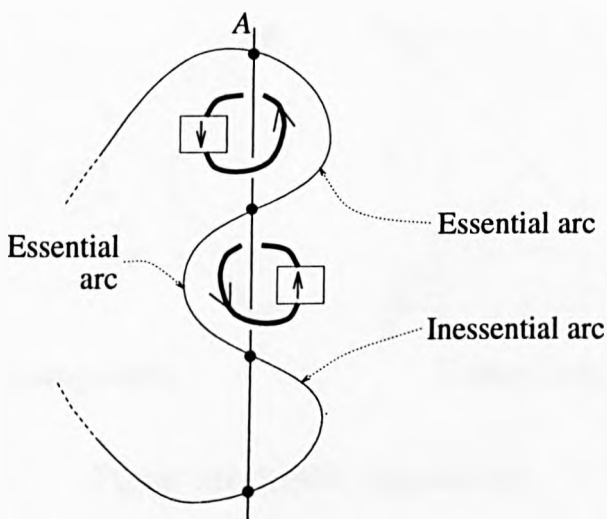


Figure 3.5: Fig. 4 of [B-M4]

centre tangency on the foliation of T , because $A \cap T = \emptyset$: this contradicts general position assumption (5a).

Since, in this case, T is braided around A , each H_t has the same number of (SCC) intersections with T . Each SCC is essential, by lemma 3.2.2. Since L is braided around A , each SCC bounds a disc D such that $D \cap L$ consists of w_0 points, for some constant $w_0 > 0$. Each disc is a meridional disc of T , and T has a non-singular foliation in which each leaf is a meridional loop. Therefore, P has the form of a type 0 pattern, as in figure 3.3.

Now suppose that $2\mu > 0$. Each non-singular leaf of $T \cap H_t$ is either an arc which joins two of the 2μ points of $A \cap T$, or an essential SCC. By general position assumption (3), and the fact that $2\mu \geq 2$, there must be singularities in the foliation of T . Each singularity is assumed to be a saddle. See figure 3.6.

There are two kinds of singularity. The first are those caused by an SCC surgered with an arc, which we call α -singularities, because the singular leaf has the topology of an ' α '. The second are caused by surgering an arc with another arc: these are called X-singularities, because the singular leaf has the topology of an 'X'. A third possibility, that of surgering two SCCs, cannot occur. (If an SCC surgers into two SCCs, both of which are essential, then either one of them is not meridional, and leads to a centre singularity, or both are meridional, which contradicts the topology of the torus.)

Let $p_1, p_2, \dots, p_{2\mu}$ be the points of $A \cap T$. Let $\theta_1, \theta_2, \dots, \theta_q$ be the t -values

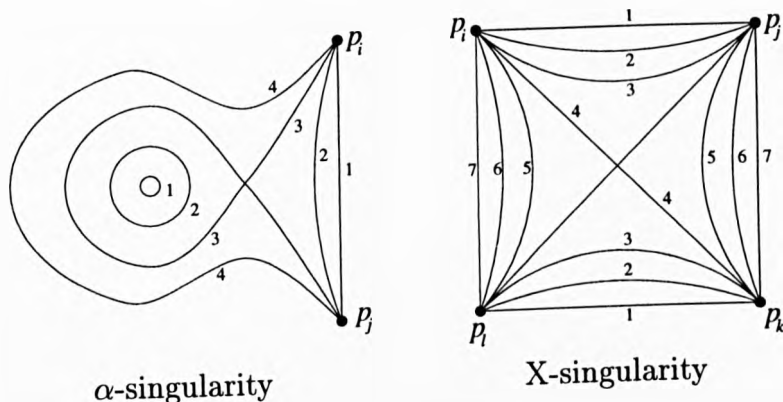


Figure 3.6: Saddle singularities

at which the singularities of the foliation occur. A singular leaf is then one of the components of $T \cap H_\theta$, for $\theta \in \{\theta_1, \dots, \theta_q\}$. The proof now leans towards the case in [B-M4] in which they consider a connected sum of two links. We adapt the situation slightly to fit our context. The idea is to reduce the number of intersections of A with T .

Choose a pair of α -singularities which are consecutive in the foliation of the torus. Either these singular leaves are separated only by leaves which are SCCs, or else there is a more complicated foliation involving points of $A \cap T$ and arc-leaves. Let our pair of α -singularities satisfy the second description. We surger T along the discs bounded by our α -singularities, to give two 2-spheres, S and S' . See figure 3.7. One of them, S' say, is now foliated, near the surgeries, by SCCs, leading to local centre singularities. The other, S , is foliated, near its surgeries, by arcs with ends on A . In what follows we will work with the foliation of S .

The 2-sphere S has an even number of point intersections with A , say $2\mu' \leq 2\mu$ of them. The foliation is one of arcs only, and each saddle singularity is an X-singularity. Then the complement in S of the singular leaves is a union of regions R_i , each with 4 edges belonging to singular leaves.

Choose one (non-singular) leaf e_i from each R_i . The union of all these leaves $\{e_i\}$ gives a cell decomposition of S ; the 0-cells are the point intersections $A \cap S$, the 1-cells are the subset $\{e_i\}$ of the non-singular leaves, and each 2-cell contains exactly one singularity of the foliation. Every 2-cell has four vertices and four edges (see figure 3.8, for example). We call our 2-cells *tiles*, and the cell decomposition a *tiling*.

We can choose the tiling so that all the point intersections of L with S occur in two tiles, the so-called 'end' tiles that were constructed from the surgery of T .

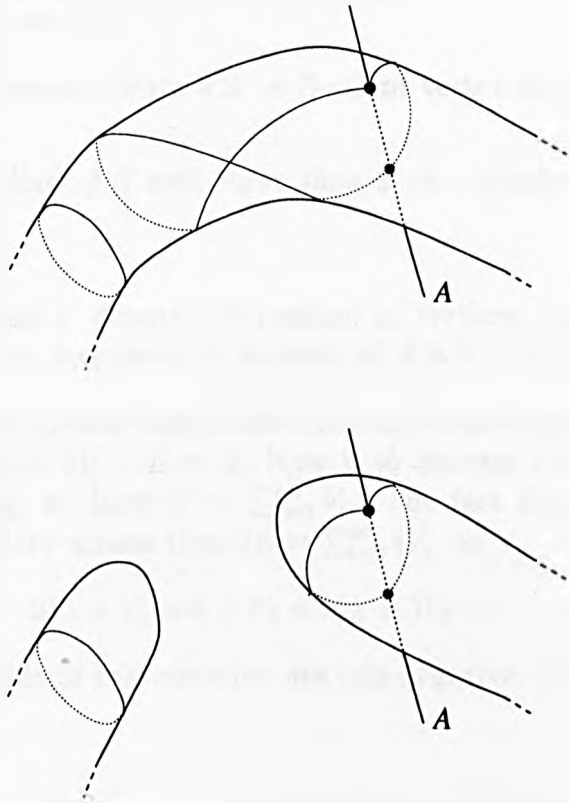


Figure 3.7: Surgering along an SCC



Moreover, the intersections of L with one of these tiles are derived from a number of parallel strings which are all travelling together, in an arbitrarily tight bunch, around A . They can therefore be treated as a single weighted string.

Following [B-M4], we define the *sign* of a tile. Each tile contains exactly one singularity of the foliation, at which T is tangent to a fibre H_θ . At such a tangency the normals of T and H_θ coincide. The orientations of these normals will either agree or disagree; the sign of the tile is accordingly *positive* or *negative*.

A vertex in the tiling is *r-valent* if it has exactly r tile-edges meeting at the vertex. Notice that an r -valent vertex is adjacent to exactly r regions and r tiles: this point will be of use later.

We show that there is always a 2- or 3-valent vertex in the tiling of S .

Lemma 3.2.3 *A tiling of S with more than 2 tiles always contains a 2- or 3-valent vertex.*

Proof. Let V , E and F denote the number of vertices, edges and tiles in the tiling of S . The Euler characteristic formula of S is $V - E + F = 2$.

Each tile has exactly four edges, and each edge is an edge of exactly two tiles, so $2F = E$, and hence $2V - E = 4$. Now if V_i denotes the number of i -valent vertices in the tiling, we have $V = \sum_{i=2}^{\infty} V_i$. The fact that each edge has two vertices in its boundary means that $2E = \sum_{i=2}^{\infty} iV_i$, so

$$2V_2 + V_3 = 8 + V_5 + 2V_6 + 3V_7 + \dots$$

The terms on each side of this equation are non-negative, and hence there is a 2- or 3-valent vertex. □

We can assume that S has non-null intersection with L , for otherwise T would be an inessential torus. Call a tile of S *good* if it is not pierced by L .

Now we can assume (a small isotopy will oblige us) that the points of $L \cap S$ lie in the complement of the set of singular leaves, that is in regions R_i . Call a region of S *bad* if it is pierced by L . We can isotop parallel strings as a single weighted string, to conclude that there exist at most two bad regions of S (namely the 'end' regions of S .) We can assume that the pierce-points also inhabit the same tile: a different choice of tile edge (as in figure 3.8) will ensure this.

Call a vertex *good* if it is adjacent only to good regions.⁶ A region is adjacent to exactly two vertices, so there are at most four bad vertices.

⁶This is another departure from [B-M4], which defines good vertices in terms of good tiles.

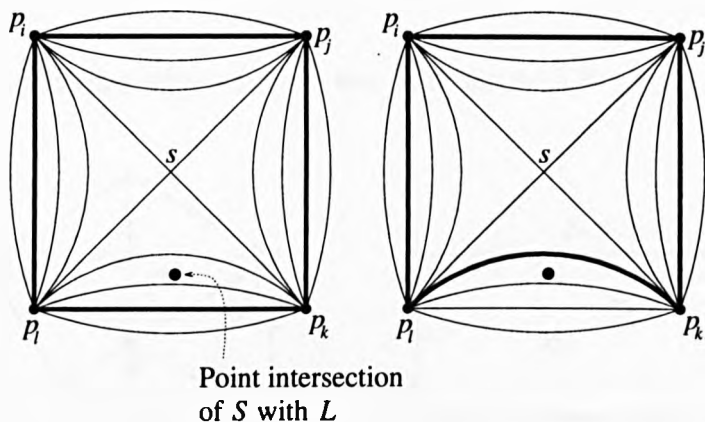


Figure 3.8: Redefining the tile edges

The next lemma discusses the existence of (possibly good) 2-valent vertices.

Lemma 3.2.4 *Either the tiling of S has a 2-valent vertex, or else there is an isotopy of S to a new 2-sphere S^* , such that the tiling of S^* has a good 2-valent vertex. Moreover, the tiles which intersect L are undisturbed by the isotopy, and the torus T^* obtained by replacing S with S^* has $c(T^*, H) \leq c(T, H)$.*

Proof. Suppose there is no 2-valent vertex in the tiling of S . Then by lemma 3.2.3 there exists a 3-valent vertex, p , which is adjacent to exactly 3 tiles. Each tile contains exactly one saddle singularity; necessarily, at least two of the three singularities (say s and s') have the same sign. We show that there is an isotopy of S which swaps the order of the two singularities s and s' in the foliation: the result reduces p to a 2-valent vertex.

We assume, to begin, that the tiles adjacent to p are all good tiles: they are not pierced by L . The argument for this runs as follows. Recall that a region (bounded by singular leaves, and foliated by non-singular leaves) is said to be *bad* if it is pierced by L . By construction there are at most two bad regions; since each region is adjacent to two vertices then there can be no more than four vertices which are adjacent to a bad region. Since there are no 2-valent vertices, then (from the proof of lemma 3.2.3) $V_2 = 0$ implies $V_3 \geq 8$, so we can find a 3-valent vertex p which is not adjacent to a bad region. If a tile adjacent to p has intersection with L then it belongs to a region which is not adjacent to p . The tile can be redefined by choosing a different edge for the tile, which excludes the intersection from the tile, though not the region. See figure 3.8.

The proof of the lemma continues as in [B-M4], and we present only a summary here.

The three good tiles adjacent to p are as in figure 3.9.

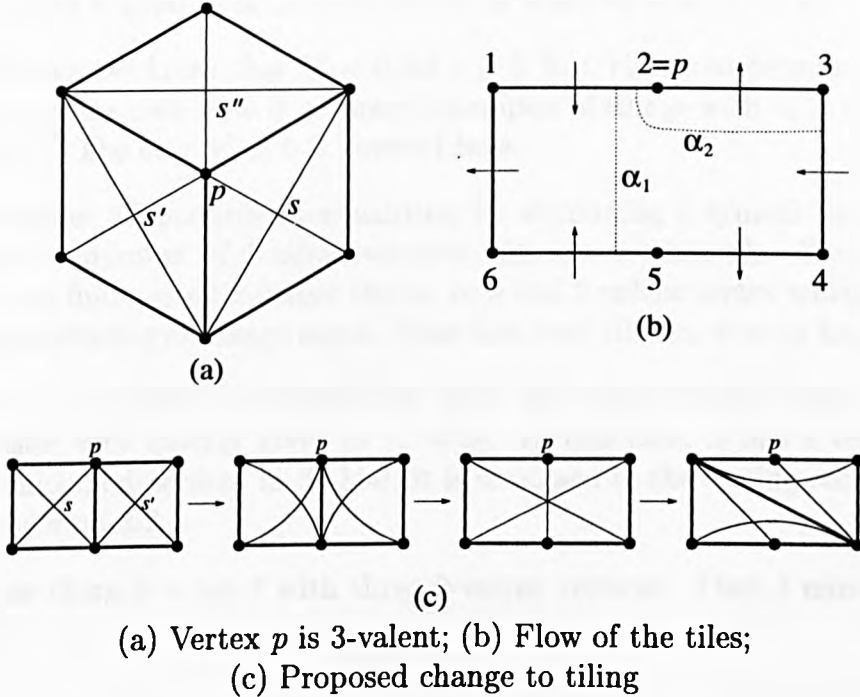


Figure 3.9: Fig. 8 of [B-M4]

Birman and Menasco reconstruct the surface around the singularities s and s' , from analysis of the foliation. They show that the surface can be isotoped so that the singularities appear in the opposite order in the foliation. The resulting change in the foliation gives the required end.

The final observation is that the change of foliation occurs only in two tiles, and the foliation in the remainder of S is unchanged. In particular this means that we can reconstruct T from the refoliated 2-sphere because the isotopy occurs away from the bad tiles: we simply undo the surgery that created S in the first place. The foliation of T is as it was, except that it inherits the change in the two tiles performed on S . Since (by [B-M4]) the complexity of S was not increased, the complexity of T is also not increased. \square

Lemma 3.2.5 *If the tiling of S contains more than two tiles, and also contains a 2-valent vertex p , then L admits an exchange. Further, after the exchange we can remove points of $A \cap T$, thus reducing the complexity.*

Proof. We consider first the case when p is not good. Recall that V_i denotes the number of i -valent vertices in the tiling. There are at most four bad vertices, so if $V_2 + V_3 \geq 5$ then we can always find a good 2- or 3-valent vertex (and hence a good 2-valent vertex, via lemma 3.2.4). Assume $V_2 + V_3 \leq 4$, and hence $V_2 \leq 4$. We know $V_2 + (V_2 + V_3) \geq 8$, and so $V_2 \geq 4$; so the only case when we might not be able to find a good 2- or 3-valent vertex is when $V_2 = 4$, $V_3 = 0$.

In this case we know that $V_i = 0$ for $i \geq 5$, but V_4 is undetermined. [B-M4] discusses only the case $V_4 = 0$, although examples of tilings with $V_4 > 0$ are easily constructed.⁷ The case $V_4 > 0$ is covered here.

We consider all possible eventualities, by examining a typical tile t , and in particular the number of 2-valent vertices adjacent to that tile. We show that either we can find a good 2-valent vertex, or a bad 2-valent vertex which admits a complexity-reducing exchange move. Note that each tile has exactly four vertices.

If t has four 2-valent vertices, then there are only two tiles (and the Euler characteristic very quickly gives us $V_4 = 0$). In this case, S has a very special position which is described in [B-M4]; it is discussed in the closing section of the proof of theorem 3.2.1.

Suppose there is a tile t with three 2-valent vertices. Then t must be as in figure 3.10.

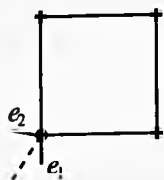


Figure 3.10: Tile with three 2-valent vertices

Necessarily there is another tile t' which has the same three 2-valent vertices. By assumption, t' has only four vertices; the fourth is the r -valent vertex ($r > 2$) adjacent to t . Using the notation of lemma 3.2.3, we have $2V_2 + V_3 = 8 + V_5 + 2V_6 + 3V_7 + \dots$, and since $V_2 = 4$, $V_3 = 0$ we can deduce that $V_i = 0$, $i \geq 5$ and so $r = 4$. Then e_1 , e_2 are different edges, and therefore t' has at least six edges. This contradicts the assumption that every tile has exactly four edges and vertices.

Suppose every tile has at most one 2-valent vertex. Each of the 2-valent

⁷I am grateful to Joan Birman and Bill Menasco for private communications concerning this point.

vertices is adjacent to exactly two regions, each of which is adjacent to an r -valent vertex ($r > 2$) at its other end (because each tile, and therefore each region, is adjacent to at most one 2-valent vertex). Since there are at most two bad regions, there are at most two bad 2-valent vertices, and hence at least two good 2-valent vertices.

We are left with the case when there is at least one tile t with two 2-valent vertices. There are two possibilities for such a tile; these are illustrated in figure 3.11.

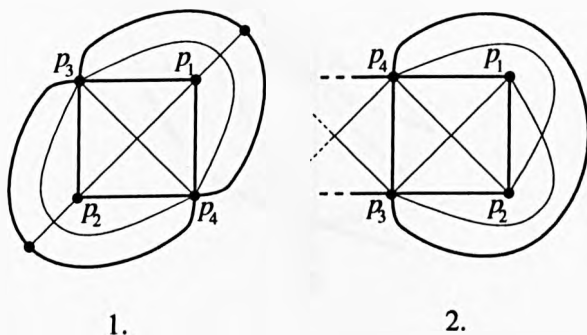


Figure 3.11: Tiles t with two 2-valent vertices

(Note: If a vertex is adjacent to a bad region then it is necessarily adjacent to a bad tile. The reverse is not true.)

There are two cases.

1. If p_1 and p_2 are both adjacent to a bad region, then choose tile edges in the bad regions so that the pierce-points are contained in t . This is enough to ensure that the other two 2-valent vertices are both good.

Otherwise, p_1 (say) is not adjacent to a bad region, and so by definition, p_1 is a good 2-valent vertex.

2. By hypothesis, each leaf in the foliation of S is essential, so L is an obstruction to its removal. Figure 3.12, illustrating the embedding of part of S , may be compared with figure 21 of [B-M4].

Since the leaves are essential, L encircles the axis $n \geq 1$ times between p_1 and p_2 , and also $m \geq 1$ times between p_3 and p_4 , inside S ; also $j \geq 1$ times between p_2 and p_3 , outside S . There is also the possibility of L piercing S in one or more places of the regions adjacent to p_1, \dots, p_4 . See figure 3.13.

Clearly, an exchange move is applicable, moving the n strings across the j strings, down so that they encircle A between p_3 and p_4 . Then the leaves

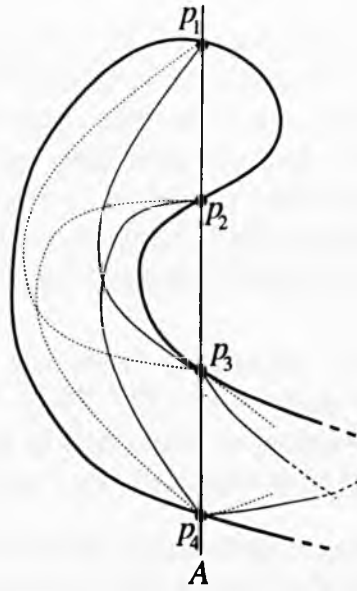


Figure 3.12: Embedding of S near the 2-valent vertices

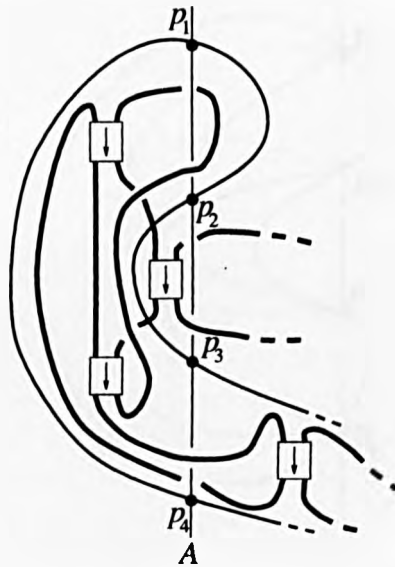


Figure 3.13: Embedding of part of L , relative to S

joining p_1 to p_2 are inessential, and can be removed, reducing the complexity by removing two points of $A \cap S$.

If p is good then the proof is as in lemma 4 of [B-M4]. (In this they explicitly describe the position of the sphere S relative to L , and show that an exchange move is applicable.) In this case, the only extra point to note is that, because p is good, all the action occurs away from the bad tiles of S : we can assume that the relevant tiles are all good by redefining some tile edges (as in figure 3.8) if necessary. Therefore, we can reconstruct T after application of lemma 3.2.5. The reduction in complexity of the foliation of S implies a reduction in $c(T, H)$. \square

Now we can complete the proof of theorem 3.2.1. The essential torus T has complexity $c(T, H) \geq (0, 0)$. The case when the complexity is $(0, 0)$ was considered at the beginning of this proof, so assume $c(T, H) > (0, 0)$. Therefore, $A \cap T \geq 2$, so necessarily there are singularities in the foliation.

We take pairs of α -singularities as described, surgering to form a sphere S , and repeatedly applying lemmas 3.2.3, 3.2.4 and 3.2.5 until S has just four 2-valent vertices in its foliation. Then S is the union of exactly two tiles, each of which has a saddle singularity. At least one of them is bad. Following the observation of [B-M4], the sphere has the form of figure 3.14.

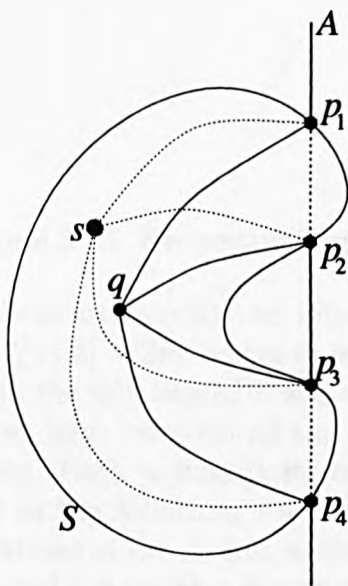


Figure 3.14: Fig. 21 of [B-M4]

If there is a good vertex, then a complexity-reducing exchange move is applicable, as described in [B-M4]. If there is no good vertex then all four 2-valent

vertices are bad, and we know that S is pierced by L in two ‘opposite’ regions, R_1 and R_3 say. This case is covered in pages 135–137 of [B-M4]. The position of S relative to A and L is deduced, and it is shown that an exchange move is possible, and that two more points of $A \cap S$ can be removed. This is done, in their words, by ‘sliding’ strings of L so that the pierce-points $L \cap R_3$ slide into R_2 , and a good 2-valent vertex is created.

The 2-sphere S now has a non-singular (North–South) foliation whose leaves are simple arcs with both ends on A . We can reconstruct T from S by reconstructing the α -singularities at either ‘end’ of S from some choice of non-singular arcs of S , and performing the inverse surgery. See figure 3.15.

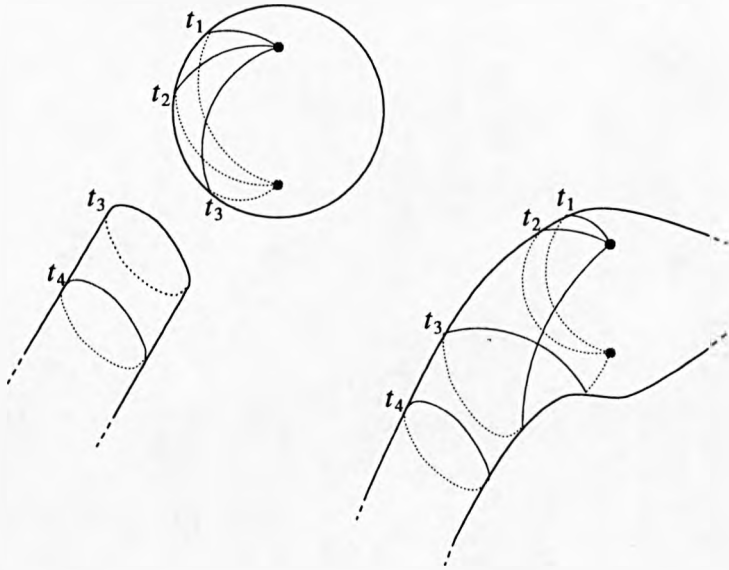


Figure 3.15: Reconstructing T

So we can assume that there are exactly two intersection points of A with T for each sphere S . We write $|T \cap A| = 2m$, where m is the number of 2-spheres S . Recall that each singularity in the foliation of T was either an α -singularity or an X-singularity: at this stage we have removed all the X-singularities, so there are only α -singularities remaining. Each α -singularity corresponds to the surgering of an SCC with an arc-leaf in the foliation; the only arc-leaves remaining are those inherited from the foliations of the S , and so the α -singularities correspond to the fusing of an SCC-foliated tube with a 2-sphere S . They must occur as in figure 3.15, and so we can deduce that there are $2m$ singularities: the complexity is $c(T, H) = (2m, 2m)$.

If $m = 1$ then the fact that each leaf is essential allows us to see that the pattern has a type 1 foliation, and is as claimed. If $m > 1$ then the essentiality

of the leaves allows us to construct part of the torus, together with four points of $A \cap T$, as in figure 3.16.

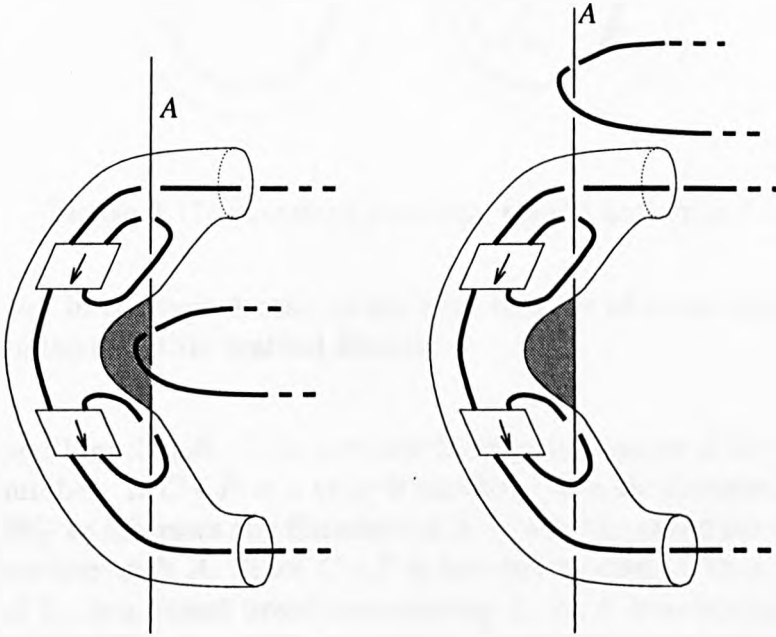


Figure 3.16: Part of the torus relative to L and A

In particular, note that by assumption, the leaf boundary of the shaded disc is essential, and so the disc itself has non-empty intersection with L . An exchange move will remove that intersection (as illustrated in figure 3.16), and so we can isotop T in a 3-space neighbourhood of the disc to remove two intersections of A with T , hence reducing the value of m and the complexity $c(T, H)$. This step is repeated until $m = 1$, and the proof of theorem 3.2.1 is complete. \square

Corollary 3.2.6 *Let $C * P$ be a type 0 or type 1 satellite, constructed by embedding a type 0 or type 1 pattern $P \subset V_P$ into the torus neighbourhood V_C of companion knot C . Then $C * P$ has braid index*

$$b(C * P) = \begin{cases} b(C).w_0 & (\text{type 0}) \\ b(C).w_0 + w_1 & (\text{type 1}) \end{cases}$$

where w_0, w_1 are the minimum weights of the strings as shown in the pattern P (figure 3.17), and $b(C)$ is the braid index of the companion.

Remark. The significance of w_0, w_1 in the diagrams is as follows. The integer w_0 is the least number of intersections $P \cap D$, over all meridional discs $D \subset V_P$.

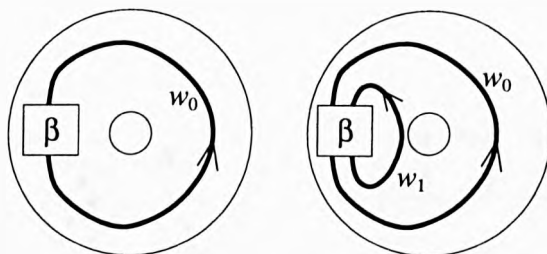


Figure 3.17: Standard patterns, type 0 and type 1

The integer w_1 , in the type 1 case, is the least number of extra strings needed to present the pattern in this braided format.

Proof of corollary 3.2.6. Take a closed braid presentation $\hat{\beta}$ of $C * P$, of minimal braid number. If $C * P$ is a type 0 satellite, then by theorem 3.2.1 we can move $T_C = \partial V_C$ to intersect the fibration of $S^3 - A$ in the standard way. Thus T_C has no intersection with A . Since $C * P$ is braided around A , then so is V_C , and so the core of V_C is a closed braid representing C , on b' braidstrings. Therefore, each page H_θ of the fibration H has exactly $b' \cdot w_0$ intersections with $C * P$. By the minimality of $b(C)$, we have $b' \geq b(C)$. If $b' > b(C)$ then an isotopy of the core of V_C in S^3 gives a presentation of C on fewer braidstrings. The same isotopy applied to V_C preserves both $C * P$ and its braidedness about A , and so gives a presentation of $C * P$ on fewer braidstrings. Thus, we can assume $b' = b(C)$. A diagram for a braid presentation of $C * P$ is shown in figure 3.18.

If $C * P$ is a type 1 satellite, then by theorem 3.2.1 we may assume A intersects T_C in precisely two points. Then a typical fibre H_θ has b' clusters of w_0 intersections, along with one cluster of w_1 intersections. The two ways that this can happen in a non-singular fibre are illustrated in figure 3.19. Then, by the same argument, $b' = b(C)$. \square

3.3 Reverse string satellites

In fact, Birman and Menasco have provided a more complete result than theorem 3.2.1, by identifying another class of patterns. The same method of proof is employed.

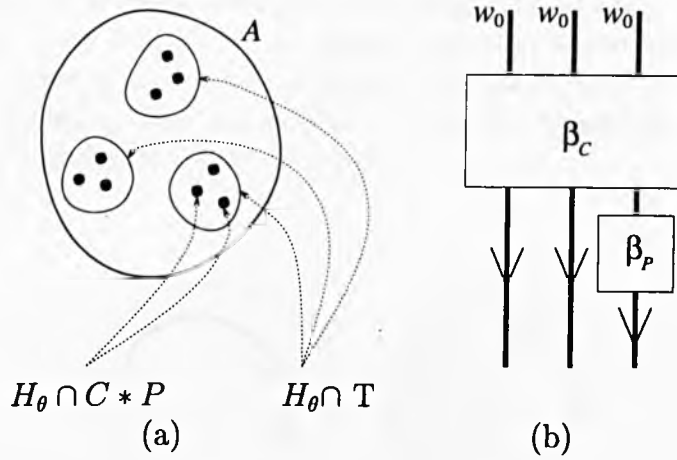


Figure 3.18: (a) A typical fibre H_θ with $C * P$ -intersections; (b) Braid presentation for $C * P$ from C and P

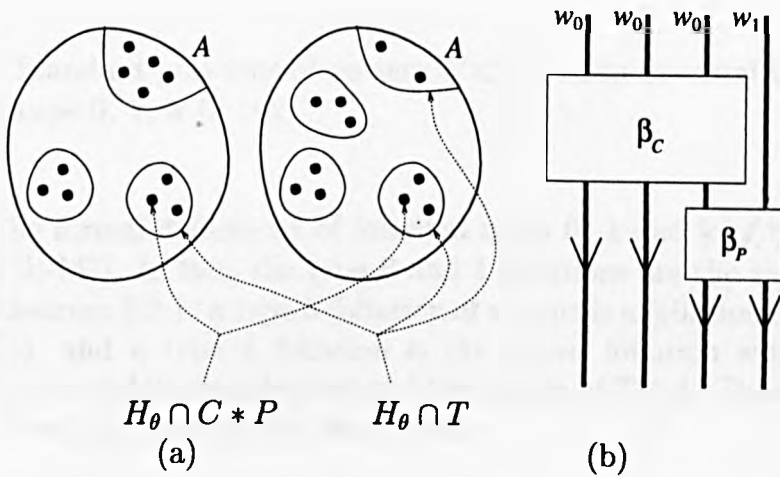


Figure 3.19: (a) Typical fibres H_θ with $C * P$ -intersections; (b) Braid presentation for $C * P$ from C and P

Theorem 3.3.1 [B-M7] *Let T be an essential, non-peripheral torus in $S^3 - L$, where L is a link which is represented as a closed braid relative to the braid axis A and fibration H . Assume that T has type **0**, **1** or **k** foliation. Let V be the solid torus which T bounds, where in the situation of type **0**, if T bounds on both sides we choose V so that $A \cap V$ is empty. Then the inclusion of $(L \cup A) \cap V$ in V in the three cases is as depicted in figure 3.20. Here, each component of $A \cap V$ is an arc, illustrated in these projections as a point. In particular, the number of such arcs is 0, 1 and k in the three cases. \square*

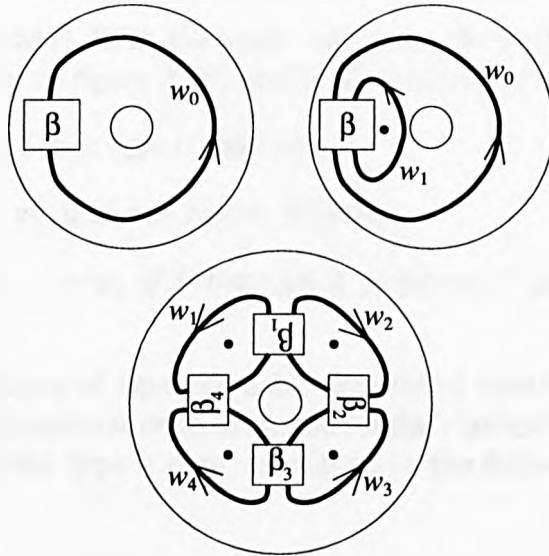


Figure 3.20: Standard positions of pattern $P \subset V_P$ when essential torus $T = \partial V$ has foliation type **0**, **1**, **k** ($k > 2$)

Remark. The formal definitions of foliation types **0**, **1** and **k** of theorem 3.3.1 are found in [B-M7]. In fact, the type **0** and **1** foliations are the torus foliations deduced by theorem 3.2.1: a type **0** foliation of a torus is a foliation by meridional circles (SCCs), and a type **1** foliation is the mixed foliation with SCCs and essential arcs, two saddle singularities and two points of $T \cap A$. These correspond to the type **0** and type **1** patterns respectively.

The type **k** foliation occurs in the case when every meridional disc of T intersects the satellite link L , with both positively *and* negatively oriented intersections. The foliation is a singular foliation in which each nonsingular leaf is a simple arc with its endpoints on A . In their proof of theorem 3.3.1, Birman and Menasco show that the foliation on T in this case induces a tiling of T , in which each 2-cell consists of four edges and contains exactly one saddle singularity; the

0-cells are the points of $T_C \cap A$ and the 1-cells are some choice of non-singular leaves. They go further, deducing from restrictions on the signs of the singularities that there is a ‘fundamental domain’ for T , consisting of $(2 \times k)$ tiles, with opposite sides identified.

The patterns corresponding to the type k foliations have the property that every meridional disc D of the essential torus V has both positive and negative intersections with L . Accordingly, we have dubbed them *reverse string patterns* (or *rs patterns*).

Theorem 3.3.2 [B-M7] *With the above notation, the pattern P having strings of weight w_i as shown in figure 3.20, and $b(L)$ denoting braid index of L , then*

$$b(L) = w_0 \cdot b(C) \text{ if } T \text{ has type } \mathbf{0} \text{ foliation;}$$

$$b(L) = w_0 \cdot b(C) + w_1 \text{ if } T \text{ has type } \mathbf{1} \text{ foliation;}$$

$$b(L) = w_1 + w_2 + \dots + w_k \text{ if } T \text{ has type } \mathbf{k} \text{ foliation, } k \geq 2. \quad \square$$

Remark. The equations of theorem 3.3.2 are stated exactly as they appear in [B-M7]. It is of some importance to draw the reader’s attention to the addendum to [B-M7], regarding the type k case, as well as to the following discussion.

In order to deduce the next corollary, we define the special braid

$$\Gamma_n^p = \prod_{j=1}^p \left(\prod_{k=1}^n \sigma_{p-j+k}^{-1} \right) \cdot \Delta(\sigma_1, \dots, \sigma_{n-1}) \cdot \Delta(\sigma_{n+1}, \dots, \sigma_{n+p-1}),$$

where $\Delta(\sigma_1, \dots, \sigma_{n-1}) = \Delta(\sigma_1, \dots, \sigma_{n-2}) \cdot \sigma_{n-1} \dots \sigma_1$; the whole braid is as shown in figure 3.21.

The significance of this is that if we have an antiparallel pair of weighted strings of weights p, n , a half-twist on them can be represented as a braid Γ_n^p in a pattern. Schematically, this is illustrated in figure 3.22. So we can control framing via the β_i in the pattern.

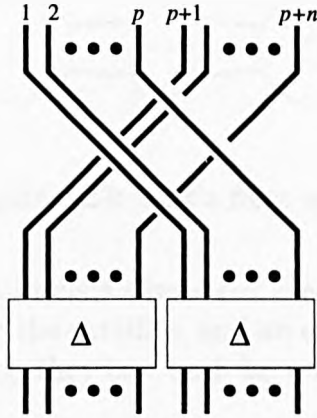


Figure 3.21: Special braid Γ_n^p

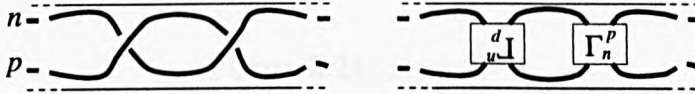


Figure 3.22: Using the pattern to control framing

Corollary 3.3.3 (A classification of reverse string patterns) *Let L be a satellite link with a reverse string pattern. Then the pattern, up to some choice of framing, is of the form of the type ‘ k ’ diagram above (the bottom diagram of figure 3.20), where*

- (i) k is even and non-negative (but could be zero)⁸;
- (ii) each braidcell β_i consists of a braidword;
- (iii) at most one of the β_i , with weighted input strings p_i, n_i is conjugate to $\Gamma_{n_i}^{p_i}$ or its inverse.

Proof. Let A be the axis which realizes L as a closed braid, and H be the fibration of $S^3 - A$ by halfplanes. Let $T \subset S^3 - L$ be the essential torus which realizes the satellite construction of L . By theorem 3.3.1, we can assume that the foliation of T induced by H is the standard type k foliation, and the pattern is as in figure 3.20. Notice that k must be even: a choice of orientation forces that. Further, suppose that β_i, β_j were conjugate to $\Gamma_{n_i}^{p_i}, \Gamma_{n_j}^{p_j}$. By a series of flypes (see figure 3.23, and [Ta] for more detail), we can assume that $|i - j| = 1$.

⁸See the remark following this proof.

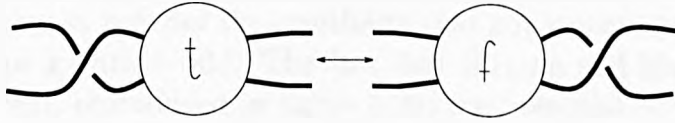


Figure 3.23: Tait's *flype* move

Then, if $\beta_i = \beta_j^{-1}$, the half twists cancel out (see figure 3.24). Otherwise, the pair contribute a full twist to the satellite, and an extra ± 1 to the framing. Since we are working *up to framing*, they can both be removed (see figure 3.25). \square



Figure 3.24: $\beta_i = \beta_j^{-1}$

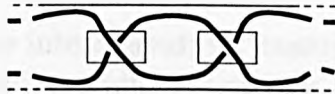


Figure 3.25: $\beta_i = \beta_j$

Remark. It is important to make a clear distinction between ‘foliation type’ (of an essential torus $T \subset S^3 - L$) and ‘pattern type’ (of a satellite $C * P$). The foliation type, the chief tool of theorem 3.3.1, will tell us what pattern type we are working with, as described in the caption accompanying figure 3.20. Pattern types resulting from a type 0 or type 1 foliation are precisely the non-reverse string type 0 and 1 patterns respectively. Pattern types resulting from a type k foliation ($k \in \mathbf{N}$, $k \geq 2$) are the reverse string type k' patterns, where k' is the number of braidboxes in a planar diagram of P , and is not unique. In particular, $k' \in 2\mathbf{N}$. The particular case $k' = 4$ is illustrated in figure 3.20, and the case $k' = 0$ (hereafter called the (x, y) -*antiparallel* pattern) has x and y strings running in an antiparallel fashion around the longitude of V , as shown in figure 3.27. If P is an antiparallel then $C * P$ is an antiparallel satellite.

One problem with their statement of theorem 3.3.1 is that, for a reverse string satellite L , it seems to rule out the possibility that any essential torus T in $S^3 - L$ has foliation type k with k odd. The fact that Birman and Menasco's example (figure 7 of [B-M7], reproduced in figure 3.26) has essential torus with foliation type 5 presents an apparent conflict.

This is explained by the observation that the *foliation* type and the *pattern* type are, to some extent, independent of each other. More accurately, the foliation type is controlled by four factors:

- (i) the pattern (and in particular the pattern type, which in the reverse string case must be even);
- (ii) the writhe $w(C)$;
- (iii) the arc index, $\alpha(C)$; and
- (iv) the choice of framing, f .

The last three factors between them force the foliation type to have either odd or even parity, as we shall see.

Some of these factors are interrelated; for example, an arc diagram of a companion comes with an implicit 'meridional twisting' (the writhe), which influences the framing. A good way to see this is to consider the most simple of reverse string patterns, namely the (1,1)-antiparallel. The discussion in the following paragraphs, in particular taking $P = (1,1)$ -antiparallel, makes the meridional twisting quite apparent. (The (1,1)-antiparallel has also been referred to as the 'British Rail' parallel, after the British Rail logo .)

Before closing this section, we make some observations on the braid index of reverse string satellites, which will be built on in later sections.

Proposition 3.3.4 *Let C be a knot with arc index $\alpha = \alpha(C)$. Let L be a satellite which has C as a companion, the pattern being reverse string; let L be braided in a positive sense around braid axis A . Then an essential torus $T \subset S^3 - L$ has foliation type at least α , with respect to the open-book fibration of $S^3 - A$.*

Proof. Suppose T_C is such an essential torus: its core is C , and T_C bounds a solid torus V_C with $L \subset V_C$. Let $H = \{H_\theta : \theta \in [0, 2\pi]\}$ be the open book decomposition of $S^3 - A$ by half-planes; this induces the foliation of T_C , of type k , with leaves $\{H_\theta \cap T_C\}$. We show that $\alpha(C) \leq k$.

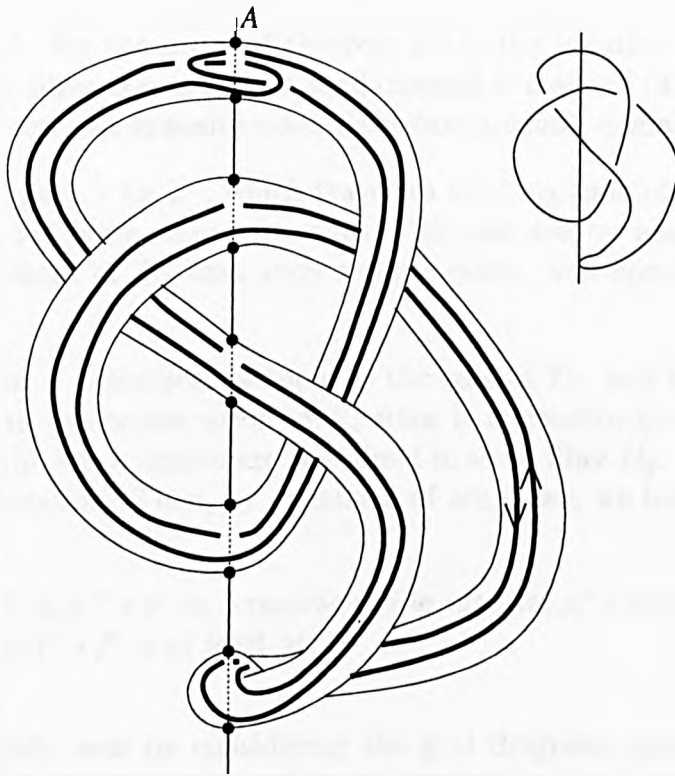


Figure 3.26: Whitehead double of a trefoil with its essential torus, from [B-M7]

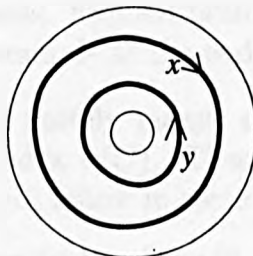


Figure 3.27: The (x, y) -antiparallel pattern

Since L is a reverse string satellite, it does not have a type 0 or type 1 pattern, and we may deduce by general position arguments and using theorem 3.2.1 that no leaf of the foliation is a simple closed curve. The general position assumptions also tell us that every non-singular leaf must be a simple arc, which joins two points of $T_C \cap A$. By the proof of theorem 3.3.1, the foliation on T_C induces a tiling of T_C : the tiling comes from a fundamental domain of $(2 \times k)$ tiles, where each tile is 4-valent, and opposite sides of the fundamental domain are identified.⁹

We choose a path γ on T_C , which traverses the longitude of T_C exactly once, constructed by following some tile-edges. We can see by examination of the fundamental domain of T_C that such a path exists, and consists of exactly k edges.

It follows that γ is ambient isotopic to the core of T_C , and hence to C itself. Moreover, γ is an arc presentation of C , since it is constructed of non-singular leaves, each of which is a simple arc contained in some fibre H_θ . There are k arcs in this arc presentation. Then, by definition of arc index, we have $\alpha(C) \leq k$. \square

Corollary 3.3.5 *Let $C * P$ be a reverse string satellite of a companion C . Then the braid index of $C * P$ is at least $\alpha(C)$.*

Proof. Most easily seen by considering the grid diagram, given by projecting $C * P$ onto the boundary of a cylindrical neighbourhood of A . There is at least one braidstring for each of the point intersections $A \cap C$ of the arc presentation of C . Further discussion of this construction follows in section 3.5. \square

It is a fact that for any knot C , there exist infinitely many inequivalent satellites $C * P$ of C with braid index $b(C * P) = \alpha(C)$. For example, an infinite family of patterns $\{P_k\}$ is given in figure 3.28; for a given companion C , these patterns give rise to an infinite family of satellites $C * P_k$, each with the same framing and the same braid index. Explicit braid presentations of these satellites can be constructed as in the example at the end of section 3.4.

There also exist (probably finitely many) satellites of C with pattern the $(1, 1)$ -antiparallel, and braid index $\alpha(C)$. These differ by virtue of a choice of framing. A discussion of this will follow in sections 3.5 and 3.6.

⁹See the remark following theorem 3.3.1, and also [B-M7].

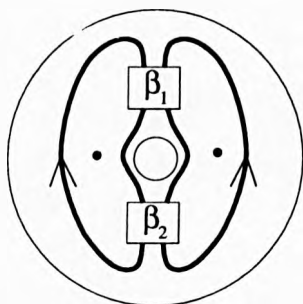


Figure 3.28: An infinite family of patterns, $\{P_k\}$, constructed by setting $\beta_1 = \sigma_1^2 \in B_2$ and $\beta_2 = \sigma_1^{2k+1} \in B_2$, $k \in \mathbb{Z}$

3.4 Braid presentations of reverse string satellites

We have already considered presenting braids of type 0 and type 1 (non-reverse string) satellites in section 3.2. The following proposition, and its proof, are of some help in understanding the embedding of a reverse string satellite and its essential torus in S^3 , relative to A .

Proposition 3.4.1 *Let $G = G(C)$ be an arc presentation of a knot C with $\alpha' \geq \alpha(C)$ arcs. Let V_C be a tubular neighbourhood of C with type α' foliation. Let P be a reverse string pattern of type k , with $k \leq \alpha'$, as described in corollary 3.3.3, P living in an unknotted solid torus V_P . Then there exists an embedding*

$$e : V_P \rightarrow V_C \subset S^3$$

such that the inclusion of P in $S^3 - A$ induced by the embedding is a closed braid with braid axis A .

Proof. The α' arcs are embedded in half-planes

$$H = \left\{ H_\theta : \theta = \frac{2n\pi}{\alpha'}, n = 1, \dots, \alpha' \right\}.$$

V_C has type α' foliation, so the set $\{V_C \cap A\}$ consists of precisely α' subarcs $a_1, a_2, \dots, a_{\alpha'}$ of A . If we think of V_C as homeomorphic to $S^1 \times D^2$, then we can fibre V_C by discs D^2 such that the subarcs a_i bisect α' of the fibres (denoted D_i^C) as shown in figure 3.29. The D_i^C dissect V_C into α' solid tubes Z_i , bounded in V_C by $D_i^C \cup D_{i+1}^C$.

The torus V_P containing P is dissected into α' solid tubes Y_j by considering a similar fibration of V_P . For $j = 1, \dots, k$, each Y_j will contain a braidcell and

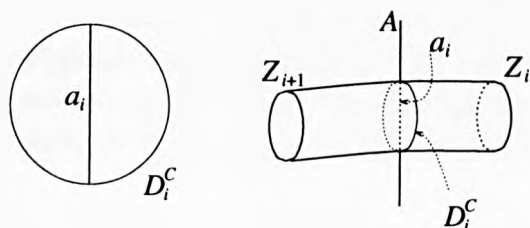


Figure 3.29: Dissecting disc D_i^C

four weighted strings. For $j = k + 1, \dots, \alpha$, each Y_j carries two parallel weighted strings as in figure 3.31. The dissecting discs D_j^P are positioned as shown in figure 3.30; they will be bisected by the preimages $e^{-1}(a_i)$, which separate the points of $P \cap D_j^P$ into algebraically positive and negative intersections. The embedding will be such that $e(Y_j) = Z_j$. Let $P_j = P \cap Y_j$.

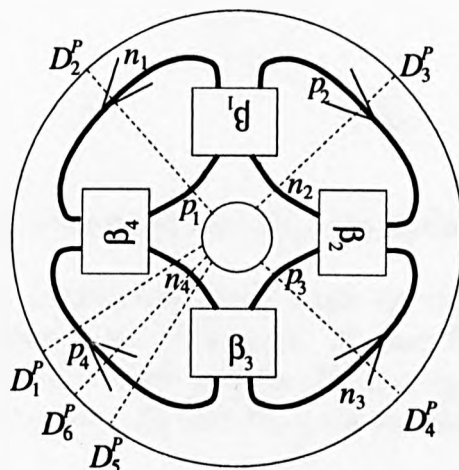


Figure 3.30: Dissecting discs D_j^P of V_P

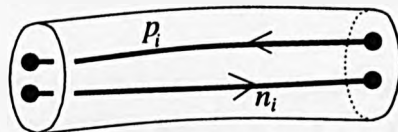


Figure 3.31: Completion tube Y_j , $j = k + 1, \dots, \alpha'$

Notice that if $Z_{j_1} \cap Z_{j_2} \neq \emptyset$, $j_1 \neq j_2$ (say $j_1 < j_2$ without loss of generality), then necessarily $|j_2 - j_1| \equiv 1 \pmod{\alpha'}$, so $Z_{j_1} \cap Z_{j_2} = D_{j_2}^C$; the intersection of $e(P)$ with the disc consists of point intersections only. Therefore $e(P_{j_1})$ and $e(P_{j_2})$ do not interweave, so we need only show that we can choose e so that the inclusion $e(P_j)$ in $S^3 - A$ is transverse to the pages of the open book decomposition, for each $j = 1, \dots, k$.

The exact position of the D_i^C are as follows. The arc contained in $H_{\theta_i} \in H$ has a tubular neighbourhood, which we call Z_i . The Z_i appear in numerical order as we traverse V_C , so the arcs of C corresponding to Z_i, Z_{i+1} meet at a point $x_j \in C \cap A$. Tubular neighbourhoods Z_i and Z_{i+1} themselves intersect in the disc D_{i+1}^C ; we choose this disc to lie in a plane R_{i+1} that bisects the angle between H_{θ_i} and $H_{\theta_{i+1}}$. See figure 3.32.

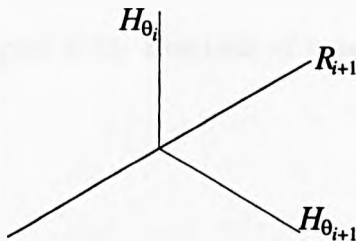


Figure 3.32: Dissecting disc D_{i+1}^C lies in the plane R_{i+1}

Arcs (in particular, consecutive arcs) must lie in distinct half-planes, by construction of arc presentation. Therefore, R_i and R_{i+1} can coincide only if $\theta_{i-1} = \theta_i - \pi = \theta_{i+1}$. (In this case, strictly, R_i and R_{i+1} differ by an angle π .) Then, if ϕ_i is the angle between R_i and R_{i+1} , we can say $0 < \phi_i < 2\pi$.

So Z_i is as shown in figure 3.33, with the planes R_i, R_{i+1} indicating the boundaries of Z_i .

We embed the pattern transversely into the pages of the open-book decomposition as shown in figures 3.34 and 3.35. The set $P \cap D_i^C$ consists of point intersections only, and so is transverse to the pages of the decomposition. \square

The proof of proposition 3.4.1 leads to a direct approach for constructing a presenting braid for a reverse string satellite $C * P$. We place the companion C , and then dress it with P , in such a way that a braid whose closure represents $C * P$ becomes apparent. The ‘sizes’ of the pattern and companion diagrams should be compatible: the number of arcs on which the companion is presented should be at least as big as the pattern type.

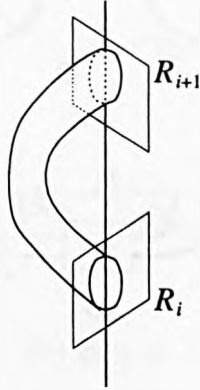
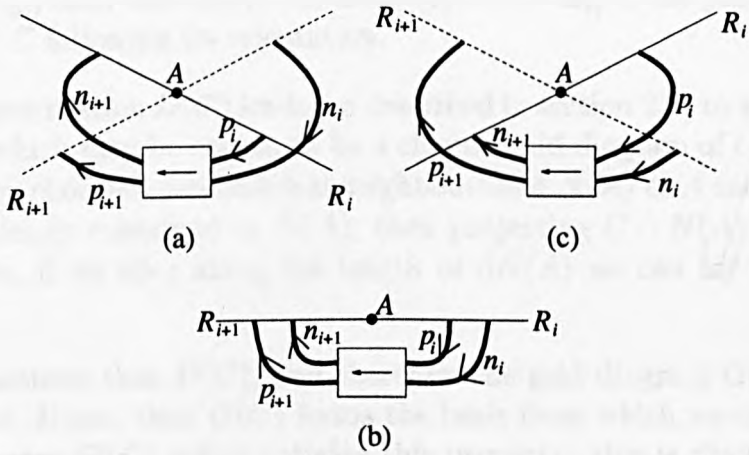


Figure 3.33: Position of tube Z_i



(a) $\phi_i \in (0, \pi)$

(b) $\phi_i = \pi$

(c) $\phi_i \in (\pi, 2\pi)$

Figure 3.34: Embedding of P_j , for $1 \leq j \leq k$

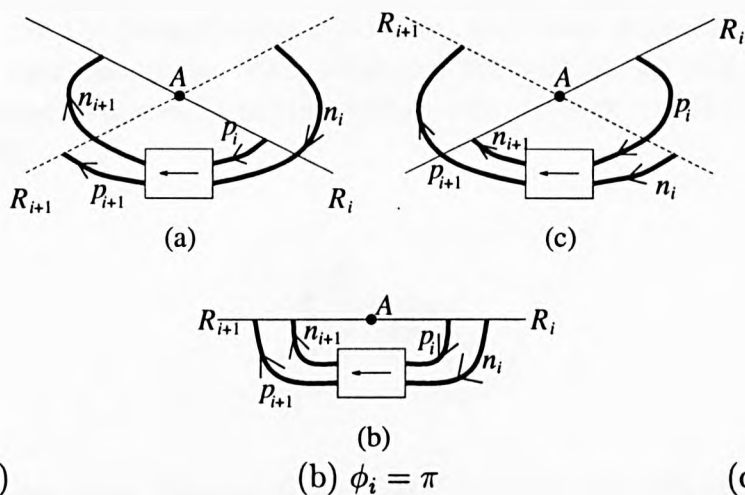


Figure 3.35: Embedding of P_j , for $k + 1 \leq j \leq \alpha'$

The algorithm begins with an arc presentation $D(C)$ for C , and a diagram of the pattern P in standard form in the torus, as in corollary 3.3.3.

We must recall some terminology and definitions. A pair of arcs in a diagram are said to be *consecutive* if they meet at a point of A . The α' arcs of $D(C)$ are embedded in fibres $H_{\theta_1}, \dots, H_{\theta_{\alpha'}}$ of $S^3 - A$. Each joins two of the α' points $x_1, \dots, x_{\alpha'}$ of A . The x_i are indexed in ascending order around A . We have an α' -cycle $\pi \in S_{\alpha'}$, such that $\pi(1) = 1$, and $\pi(j) = i \Leftrightarrow H_{\theta_i}$ is the j th plane visited if we traverse C following its orientation.

The arc presentation $D(C)$ leads (as described in section 2.2) to a grid diagram $G(C)$ for C , which may be chosen to be a closed braid diagram of C . Essentially, this is given by choosing a cylindrical neighbourhood $N(A)$ of A such that no arc of C is completely contained in $N(A)$; then projecting $C \cap N(A)$ radially onto $\partial N(A)$. Then, if we slice along the length of $\partial N(A)$ we can lay it flat on the plane.

We may assume that $D(C)$, and therefore the grid diagram $G(C)$, each has at least k arcs. If not, then $G(C)$ forms the basis from which we can generate a new grid diagram $G'(C)$ which satisfies this property: this is discussed in more detail in the sections on framing (sections 3.5 and 3.6).

(In the grid diagram $G(C)$, we can assume that the x_i are represented by the horizontal lines, with x_1 highest, and $x_{\alpha'}$ lowest. Also we have the halfplanes represented by the vertical lines with H_{θ_1} left-most, and $H_{\theta_{\alpha'}}$ right-most.)

At any rate, in $G(C)$ we get a number of vertical and horizontal lines. The vertical lines are the (slightly trimmed) arcs, with both ends on the plane, and bridging out over the plane. The horizontal lines lie in the plane, and simply identify the appropriate ends of consecutive arcs, as they would have met at A . See figure 3.36.

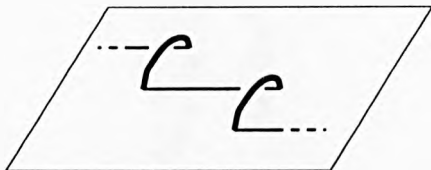


Figure 3.36: Two consecutive arcs bridging over the plane

From $G(C)$ we can construct a diagram of how V_C lies relative to $\partial N(A)$. Each arc is thickened into a solid cylinder; its endpoints thicken into the discs D_i^C . Figure 3.37 helps to illustrate this. These discs lie embedded in $\partial N(A)$, and there are two copies of each D_i^C . The pair have oppositely oriented boundaries as they appear on $\partial N(A)$ (one clockwise, one counter-clockwise, inherited from the orientation of V_C); identification of corresponding pairs will reconstruct V_C .

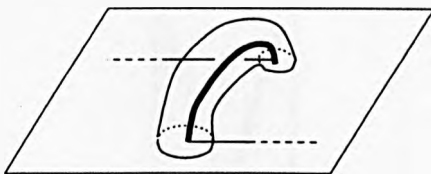


Figure 3.37: A thickened arc Z_i bridging over the plane

Meanwhile, the pattern is dissected as in the proof, using dissecting discs D_j^P , to give tubes Y_j containing sections of the pattern. The first k of the Y_j each contain a braid cell B_j , $1 \leq j \leq k$, and the remainder carry a pair of oppositely oriented parallel weighted strings p_i and n_i . The reader is referred to figure 3.31 in the proof of proposition 3.4.1.

The first k of the Y_j are embedded into the cylindrical neighbourhoods of the first k consecutive arcs, as shown. The choice of ‘first arc’ is not unique, but the satellite is independent of this choice. The horizontal ‘identifying’ semi-loops of $G(C)$ are replaced by weighted parallel strings p_i , and the opposite choice of semi-loops replaced by weighted parallel strings n_i . If we declare that the p_i follow the chosen orientation of C in order of their indices, then there is only one way to embed each of the following Y_j , $j \leq k$. See figure 3.38.

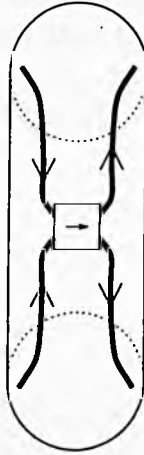


Figure 3.38: The embedding $Y_j \subset Z_{\pi(j)}$, $1 \leq j \leq k$

The remaining Z_j , $k + 1 \leq j \leq \alpha'$, each have embedded a completion tube Y_j , carrying the two antiparallel weighted strings. They project onto $\partial N(A)$ as in figure 3.39.

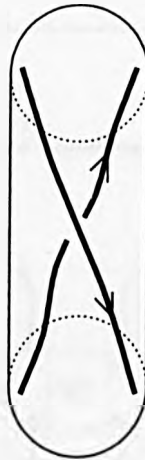


Figure 3.39: The embedding $Y_j \subset Z_{\pi(j)}$, $k + 1 \leq j \leq \alpha'$

There are two choices for this embedding: the crossing of p_i with n_i ensures braidedness, but the braidedness is independent of the *choice* of crossing. This choice is discussed further under consideration of framing (sections 3.5 and 3.6).

Example. Figure 3.40 shows a reverse string satellite of a trefoil, with a ‘type 4’ reverse string pattern as shown. Note that the framing has been chosen implicitly so that the number of braidstrings of the satellite is equal to the arc index of the companion. The essential non-peripheral torus in the complement of this satellite has foliation type 5.

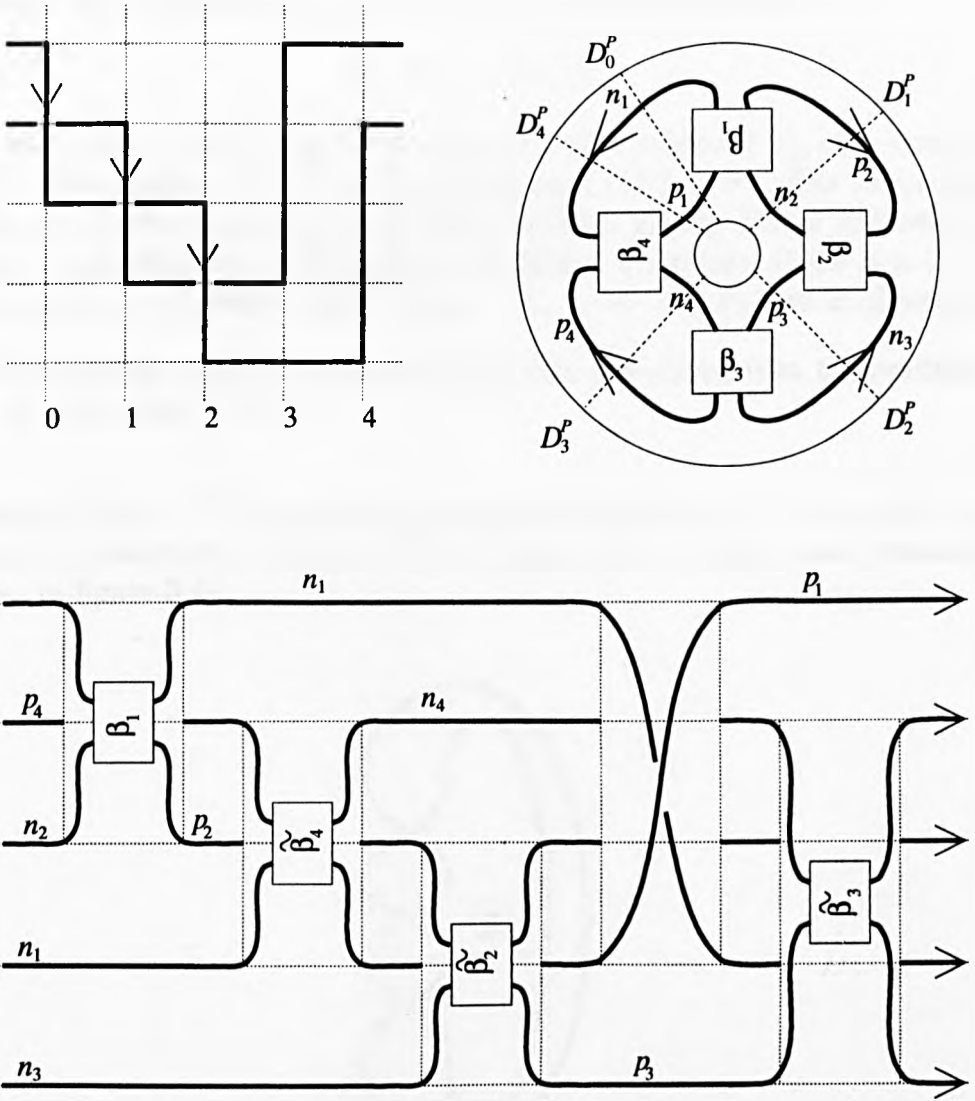


Figure 3.40: Reverse string satellite presented as a closed braid

3.5 Concerning the framing of satellite links

So far in this discussion of satellites as closed braids we have consciously chosen to ignore one vital concept, namely that of framing. In this section we discuss how the framing fits into our theory.

Recall that the satellite $C * P$ is constructed by an embedding

$$e : V_P \rightarrow V_C \subset S^3$$

of an unknotted torus V_P into the toroidal neighbourhood V_C of a companion knot C . The satellite $C * P$ itself is the image $e(P) \subset S^3$. The embedding is not unique: e may introduce any whole number of meridional full-twists into the torus, and still be a continuous embedding. Therefore, there is a bijection between the set of possible embeddings $e : V_P \rightarrow V_C$ and the set \mathbf{Z} of integers.

The following examples illustrate how this non-uniqueness is manifested in braid presentations of $e(P)$.

Example. Let $C * P$ be a satellite link with companion $C = 3_1$, and a type 1 pattern. To construct a braid for $C * P$, begin with a closed braid presentation of C , as in figure 3.41.

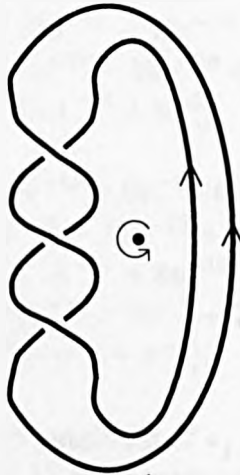


Figure 3.41: Closed braid presenting $C = 3_1$

Closed braid presentations of $C * P$ are then easily constructed, as in figure 3.42.

Both are equally good satellites, in so far as they satisfy the definition of a satellite. They are, however, different links, distinguishable by comparing Homfly

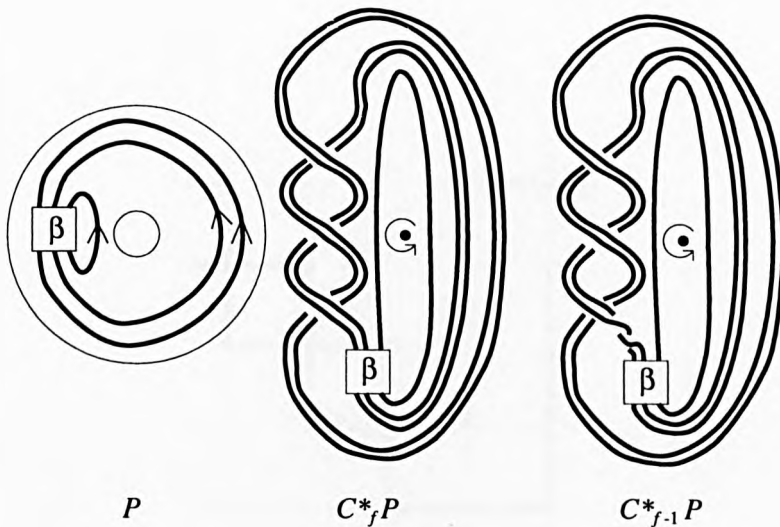


Figure 3.42: Closed braids presenting two possible satellites $C *_f P$ and $C *_{f-1} P$

or Jones polynomials. As an example, consider the case where each string is of weight 1, and β is the trivial braid on three strings¹⁰:

$$\begin{aligned}
 \mathcal{P}_{C *_f P}(v, z) &= z^{-2} (v^{-16} - 6v^{-14} + 13v^{-12} - 12v^{-10} + 4v^{-8}) \\
 &\quad + (-5v^{-14} + 26v^{-12} - 40v^{-10} + 19v^{-8}) \\
 &\quad + z^2 (-v^{-14} + 22v^{-12} - 57v^{-10} + 36v^{-8}) \\
 &\quad + z^4 (8v^{-12} - 36v^{-10} + 28v^{-8}) \\
 &\quad + z^6 (v^{-12} - 10v^{-10} + 9v^{-8}) \\
 &\quad + z^8 (-v^{-10} + v^{-8}),
 \end{aligned}$$

$$\begin{aligned}
 \mathcal{P}_{C *_{f-1} P}(v, z) &= z^{-2} (v^{-14} - 6v^{-12} + 13v^{-10} - 12v^{-8} + 4v^{-6}) \\
 &\quad + (v^{-14} - 46v^{-12} + 19v^{-10} - 26v^{-8} + 12v^{-6}) \\
 &\quad + z^2 (-v^{-12} + 8v^{-10} - 22v^{-8} + 15v^{-6}) \\
 &\quad + z^4 (v^{-10} - 8v^{-8} + 7v^{-6}) \\
 &\quad + z^6 (-v^{-8} + v^{-6}).
 \end{aligned}$$

Example. Let us construct two satellites $C *_f P$, $C *_{f+1} P$, for some f , where C is the knot 3_1 , and P is the (1,1)-antiparallel pattern. Construct each satellite as a closed braid, via the algorithm of section 3.4.

Begin with a grid presentation $G(C)$ of C with 5 arcs, as in figure 3.43.

This is then dressed with the pattern, as described in the previous section, and illustrated in figure 3.44.

¹⁰In this case, both links are both distant unions, and so have Conway polynomial 0.

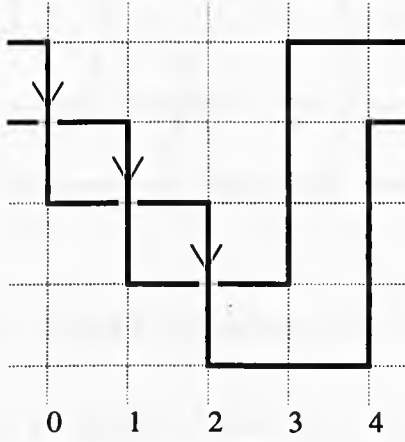


Figure 3.43: Grid presentation $G(C)$, $C = 3_1$

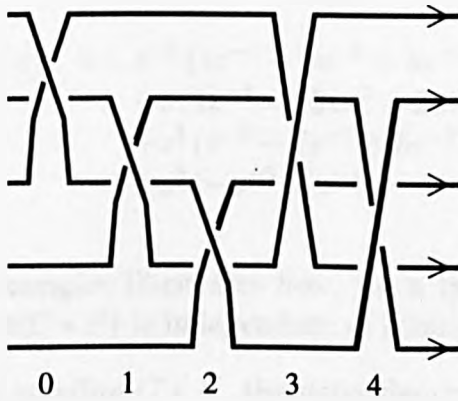


Figure 3.44: Closed braid presentation for $C *_f P$

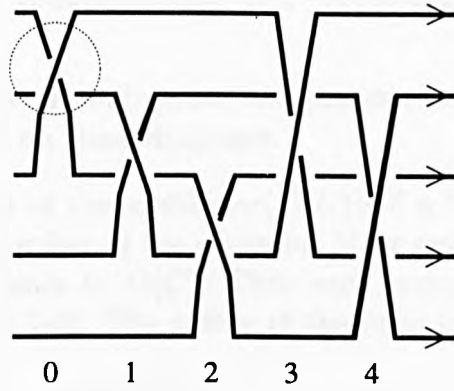


Figure 3.45: Closed braid presentation for $C *_{f+1} P$

There is no unique way to do this. A full twist of the torus manifests itself as a full twist of a cylindrical neighbourhood Y_j of one of the arcs. This induces in the presentation a change of sign of a crossing, located in the projection of that Y_j . See figure 3.45. This change of framing is discussed further in section 3.6.

Again, each of these links satisfies the definition of ‘satellite link’, but they are inequivalent links, as their Homfly polynomials confirm:

$$\begin{aligned} \mathcal{P}_{C*_f P}(v, z) &= z^{-1} (4v^{-3} - 8v^{-1} + 5v - v^3) \\ &\quad + z (4v^{-3} - 15v^{-1} + 10v - v^3 - v^5) \\ &\quad + z^3 (v^{-3} - 7v^{-1} + 6v) \\ &\quad + z^5 (-v^{-1} + v), \end{aligned}$$

$$\begin{aligned} \mathcal{P}_{C*_{f+1} P}(v, z) &= z^{-1} (4v^{-5} - 8v^{-3} + 5v^{-1} - v) \\ &\quad + z (4v^{-5} - 15v^{-3} + 9v^{-1} - v - v^3) \\ &\quad + z^3 (v^{-5} - 7v^{-3} + 6v^{-1}) \\ &\quad + z^5 (-v^{-3} + v^{-1}). \end{aligned}$$

The first of these examples illustrates how, for a type 0 or type 1 satellite $C * P$, the braid index $b(C * P)$ is independent of framing.

For a reverse string satellite $C * P$, the dependence of $b(C * P)$ on framing was conjectured by Birman and Menasco in [B-M7]. This dependence is analysed below. Observations, based on the explicit braid presentations of $C * P$, provide us with an upper bound for $b(C * P)$. Analysis of the Homfly polynomial gives us a lower bound for $b(C * P)$, via the MFW inequality.

3.6 A formal definition for framing

Since we are working via our 2-dimensional representations of links, our definition of framing is also based on these diagrams.

Recall the definition of the *writhe* $wr(D(C))$ of a link diagram $D(C)$: it is the algebraic crossing number of the diagram. More explicitly, we first assign an orientation to C , and hence to $D(C)$. Then each crossing c of $D(C)$ has a *sign* $\varepsilon(c)$, according to figure 3.46. The writhe of the diagram is

$$wr(D(C)) = \sum_{c \in D(C)} \varepsilon(c).$$

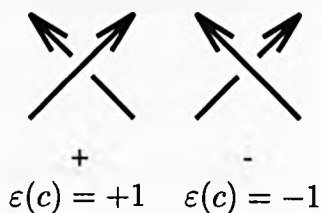


Figure 3.46: Sign of a crossing

Given a diagram $D(C)$ of a link C , there is a natural way to draw a diagram of the (1,1)-antiparallel satellite, based on $D(C)$. Simply, one draws in another strand which runs along the side of $D(C)$. This is known as the *blackboard antiparallel*, for obvious reasons, and its framing is called the *blackboard framing*.

Generally, we can define the *framing* of such a satellite as being the writhe of the underlying companion diagram. Equally, this is given by finding the winding number of one component around the other (this is counted by summing the signs of all crossings in which one component of the link crosses *over* the other), and taking the negative of this result.

As an example of this, consider figure 3.47. Here, the diagram of the trefoil has writhe 3. Constructing its blackboard (1,1)-antiparallel, we find that the blackboard framing is 3.

Proposition 3.6.1 *In this case, the framing of the (1,1)-antiparallel of $D(C)$ with blackboard framing is $wr(D(C))$.*

Proof. The only crossings that can possibly contribute to the winding number of the two components occur near the crossings of $D(C)$. A positive crossing



Figure 3.47: Trefoil and its blackboard antiparallel

of $D(C)$ contributes -1 to the winding number; a negative crossing of $D(C)$ contributes $+1$. \square

In particular, if the diagram $D(C)$ of C is a grid diagram $G(C)$, then proposition 3.6.1 still holds.

Example.

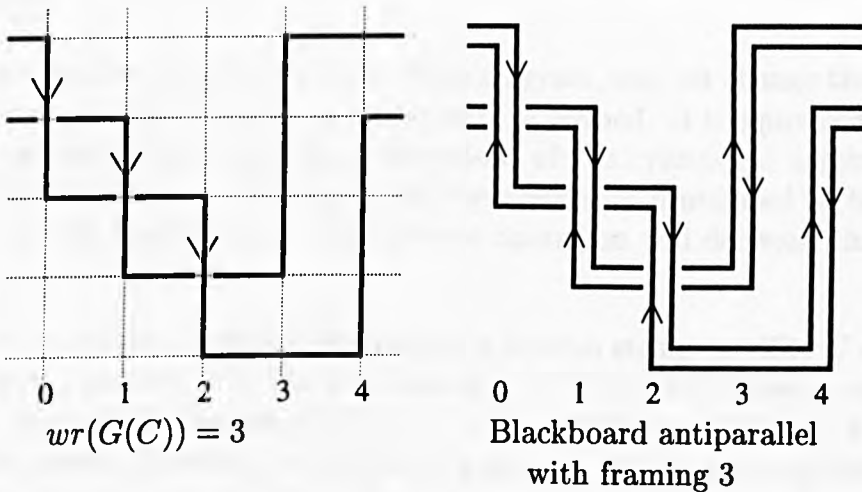


Figure 3.48: Grid diagram $G(C)$ and its blackboard antiparallel

The $(1,1)$ -antiparallel of $C * P$ (P is the $(1,1)$ -antiparallel) has two oppositely oriented components, L_1 and L_2 , say. Suppose that the orientation of L_1 agrees with that of C . Each of these components, when considered alone, is a braided grid diagram for C . If we take the opposite choice of semi-loops for one of them, then they are braided in the same direction. This is equivalent to pushing the existing semi-loops of this component down, through a point at infinity, and back up into their alternative positions. Compare figures 3.48 and 3.49. Since the horizontal lines in the grid never *over*-cross another part of the link, this move is an ambient isotopy of $C * P$ in S^3 and the link type is preserved. Since the link type of $C * P$ is preserved, the framing of the companion is also preserved.

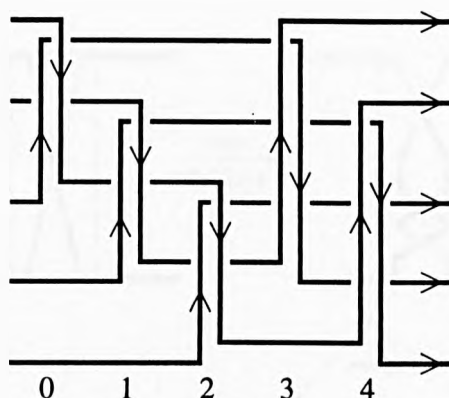


Figure 3.49: Braided diagram of the blackboard antiparallel

We conclude that at each embedded tube Y_j , the components L_1 and L_2 cross; and if L_1 crosses *over* L_2 at each of these singularities, then the framing is equal to $wr(G(C))$.

We can preserve the satellite form of the diagram, and yet change the framing, by altering one of the crossings, as previously described. It is equivalent to a full twist (in an appropriate meridional direction) of the cylindrical neighbourhood of the corresponding arc. For example, the operation illustrated in figure 3.50 will increase the framing by 1. The reverse operation will decrease the framing by 1.

We can construct a braided diagram of a reverse string satellite $C *_f P$ with companion C , pattern $P \subset V_P$ and framing $f \in \mathbf{Z}$, in the following way. First construct some grid diagram $G(C)$ of C with writhe $wr(G(C))$. In order to achieve the correct framing, we will need a number of ‘completion tubes’ of the appropriate type: they should number at least $|f - wr(G(C))|$. To ensure that $G(C)$ has sufficiently many arcs, we can apply Cromwell’s moves III and IV if necessary. See section 2.3.

Dress the diagram $G(C)$ as described in section 3.5. Finally, alter the sign of the crossing of sufficiently many of the completion tubes, so that the framing is correct.

In the example of figures 3.48 and 3.49, there is sufficient possibility to easily produce braidwords for framings $1 \leq f \leq 6$. If $C *_f P$ were a satellite with framing f outside this range, then we would need to start with an alternative grid diagram $G(C)$. For example, see figure 3.51.

So for a certain grid diagram $G(C)$, we can construct satellites with framing

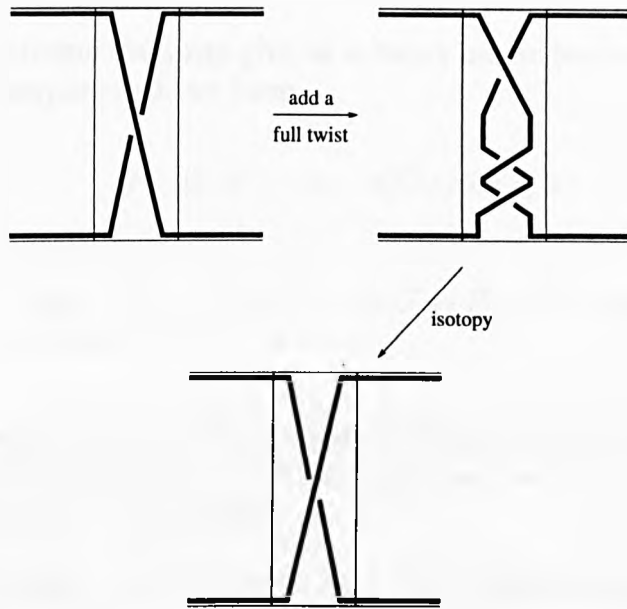


Figure 3.50: Changing the framing

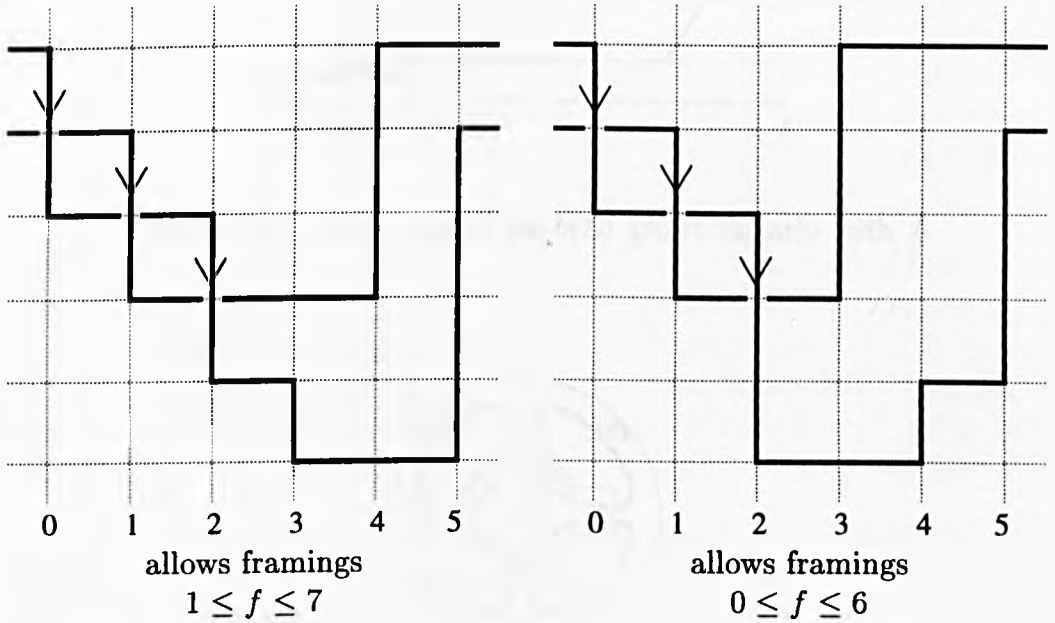


Figure 3.51: Some other grid diagrams for C

f inside a certain range. Outside that range, a different choice of grid diagram for C will suffice.

Hence, more extreme framings give us a larger upper bound for $b(C *_f P)$. In the case of the example cited, we have

$$f \in [1, 6] \Rightarrow b(C *_f P) \leq 5$$

$$\left. \begin{array}{l} f = 1 - k \\ \text{or} \\ f = 6 + k \end{array} \right\}, k \geq 1 \Rightarrow b(C *_f P) \leq 5 + k.p_1,$$

where p_1 is the weight of one of the weighted strings in the diagram of P (figure 3.53). In fact, we can choose p_1 to be the minimum, over all i , of the weights of the weighted strings p_i in the diagram.

Therefore the upper bound is linear in f for f outside a special range, with coefficient p_1 . Figure 3.52 describes the relationship.

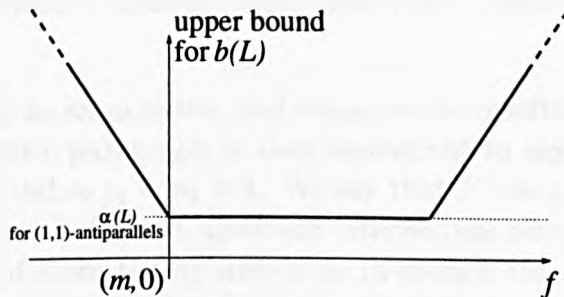


Figure 3.52: Upper bound for $b(L)$ grows linearly with f

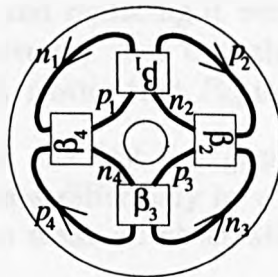


Figure 3.53: General diagram of a reverse string pattern

3.7 A linear relation between framing and Homfly polynomial

For a lower bound for $b(C *_f P)$ we can turn to the Homfly polynomial, and in particular to the MFW inequality (see theorem 1.5.1(i)). It would be satisfying to find that the upper bounds (from the explicit diagrams of the previous section) and the lower bounds (from MFW) are sufficiently close that the braid index of a given satellite can be accurately deduced from either of these methods. There is certainly evidence to support this, in some cases: section 3.8 discusses a preliminary result.

In this section, we see how the linear dependence of the upper bound on framing is also exhibited in the lower bound, at least for an infinite subclass of reverse string satellites.

Recall that for a general link L , we define $\text{spr}_v(\mathcal{P}_L(v, z))$ to be the difference between the greatest and least powers of v in $\mathcal{P}_L(v, z)$. We study a subclass of reverse string satellites $C *_f P$ whose patterns have *geometric winding number* 2 around the longitude of $V(C)$.¹¹ That is to say, there exists a meridional disc D of V_P which intersects P exactly twice (and those intersections have opposite signs).

Let us project V_P to an annulus, and examine the resulting diagram of P (see figure 3.53). The above paragraph is then equivalent to saying that, for some i , we have $p_i + n_i = 2$, and so $p_i = n_i = 1$. We say that P has *geometric intersection number* $p_i + n_i = 2$ with D , and *algebraic intersection number* $p_i - n_i = 0$ with D . An application of skein theory allows us to deduce the linear dependence of $\text{spr}_v(\mathcal{P}_{C *_f P}(v, z))$ on the framing f of $C *_f P$. This leads to a conjecture that such linear behaviour extends to all reverse string satellites.

In order to state the first theorem, we need the following definition. Let the pattern $P \subset V_P$, and the disc $D \subset V_P$ be as described in the previous paragraph. Let \tilde{D} be a cylindrical neighbourhood of D , as in figure 3.54 (top). We construct P_∞ by removing \tilde{D} from V_P , and replacing it with a cylindrical neighbourhood of D in V_P as in figure 3.54 (bottom), such that the orientations of strings on the disc boundaries are coincident. Notice that P_∞ is not a ‘proper’ pattern.

There are two results here: the first is a general result relating the Homfly polynomials of two satellites that differ only by a choice of framing. The second result employs this relation, to make an observation about how $\text{spr}_v \mathcal{P}_{C *_f P}(v, z)$ relates to framing.

¹¹So in particular, this applies when P is the (1,1)-antiparallel: the first result is therefore a generalization of proposition 4.3.1, which is a theorem of Lee Rudolph.

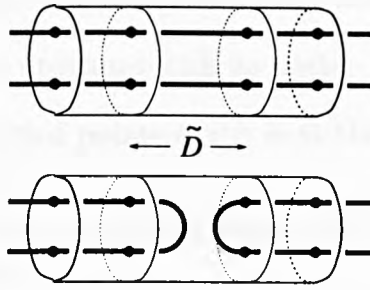


Figure 3.54: Replacing \tilde{D} to give P_∞

Theorem 3.7.1 *Let C be a knot, and $P \subset V_P$ be a reverse string pattern. Suppose there exists a meridional disc D of V_P such that $D \cap P$ consists of two points, of opposite signs. Also, for $f \in \mathbf{Z}$, let $C *_f P$ be the satellite with companion C , pattern P and framing f . Let $C *_\infty P$ be the satellite with companion C and pattern P_∞ (notice that $C *_\infty P$ is independent of framing, since P_∞ is not proper). Then for any $f, s \in \mathbf{Z}$,*

$$\delta \mathcal{P}_{C *_f P}(v, z) - \mathcal{P}_{C *_\infty P}(v, z) = v^{2s} (\delta \mathcal{P}_{C *_{f+s} P}(v, z) - \mathcal{P}_{C *_\infty P}(v, z)).$$

Theorem 3.7.2 *With the hypotheses of theorem 3.7.1, suppose also that the two points of $D \cap P$ belong to different components of P . Then there exist integers m, M and d with $m \leq M$ and $d > 0$, independent of f , such that*

$$\begin{aligned} f \leq m &\Rightarrow \operatorname{spr}_v \left(\mathcal{P}_{C *_f P}(v, z) \right) = d + 2|m - f| \\ m \leq f \leq M &\Rightarrow \operatorname{spr}_v \left(\mathcal{P}_{C *_f P}(v, z) \right) = d \\ M \leq f &\Rightarrow \operatorname{spr}_v \left(\mathcal{P}_{C *_f P}(v, z) \right) = d + 2|M - f|. \end{aligned}$$

3.7.I Development of the tools

Skein theory is the key to these results, and some important definitions are covered now. The reader is also referred to chapter 1, and to Morton's NATO lecture notes [Mo1].

We study the links involved via their projections onto planar surfaces. Let F be a planar surface, with a finite (possibly empty) set of specified points on its boundary, if it has one. In this section, our discussion deals first with general F , and then specializes to the cases $F = S^2$, and $F = \mathcal{R}_2^2$ (to be defined below).

A *diagram* in F is a number of closed curves on F , together with arcs joining the specified points of ∂F , such that

- (i) there are finitely many singular points, and that they are double points;
- (ii) the double points are crossings with an under- and over-crossing;
- (iii) every one of the specified points of ∂F is at the end of some arc.

Let Λ denote the ring $\mathbf{Z}[v^{\pm 1}, z^{\pm 1}]$; then define $\mathcal{D}(F)$ to be the set of Λ -linear combinations of diagrams in F .

Let R_n^m denote a rectangular disc with m specified points on the top edge, and n on the bottom. A *diagram* in R_n^m is an (m, n) -tangle. Let \mathcal{R}_2^2 denote the set of diagrams in R_2^2 , with the extra structure that for any $D \in \mathcal{R}_2^2$, the curves of D have the choice of orientation at the boundary as illustrated in figure 3.55.

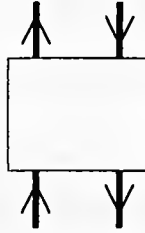


Figure 3.55: Orientation in \mathcal{R}_2^2

In particular, we define special tangles in \mathcal{R}_2^2 as in figure 3.56.

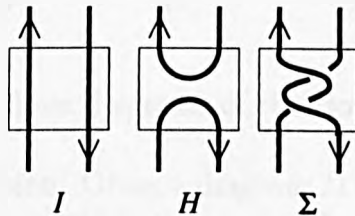


Figure 3.56: Special tangles $I, H, \Sigma \in \mathcal{R}_2^2$

There is a natural multiplication in \mathcal{R}_2^2 , given by juxtaposition of the tangles, as in figure 3.57.

Note that $X.I = X$, for all $X \in \mathcal{R}_2^2$, and also that Σ has a natural multiplicative inverse $\Sigma^{-1} \in \mathcal{R}_2^2$.



Figure 3.57: Multiplication in \mathcal{R}_2^2

The *Homfly skein* $\mathcal{S}(F)$ of F is the quotient of $\mathcal{D}(F)$ by the Homfly relations

$$D_+ = v^2 D_- + vz D_0 \quad (3.1)$$

$$D \sqcup O = \delta D \quad (3.2)$$

where \sqcup denotes distant union, $\delta = \frac{v^{-1}-v}{z}$, and $D_+, D_-, D_0 \in \mathcal{D}(F)$ are diagrams which are identical except in the neighbourhood of a double point, in which they appear as in figure 3.58.



Figure 3.58: The three diagrams of the Homfly skein relation

We need one more definition. Given a diagram $D \in \mathcal{D}(F)$, let each component have a unique label s_i , $1 \leq i \leq |D|$. Let each s_i have a base point $p_i \subset s_i$; the s_i are oriented, so if s_i has intersection with the boundary of F , we let p_i be the initial point of s_i on the boundary. We follow a path along $s_1, \dots, s_{|D|}$ in order, following each s_i in the direction of its orientation starting from p_i .

Now say that the diagram D is *descending* if there exists a choice of s_i, p_i such that, as one travels the path described, each crossing of D is first encountered as an overpass.

Remark. It is well-known (for example, [L-M] p.113) that any descending diagram in $\mathcal{D}(S^2)$ is a diagram of an unlink.

We continue with a sequence of lemmas.

Lemma 3.7.3 $\mathcal{S}(F)$ is spanned, as a Λ -module, by descending diagrams with no null-homotopic closed curves.

Proof. By induction, first on the number of crossings in a diagram, and second on the number of null-homotopic closed curves.

Let D be a non-descending diagram in $\mathcal{D}(F)$; so every choice of labels $\{s_i\}$ of the components gives a crossing (c , say) of D which is first met as an underpass. We use the Homfly skein relation to write D as a linear combination (over Λ) of diagrams D' , D'' , which are identical to D except in a neighbourhood of c . In D' , the sign of c is negated, and so is first met as an overpass. In D'' , the crossing is smoothed over. Therefore, D is expressible in $\mathcal{S}(F)$ as a linear combination of descending diagrams and diagrams with fewer crossings. When there are no crossings, a null-homotopic closed curve is removable at the expense of multiplying by δ . \square

The following two lemmas can then be deduced.

Lemma 3.7.4 $\mathcal{S}(S^2)$ is spanned, as a Λ -module, by the empty diagram. \square

Lemma 3.7.5 $\mathcal{S}(\mathcal{R}_2^2)$ is spanned, as a Λ -module, by the diagrams I , H . \square

Now, we are studying diagrams of satellites in $\mathcal{D}(S^2)$ via $(2, 2)$ -tangles in $\mathcal{D}(\mathcal{R}_2^2)$, as will become apparent. The following (general) definition describes how we relate $\mathcal{D}(\mathcal{R}_2^2)$ to $\mathcal{D}(S^2)$.

For planar surfaces F , F' , we define a *wiring* W of F into F' to be a choice of inclusion of F in F' , together with a fixed diagram of closed curves and arcs in $F' - F$ whose endpoints are the specified points of ∂F and $\partial F'$. The wiring W then determines a linear map

$$\mathcal{D}_W : \mathcal{D}(F) \rightarrow \mathcal{D}(F')$$

by the inclusion $D \mapsto W \cup D$.

We choose a wiring W of \mathcal{R}_2^2 into S^2 by wiring a $(2, 2)$ -tangle into a link.

Lemma 3.7.6 A wiring W of \mathcal{R}_2^2 into S^2 induces a linear map

$$\mathcal{S}_W : \mathcal{S}(\mathcal{R}_2^2) \rightarrow \mathcal{S}(S^2),$$

defined on a diagram T in \mathcal{R}_2^2 by $T \mapsto W \cup T$.

Proof. Specialization of theorem 1.5 of [Mo1], using a different skein relation. \square

Composition $X_1.X_2.\dots.X_n$ in $\mathcal{D}(\mathcal{R}_2^2)$ induces a multilinear map

$$\mathcal{S}(\mathcal{R}_2^2) \times \mathcal{S}(\mathcal{R}_2^2) \times \dots \times \mathcal{S}(\mathcal{R}_2^2) \rightarrow \mathcal{S}(\mathcal{R}_2^2),$$

via a wiring.

Given a reverse string satellite $C *_f P$, let us begin with a diagram $D(C *_f P) \in \mathcal{D}(S^2)$ which has the property that the companion and the pattern are easily discernible: for example, if L was a Whitehead double of the trefoil, then $D(C *_f P)$ might be as in figure 3.59.

Since $C *_f P$ has pattern P which has geometric winding number 2, there exists a rectangle Γ in S^2 which decomposes S^2 into two planar areas F_1 and F_2 , in such a way that the part of $D(C *_f P)$ in F_1 , say, is the $(2, 2)$ -tangle $I \in \mathcal{R}_2^2$. Such a rectangle Γ is illustrated in figure 3.59.

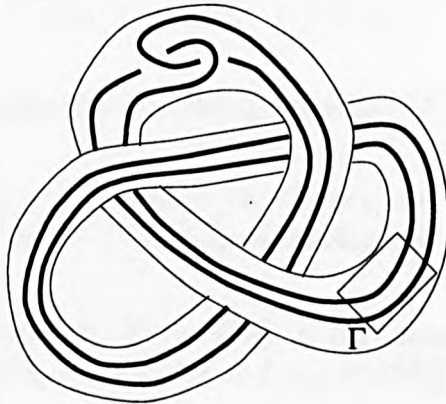


Figure 3.59: Diagram $D(C *_f P)$ of satellite $C *_f P$

We study framing via $\mathcal{S}(\mathcal{R}_2^2)$, since a change in framing (which is induced by meridional full-twists of the essential torus V_C) is represented in $D(L)$ by replacing $I \subset F_1$ by some power of Σ . The sub-diagram $D(L) \cap F_2$ gives us a wiring W of the $(2, 2)$ -tangle into S^2 ; results in $\mathcal{S}(\mathcal{R}_2^2)$ are extended to results in $\mathcal{S}(S^2)$ via the linear map $\mathcal{S}_W : \mathcal{S}(\mathcal{R}_2^2) \rightarrow \mathcal{S}(S^2)$.

The Homfly relations in $\mathcal{S}(\mathcal{R}_2^2)$ quickly give us the following relations:

$$\Sigma = v^2 I + v z H \tag{3.3}$$

$$\Sigma^{-1} = v^{-2} I - v^{-1} z H. \tag{3.4}$$

The first thing to check in $\mathcal{S}(\mathcal{R}_2^2)$ is the effect of multiplying Σ by the basis elements I and H .

Lemma 3.7.7 *In $\mathcal{S}(\mathcal{R}_2^2)$, we have $\Sigma I = \Sigma$ and $\Sigma H = H$.*

Proof. Multiplication of pure tangles is by juxtaposition; the lemma is obvious from the diagrams. \square

By equation 3.3 and lemma 3.7.7, we can say that multiplication by Σ in $\mathcal{S}(\mathcal{R}_2^2)$ has a 2×2 matrix

$$\begin{pmatrix} v^2 & 0 \\ vz & 1 \end{pmatrix}$$

with respect to basis $\{I, H\}$ of $\mathcal{S}(\mathcal{R}_2^2)$. That is, if $X = a_1 I + a_2 H \in \mathcal{S}(\mathcal{R}_2^2)$ is written as a column vector $\begin{pmatrix} a_1 \\ a_2 \end{pmatrix}$, then

$$\Sigma \begin{pmatrix} a_1 \\ a_2 \end{pmatrix} = \begin{pmatrix} v^2 & 0 \\ vz & 1 \end{pmatrix} \begin{pmatrix} a_1 \\ a_2 \end{pmatrix}.$$

The matrix is diagonalized by choosing the basis $\{\delta^{-1}H, I - \delta^{-1}H\}$.

Lemma 3.7.8 *In $\mathcal{S}(\mathcal{R}_2^2)$, $\delta^{-1}H$ and $I - \delta^{-1}H$ are idempotent and mutually orthogonal. Therefore $\{\delta^{-1}H, I - \delta^{-1}H\}$ is an orthogonal basis for $\mathcal{S}(\mathcal{R}_2^2)$.*

Proof. Diagrams confirm that $H^2 = H.H = \delta H$, and hence $\delta^{-2}H^2 = \delta^{-1}H$. Now write $g = \delta^{-1}H$ and $h = I - \delta^{-1}H = I - g \in \mathcal{S}(\mathcal{R}_2^2)$. Then

$$h^2 = (I - g)^2 = I^2 - 2I.g + g^2 = I - 2g + g = I - g = h.$$

Also, $gh = g(I - g) = g - g^2 = g - g = 0$. Similarly, $hg = 0$.

Since $\mathcal{S}(\mathcal{R}_2^2)$ is a 2-dimensional module (by lemma 3.7.5), $\{g, h\}$ forms an orthogonal basis for $\mathcal{S}(\mathcal{R}_2^2)$. \square

We retain the notation g and h for $\delta^{-1}H$, $I - \delta^{-1}H$ in what follows. We can now write the composite tangles $\Sigma.I$, $\Sigma.H$, $\Sigma^{-1}.I$ and $\Sigma^{-1}.H$ in terms of the orthogonal basis. For example,

$$\begin{aligned} \Sigma.I &= v^2 I + vz H \\ &= v^2 I + \frac{1-v^2}{\delta} H \\ &= \delta^{-1} H + v^2 (I - \delta^{-1} H) \\ &= g + v^2 h. \end{aligned}$$

Similarly, $\Sigma^{-1}.I = g + v^{-2}h$. Also, $\Sigma^{\pm 1}.H = H = \delta.\delta^{-1}H = \delta g$. The following lemma now comes easily.

Lemma 3.7.9 *In $\mathcal{S}(\mathcal{R}_2^2)$, we have $\Sigma^n = g + v^{2n}h$.*

Proof. By induction. This is certainly true for $|n| \leq 1$, by the above. Further, if we assume the result for indices m and n then

$$\begin{aligned}\Sigma^{m+n} &= \Sigma^m \Sigma^n \\ &= (g + v^{2m}h)(g + v^{2n}h) \\ &= g + v^{2(m+n)}h.\end{aligned}$$

□

It is easy to check that $\Sigma g = g$, and $\Sigma h = v^2h$. We can interpret this as saying that multiplication by Σ has been diagonalized. Now writing $X = a_1g + a_2h \in \mathcal{S}(\mathcal{R}_2^2)$ as a column vector $\begin{pmatrix} a_1 \\ a_2 \end{pmatrix}$, we get

$$\Sigma \begin{pmatrix} a_1 \\ a_2 \end{pmatrix} = \begin{pmatrix} 1 & 0 \\ 0 & v^2 \end{pmatrix} \begin{pmatrix} a_1 \\ a_2 \end{pmatrix}$$

with respect to basis $\{g, h\}$.

Now we apply lemma 3.7.9, via the linear map $\mathcal{D}_W : \mathcal{D}(\mathcal{R}_2^2) \rightarrow \mathcal{D}(S^2)$, where W is the wiring defined (as previously described) by the diagram of $C *_f P$. If $C *_f P = \mathcal{D}_W(I)$ has framing f , then the satellite $\mathcal{D}_W(\Sigma^n) = C *_f P$ has framing $f - n$.

The linear map \mathcal{D}_W induces a linear skein map $\mathcal{S}_W : \mathcal{S}(\mathcal{R}_2^2) \rightarrow \mathcal{S}(S^2)$, so that $\mathcal{S}_W(\Sigma^n)$ gives us the Homfly polynomial of the framing $(f - n)$ satellite. From lemma 3.7.9, and the linearity of \mathcal{S}_W , we have for $n \in \mathbf{Z}$,

$$\mathcal{S}_W(\Sigma^n) = \mathcal{S}_W(g) + v^{2n}\mathcal{S}_W(h).$$

3.7.II Proof of theorems 3.7.1 and 3.7.2

Proof of theorem 3.7.1. We choose a diagram D_f of $C *_f P$ in $\mathcal{D}(S^2)$, such that we can pick out a rectangle Γ as described; Γ bounds two rectangular discs F_1 and F_2 on S^2 . The wiring diagram W is $D_f \cap F_2$, and $D_f \cap F_1 = I \in \mathcal{R}_2^2$.

Therefore, by the work in the previous subsection,

$$\mathcal{S}_W(\Sigma^n) = \mathcal{S}_W(g) + v^{2n}\mathcal{S}_W(h).$$

By the linearity of the skein map, we deduce

$$\begin{aligned} \mathcal{S}_W(\Sigma^n) &= \mathcal{S}_W(\delta^{-1}H) + v^{2n}\mathcal{S}_W(I - \delta^{-1}H) \\ &= \delta^{-1}\mathcal{S}_W(H) + v^{2n}(\mathcal{S}_W(I) - \delta^{-1}\mathcal{S}_W(H)). \end{aligned}$$

The theorem follows easily from the observation that, in $S(S^2)$, the term $\mathcal{S}_W(I)$ equally represents the satellite link $C *_f P$, and also its Homfly polynomial $\mathcal{P}_{C *_f P}(v, z)$. Notice that $\mathcal{S}_W(\Sigma^n)$ corresponds to $C *_f P$, and $\mathcal{S}_W(H)$ corresponds to $C *_\infty P$. \square

Proof of theorem 3.7.2. Assume for the moment that $\mathcal{S}_W(g)$ and $\mathcal{S}_W(h)$ are both non-zero. Write

$$\begin{aligned} \mathcal{S}_W(g) &= \sum_{i=r}^R v^i Z_i(z) \\ \mathcal{S}_W(h) &= \sum_{i=s}^S v^i Y_i(z) \end{aligned}$$

such that $Z_i(z), Y_i(z) \in \mathbf{Z}[z^{\pm 1}]$, and $Z_r(z), Z_R(z), Y_s(z)$ and $Y_S(z)$ are all non-zero. Then we can deduce

$$\text{spr}_v(\mathcal{S}_W(\Sigma^n)) = \max(R, S + 2n) - \min(r, s + 2n).$$

Then there are two cases to consider.

1. $R - r \geq S - s$. Then

$$\text{spr}_v(\mathcal{S}_W(\Sigma^n)) = \begin{cases} R - (s + 2n) & \text{if } n \leq \frac{r-s}{2} \\ R - r & \text{if } \frac{R-S}{2} \geq n \geq \frac{r-s}{2} \\ (2n + S) - r & \text{if } n \geq \frac{R-S}{2} \end{cases}$$

In this case, $d = R - r$, $m = \frac{r-s}{2}$, $M = \frac{R-S}{2}$.

2. $R - r \leq S - s$. Then

$$\text{spr}_v(\mathcal{S}_W(\Sigma^n)) = \begin{cases} R - (s + 2n) & \text{if } n \leq \frac{R-S}{2} \\ S - s & \text{if } \frac{R-S}{2} \leq n \leq \frac{r-s}{2} \\ (2n + S) - r & \text{if } n \geq \frac{r-s}{2}. \end{cases}$$

In this case, $d = S - s$, $m = \frac{R-S}{2}$, $M = \frac{r-s}{2}$.

One can easily check that these equations are then those of the theorem.

We only have to check that $\mathcal{S}_W(g)$ and $\mathcal{S}_W(h)$ are both non-zero in $\mathcal{S}(S^2)$. Since $F_2 \cap D_f$ is another $(2, 2)$ -tangle in \mathcal{R}_2^2 , then $W \in \mathcal{D}(\mathcal{R}_2^2)$, and so within the skein module $\mathcal{S}(\mathcal{R}_2^2)$ we may write

$$W = a_1 \cdot g + a_2 \cdot h$$

with $a_1, a_2 \in \Lambda$, since $\mathcal{S}(\mathcal{R}_2^2)$ is a 2-dimensional module spanned by g, h . Now use the bilinear map

$$\begin{aligned} \mathcal{S}(\mathcal{R}_2^2) \times \mathcal{S}(\mathcal{R}_2^2) &\rightarrow \mathcal{S}(\mathcal{R}_2^2) \\ W \times \Sigma^n &\mapsto W \cdot \Sigma^n \\ &= (a_1 \cdot g + a_2 \cdot h)(g + v^{2n} \cdot h) \\ &= a_1 \cdot g + v^{2n} a_2 \cdot h. \end{aligned}$$

Finally we wire them together into $\mathcal{S}(S^2)$ using the wiring W_I as in figure 3.60. The corresponding linear map $\mathcal{S}(W_I) : \mathcal{S}(\mathcal{R}_2^2) \rightarrow \mathcal{S}(S^2)$ gives

$$\begin{aligned} \mathcal{S}_{W_I}(W \cdot \Sigma^n) &= \mathcal{S}_{W_I}(a_1 \cdot g + v^{2n} a_2 \cdot h) \\ &= a_1 \mathcal{S}_{W_I}(g) + v^{2n} a_2 \mathcal{S}_{W_I}(h). \end{aligned}$$

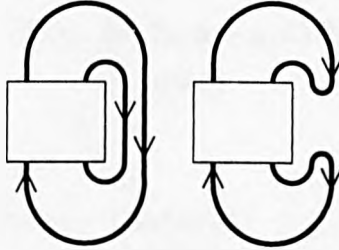


Figure 3.60: Wirings W_I and W_H

Now $\mathcal{S}_{W_I}(W \cdot \Sigma^n) = \mathcal{S}_W(\Sigma^n)$, so the triviality of $\mathcal{S}_W(g)$ and $\mathcal{S}_W(h)$ comes down to the triviality of $a_1, a_2, \mathcal{S}_{W_I}(g)$ and $\mathcal{S}_{W_I}(h)$. We discuss three of them in the following lemma.

Lemma 3.7.10 *In $\mathcal{S}(S^2)$, we have $a_1, \mathcal{S}_{W_I}(g)$ and $\mathcal{S}_{W_I}(h)$ are all non-zero.*

Proof. Let U_n denote the unlink of n components. Then working in $\mathcal{S}(S^2)$,

$$\begin{aligned}
\mathcal{S}_{W_I}(g) &= \delta^{-1}\mathcal{S}_{W_I}(H) \\
&= \delta^{-1}.U_1 \\
&= \delta^{-1} \\
&\neq 0
\end{aligned}$$

and

$$\begin{aligned}
\mathcal{S}_{W_I}(h) &= \mathcal{S}_{W_I}(I) - \delta^{-1}\mathcal{S}_{W_I}(H) \\
&= U_2 - \delta^{-1}.U_1 \\
&= \delta - \delta^{-1} \\
&\neq 0.
\end{aligned}$$

Also, $W = a_1.g + a_2.h = (a_1 - a_2).g + a_2(g + h) = (a_1 - a_2)\delta^{-1}.H + a_2.I$, so using the wiring W_H ,

$$\begin{aligned}
\mathcal{S}_{W_H}(W) &= \mathcal{S}_{W_H}((a_1 - a_2)\delta^{-1}.H + a_2.I) \\
&= (a_1 - a_2)\delta^{-1}\mathcal{S}_{W_H}(H) + a_2\mathcal{S}_{W_H}(I) \\
&= (a_1 - a_2)\delta^{-1}.U_2 + a_2U_1 \\
&= (a_1 - a_2)\delta^{-1}.\delta + a_2 \\
&= a_1.
\end{aligned}$$

So we see that a_1 is the Homfly polynomial of a link, and hence is non-zero. \square

Finally, we must deal with a_2 . Note that in $\mathcal{S}(\mathcal{R}_2^2)$,

$$\begin{aligned}
W.h &= (a_1g + a_2h).h \\
&= a_2h,
\end{aligned}$$

and therefore in $\mathcal{S}(S^2)$,

$$\begin{aligned}
\mathcal{S}_{W_I}(W.h) &= \mathcal{S}_{W_I}(a_2h) \\
&= a_2\mathcal{S}_{W_I}(h) \\
&= a_2\mathcal{S}_{W_I}(I - \delta^{-1}H) \\
&= a_2\mathcal{S}_{W_I}(I) - a_2\delta^{-1}\mathcal{S}_{W_I}(H) \\
&= a_2.U_2 - a_2\delta^{-1}.U_1 \\
&= a_2(\delta - \delta^{-1}).
\end{aligned}$$

Now $\delta - \delta^{-1} \neq 0$, so

$$\begin{aligned}
a_2 = 0 &\Leftrightarrow \mathcal{S}_{W_I}(W.h) = 0 \\
&\Leftrightarrow \mathcal{S}_{W_I}(W.(I - \delta^{-1}H)) = 0 \\
&\Leftrightarrow \mathcal{S}_{W_I}(W.I) - \delta^{-1}\mathcal{S}_{W_I}(W.H) = 0 \\
&\Leftrightarrow \delta\mathcal{S}_{W_I}(W) - \mathcal{S}_{W_I}(W.H) = 0 \\
&\Leftrightarrow \mathcal{S}_{W_I}(W.I \sqcup U_1) = \mathcal{S}_{W_I}(W.H).
\end{aligned}$$



Figure 3.61: Orientation of W at boundary

Now recall that as a $(2, 2)$ -tangle, $W \in \mathcal{D}(\mathcal{R}_2^2)$ has orientation at the boundary as in figure 3.61.

Consider the component W_1 (say) of W which enters the rectangle Γ at the top-right corner. Now by consideration of orientation, W_1 must exit Γ at either the bottom-right or top-left corner, but not the bottom-left corner. Since the two point intersections of P with D come from different components of P , W_1 must exit R_2^2 at the bottom-right corner. In this case, $\mathcal{D}_{W_I}(W.I)$ has one more component than $\mathcal{D}_{W_I}(W.H)$. See figure 3.62.

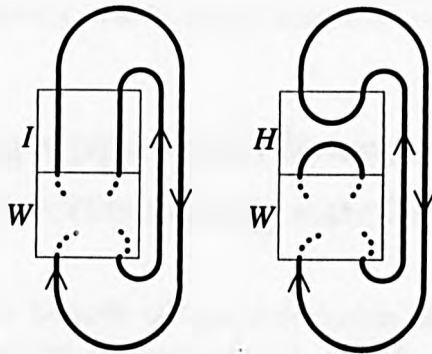


Figure 3.62: $\mathcal{D}_{W_I}(W.I)$ and $\mathcal{D}_{W_I}(W.H)$

Therefore, $\mathcal{D}_{W_I}(W.I \sqcup U_1)$ has two more components than $\mathcal{D}_{W_I}(W.H)$. By theorem 1.5.1(ii), $\text{mindeg}_z \mathcal{P}_L = 1 - |L|$; and therefore, the Homfly polynomials of these links cannot be equal. Hence, for patterns which satisfy the hypotheses, $a_2 \neq 0$.

The proof of theorem 3.7.2 is now complete. □

There are in fact many patterns for which the result of theorem 3.7.2 holds, although they do not satisfy the hypotheses of the theorem; the Whitehead doubles are an example of such. The only problem is in asserting that a_2 is non-zero,

as in the proof of theorem 3.7.2. There may be a number of ways around this: for example, a positive assertion that (for a general link L) δ^n divides $\mathcal{P}_L(v, z)$ if, and only if, $L = U_n \sqcup L'$, for some other link L' , would be enough. In fact, we take the conjecture one step further.

Conjecture 3.7.11 *Let P be a general reverse string pattern, and let D be a meridional disc which intersects P in p_1 positive intersections and n_1 negative intersections. We may suppose without loss of generality that $p_1 \leq p_i, n_i$ for all i . Then I conjecture that the coefficient of linearity in the theorem in the cases $f \leq m$ and $f \geq M$ is equal to $2p_1$. In other words, there exist integers m, M and d with $m \leq M$, independent of f , such that*

$$\begin{aligned} f \leq m &\Rightarrow \operatorname{spr}_v \left(\mathcal{P}_{C *_f P}(v, z) \right) = d + 2p_1 |m - f| \\ m \leq f \leq M &\Rightarrow \operatorname{spr}_v \left(\mathcal{P}_{C *_f P}(v, z) \right) = d \\ M \leq f &\Rightarrow \operatorname{spr}_v \left(\mathcal{P}_{C *_f P}(v, z) \right) = d + 2p_1 |M - f|. \end{aligned}$$

Such a conjecture is supported by theorem 3.7.2, which shows it to be true in a special case; also from the fact that $\operatorname{spr}_v \left(\mathcal{P}_{C *_f P}(v, z) \right)$ provides a lower bound for the braid index $b(C *_f P)$, from the MFW inequality, and its upper bound (from construction of explicit braids, in sections 3.5 and 3.6) behaves similarly.

3.8 Comparing upper and lower bounds for braid index of reverse string satellites

We have upper and lower bounds of the braid index of a reverse string satellite $C *_f P$. What is more, we know about the linear behaviour of the upper bound (from explicit braid representations of $C *_f P$) and of the lower bound (for certain patterns, from examination of the Homfly polynomial) as the framing f varies in \mathbf{Z} .

The question remains as to how well these bounds compare: is it possible for the upper and lower bounds to be equal, and hence give a precise value for $b(C *_f P)$? Preliminary experimentation has produced the following result.

Theorem 3.8.1 *Let K be a knot with $\alpha(K) \leq 9$, and $K \neq 10_{132}$. Let P be the $(1,1)$ -antiparallel pattern. Then there exists $f_+, f_- \in \mathbf{Z}$ such that $f_+ - f_- = \alpha(K)$, and*

$$f \in [f_-, f_+] \Leftrightarrow 1 + \frac{1}{2} \operatorname{spr}_v \left(\mathcal{P}_{(K *_f P)}(v, z) \right) = \alpha(K).$$

Remark. In the case $K = 10_{132}$, we find that there exists $f_+, f_- \in \mathbf{Z}$ such that $f_+ - f_- = \alpha(K) - 1$, and

$$f \in [f_-, f_+] \Leftrightarrow 1 + \frac{1}{2} \text{spr}_v \left(\mathcal{P}_{(K *_f P)}(v, z) \right) = \alpha(K) - 1.$$

It may be of some interest to note that $K = 10_{132}$ is the only knot with arc index $\alpha(K) \leq 9$ which shares its Homfly polynomial with a knot of smaller arc index.

Proof of theorem 3.8.1. By observation, following the computation of explicit Homfly polynomials. All knots K of arc index $\alpha(K) \leq 9$ are positively identified by the computer algorithm in chapter 5. Arc presentations are also generated by the algorithm, and so braid presentations of $K *_f P$ (as in the example in figures 3.44 and 3.45), for variable f , can be easily generated using a simple PASCAL algorithm. Then Short's polynomial program [M-S] is employed to compute $\mathcal{P}_{(K *_f P)}$. \square

Remark. It remains unknown whether there exists a family $\{K *_f P : f \in \mathbf{Z}\}$ of reverse string satellites, and a constant k for which $b(K *_f P) < k$, for all $f \in \mathbf{Z}$.

Chapter 4

The modulus of quasipositivity

4.1 Introduction

The work of Rudolph [Ru2, Ru3, Ru4] provides us with material which compares well with the constructions seen so far in this thesis. Some of his ideas can be exploited here.

The property of *quasipositivity* of a knot K , and an associated knot invariant, the *modulus of quasipositivity* $q(K)$, were used as tools in the study of complex plane curves. Rudolph studies quasipositivity, as it occurs in ordinary knot theory, via a certain type of satellite, the (1,1)-antiparallel.

In section 4.2 we make a number of important definitions, and a connection is made between the (1,1)-antiparallels of chapter 3 and Rudolph's quasipositive annuli [Ru4]. In section 4.3 we state some results relating to polynomial invariants from the context of Rudolph's work: in section 4.4 these are used to deduce a lower bound for arc index from the Kauffman polynomial $F_L(a, x)$, which bears a striking similarity to a result relating crossing index to Jones' polynomial $V_L(t)$. Further comments and observations serve to reinforce this similarity.

4.2 Quasipositivity and arc index

Rudolph defines the (1,1)-antiparallel satellite of a knot C with framing f as follows. Let $A(C, f)$ be an oriented annulus in S^3 with $C \subset \partial A(C, f)$, and $\text{lk}(C, \partial A(C, f) - C) = -f$. It should be noted that the orientation on $A(C, f)$ induces an orientation on its boundary, so that $\partial A(C, f)$ is the (1,1)-antiparallel

satellite of C with framing f . Rudolph's notation for this will be of use throughout this chapter.

A *positive embedded band* $\sigma_{i,j} \in B_n$ is a braid

$$\sigma_{i,j} = (\sigma_i \sigma_{i+1} \dots \sigma_{j-2}) \sigma_{j-1} (\sigma_{j-2}^{-1} \dots \sigma_{i+1}^{-1} \sigma_i^{-1}), 1 \leq i < j \leq n.$$

A *negative embedded band* is the inverse of a positive embedded band:

$$\sigma_{i,j}^{-1} = (\sigma_i \sigma_{i+1} \dots \sigma_{j-2}) \sigma_{j-1}^{-1} (\sigma_{j-2}^{-1} \dots \sigma_{i+1}^{-1} \sigma_i^{-1}).$$

This is illustrated in figure 4.1.

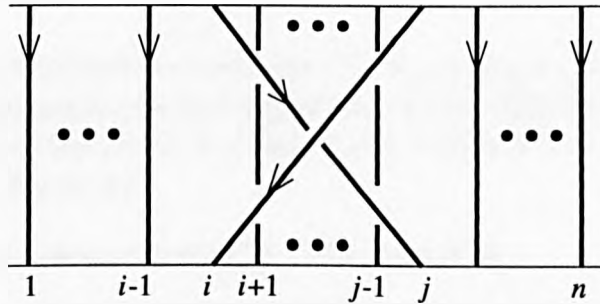


Figure 4.1: A positive embedded band $\sigma_{i,j} \in B_n$

In particular, every elementary braid generator σ_i is a positive embedded band $\sigma_{i,i+1}$, so every link has an embedded band representation.

We say that a braid representation $\beta = \prod_{s=1}^k \sigma_{i(s)}^{\varepsilon(s)}$ is *positive* if each $\varepsilon(s) = 1$; similarly we say that an embedded band representation $\beta = \prod_{s=1}^k \sigma_{i(s),j(s)}^{\varepsilon(s)}$ is *quasipositive* if each $\varepsilon(s) = 1$. Naturally, β is *quasinegative* if each $\varepsilon(s) = -1$. So β positive $\Rightarrow \beta$ quasipositive, but the reverse is not true.

A link L is *quasipositive* if there exists a quasipositive braid β whose closure $\hat{\beta}$ is ambient isotopic to L .

At this point, we make the observation that the braid representations of (1,1)-antiparallel satellites generated in section 3.5 were all embedded band representations. For example, the trefoil antiparallel was presented as the closure of the braid given in figure 4.2.

This braid can be written in B_5 as $\beta = \sigma_{3,4} \sigma_{2,3} \sigma_{1,2} \sigma_{2,4}^{-1} \sigma_{1,3}^{-1}$. The ‘change of framing’ description of figure 3.50, section 3.6 (and also illustrated in figures 3.44 and 3.45) amounts to reversing the sign of an embedded band $\sigma_{i,j}^{\pm 1}$. By changing

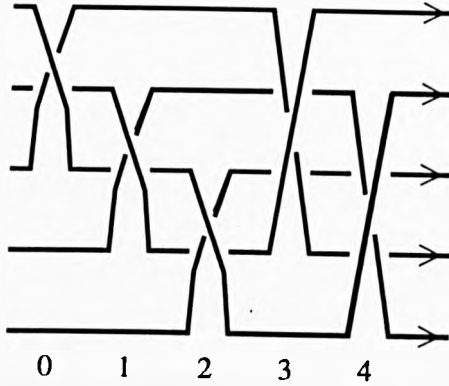


Figure 4.2: Braid representing trefoil antiparallel

the signs of the last two factors of β we get $\beta = \sigma_{3,4}\sigma_{2,3}\sigma_{1,2}\sigma_{2,4}\sigma_{1,3}$, which is a braid representing a *quasipositive* antiparallel of the trefoil. Similarly, a *quasinegative*-framed antiparallel of the trefoil is given by the closure of $\beta = \sigma_{3,4}^{-1}\sigma_{2,3}^{-1}\sigma_{1,2}^{-1}\sigma_{2,4}^{-1}\sigma_{1,3}^{-1}$. Both are shown in figure 4.3.

The *modulus of quasipositivity* $q(K)$ of a knot K is

$$q(K) = \sup \{ f \in \mathbf{Z} : \partial A(K, f) \text{ is quasipositive} \}.$$

Similarly, the *modulus of quasinegativity* $r(K)$ is defined as

$$r(K) = \inf \{ f \in \mathbf{Z} : \partial A(K, f) \text{ is quasinegative} \}.$$

Theorem 4.2.1 [Ru2, Ru4] *For any knot K , $\infty > q(K) > -\infty$.* □

The first of these inequalities is deduced from an observation of the Homfly polynomial (see theorem 4.2.6). The second is a corollary of the following.

Theorem 4.2.2 [Ru2] *Let $\beta \in B_n$ be a braid on n strings, with exponent sum e , and closure $\hat{\beta} = K$. Then $q(K) \geq e - n$.* □

Using the braid diagrams of sections 3.5 and 3.6, we can now make a direct relation between arc index and modulus of quasipositivity.

Proposition 4.2.3 *For any knot K , $\alpha(K) \geq r(K) - q(K)$.*

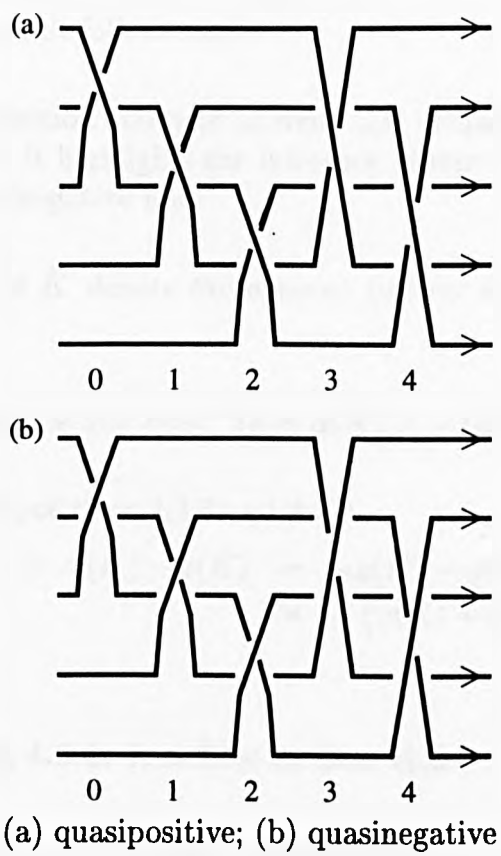


Figure 4.3: Quasipositive and quasinegative antiparallels of the trefoil

Remark. In theorem 4.2.7 we shall see that for all knots K , the value of $r(K) - q(K)$, and hence of $\alpha(K)$, is at least 2.

Proof of proposition 4.2.3. Let $G(K)$ be a grid diagram of K , based on an arc presentation of K using $\alpha(K)$ arcs. By the description in section 3.6 (figures 3.48 and 3.49), we can use $G(K)$ to construct an embedded band presentation of $\partial A(K, f)$ (for some f), similar to figure 4.2. From this, we can easily construct a quasipositive-framed antiparallel (call it $\partial A(K, f_+)$) and also a quasinegative-framed antiparallel, $\partial A(K, f_-)$ (compare to figure 4.3). From the construction, $\alpha(K) = f_- - f_+$. By the definitions of $q(K)$ and $r(K)$ we know that $f_+ \leq q(K)$ and $f_- \geq r(K)$. The result follows easily. \square

The following proposition allows us to write this inequality using the modulus of quasipositivity only. It highlights the influence of mirror images in comparing quasipositive and quasinegative links.

Proposition 4.2.4 *Let \bar{K} denote the obverse (mirror image) of K . Then we have $q(K) = -r(\bar{K})$.*

Corollary 4.2.5 *Let K be any knot. Then $\alpha(K) \geq -(q(\bar{K}) + q(K))$.*

Proof. Combining propositions 4.2.3 and 4.2.4,

$$\begin{aligned} \alpha(K) &\geq r(K) - q(K) = -q(\bar{K}) - q(K) \\ &= -(q(\bar{K}) + q(K)). \end{aligned}$$

\square

Proof of proposition 4.2.4. It suffices to show that

- (i) the obverse of a quasipositive link is quasinegative;
- (ii) the framing is negated by reflection.

Then $\overline{\partial A(K, q(K))}$ is quasinegative by (i), and has framing $-q(K)$ by (ii). So we can write $\overline{\partial A(K, q(K))} = \partial A(\bar{K}, -q(K))$.

Now if $-q(K) \neq r(\bar{K})$ then we must have $r(\bar{K}) < -q(K)$, because $r(\bar{K})$ is the *least* value of f which ensures that $\partial A(\bar{K}, f)$ is quasinegative. In particular, we can deduce that $\partial A(\bar{K}, -q(K) - 1)$ is quasinegative. This implies that $\partial A(K, q(K) + 1)$ is quasipositive; but we have that

$$q(K) + 1 > \sup \{ f : \partial A(K, f) \text{ is quasipositive} \},$$

giving a contradiction.

To prove (i): let L be a quasipositive link, and β be a quasipositive embedded band representation of L . Then $\beta = \prod_{s=1}^k \sigma_{i(s),j(s)}$. Now the obverse of a positive embedded band is a negative embedded band:

$$\overline{\sigma_{i,j}} = \sigma_{n-j,n-i}^{-1} \in B_n.$$

A quick sketch will convince the reader of this. The obverse, \bar{L} , is represented by $\bar{\beta}$, which is given by

$$\bar{\beta} = \prod_{s=1}^k \overline{\sigma_{i(s),j(s)}} = \prod_{s=1}^k \sigma_{n-j(s),n-i(s)}^{-1},$$

and hence \bar{L} is quasinegative.

To prove (ii): note that the framing is extracted by a count of the signs of certain crossings. By reflecting, the signs of all the crossings, and in particular those relevant to the framing, are negated. We deduce that framing is negated by reflection. \square

Remark. Using theorem 4.2.2, we can quickly deduce that the inequality of proposition 4.2.3 (and corollary 4.2.5) is sometimes strict. Writing $\beta = \prod_{s=1}^k \sigma_{i(s)}^{\varepsilon(s)} \in B_n$, and $K = \hat{\beta}$, we have by theorem 4.2.2

$$q(K) \geq \left(\sum_{s=1}^k \varepsilon(s) \right) - n,$$

and

$$\begin{aligned} q(\bar{K}) &\geq \left(\sum_{s=1}^k (-\varepsilon(s)) \right) - n \\ &\geq - \left(\sum_{s=1}^k \varepsilon(s) \right) - n. \end{aligned}$$

Putting these together we get

$$- \left(q(K) + q(\bar{K}) \right) \leq 2n.$$

Now let us suppose that the inequality is never strict, *i.e.* for any knot K , we have $\alpha(K) = - \left(q(K) + q(\bar{K}) \right)$. This implies $\alpha(K) \leq 2b(K)$. We already know (by proposition 2.5.1) that $\alpha(K) \geq 2b(K)$, and so we conclude that for all knots,

$$\alpha(K) = 2b(K).$$

This we know not to be true. A rich source of counter-examples are the (l, m) torus links, for $l \neq m$.

Rudolph's study of upper bound for $q(K)$ allows us to relate $q(K)$ and $r(K)$. We define the polynomial $R_K(v) \in \mathbf{Z}[v^{\pm 1}]$ by

$$R_K(v) = z^{|K|-1} \mathcal{P}_K(v, z)|_{z=0}.$$

Since $\text{mindeg}_z \mathcal{P}_K(v, z) = 1 - |K|$, we know $R_K(v)$ must be non-zero, and so $\text{spr}_v R_K(v) \geq 0$.

Theorem 4.2.6 [Ru4] *For any knot K , we have $q(K) \leq -1 + \text{mindeg}_v R_K$. \square*

We can deduce the following.

Theorem 4.2.7 *For any knot K , we have $r(K) > q(K) + 1$.*

Proof. By theorem 4.2.6,

$$q(K) \leq -1 + \text{mindeg}_v R_K.$$

Also,

$$\begin{aligned} q(\bar{K}) &\leq -1 + \text{mindeg}_v R_{\bar{K}} \\ \Rightarrow q(\bar{K}) &\leq -1 - \text{maxdeg}_v R_K. \end{aligned}$$

Therefore

$$\begin{aligned} q(K) + q(\bar{K}) &\leq -2 - (\text{maxdeg}_v R_K - \text{mindeg}_v R_K) \\ &\leq -2 - \text{spr}_v R_K \\ &\leq -2. \end{aligned}$$

So $q(K) - r(K) \leq -2$, by proposition 4.2.4. \square

Corollary 4.2.8 *Let K be any knot. Then*

- (i) *there exists $f \in \mathbf{Z}$, $\infty > f > -\infty$ such that $\partial A(K, f)$ is quasipositive;*
- (ii) *there exists $f \in \mathbf{Z}$, $\infty > f > -\infty$ such that $\partial A(K, f)$ is quasinegative;*
- (iii) *there does not exist any $f \in \mathbf{Z}$ such that $\partial A(K, f)$ is both quasipositive and quasinegative; further,*
- (iv) *there exists $f \in \mathbf{Z}$ such that $\partial A(K, f)$ is neither quasipositive nor quasinegative.*

Proof. These statements are deduced directly from theorems 4.2.1 and 4.2.7. \square

4.3 The framed polynomial

In this section we meet a polynomial which is an invariant of links up to regular isotopy, introduced into the work of Rudolph in [Ru5]. We also state a couple of results of Rudolph, pertaining to this polynomial invariant, which are of use in the following section.

Recall the definition $\partial A(C, f)$ for the (1,1)-antiparallel of C . We extend it slightly, so that for a general link L , $A(L, f)$ is a choice of disjoint annuli, such that $L \subset \partial A(L, f)$, and also $\text{lk}(L_i, \partial A(L_i, f_i)) = f_i$, where L_i are the components of L . So $A(L, f)$ defines a choice of parallel to each component of L , which is completely determined by the f_i .

Since both Kauffman and Homfly polynomials are used here, it is useful to adopt the notation $\delta_F(a, x) = F_{U_2}(a, x) = \frac{a^{-1}-x+a}{x}$, $\delta_P(v, z) = \mathcal{P}_{U_2}(v, z) = \frac{v^{-1}-v}{z}$.

The *framed polynomial* is defined to be

$$\mathcal{A}_{L,f}(v, z) = (-1)^{|L|} \left(1 + \delta_P \sum_{L'} (-1)^{|L'|} \mathcal{P}_{\partial A(L', f|_{L'})} \right)$$

where L' runs through the non-empty sublinks of L .

Proposition 4.3.1 [Ru4] *Given an antiparallel satellite $\partial A(L, f)$, define its total framing $\phi(L, f)$ to be $\phi(L, f) = \sum_i f_i$. Then*

$$\mathcal{A}_{L,f}(v, z) = v^{-2\phi(L,f)} \mathcal{A}_{L,0}(v, z).$$

□

In the case $|L| = 1$, then $\mathcal{A}_{L,f}(v, z) = \delta_P \mathcal{P}_{\partial A(L,f)}(v, z) - 1$, and $\phi(L, f) = f$. So the case $|L| = 1$ is a corollary of theorem 3.7.1.

The second proposition is a rather curious result which relates the Homfly and Kauffman polynomials via the framed polynomial.

Proposition 4.3.2 [Ru5] *Given a link L with components L_i , $i = 1, \dots, |L|$, define its total linking number $\tau(L)$ to be $\tau(L) = \sum_{i < j} \text{lk}(L_i, L_j)$. Then*

$$\delta_F(v^{-2}, z^2) F_L(v^{-2}, z^2) \equiv v^{4\tau(L)} \mathcal{A}_{L,0}(v, z), \text{ mod } 2.$$

□

The apparent complexity of this congruence is reduced if it is rewritten in terms of Kauffman and Homfly polynomials with the alternative normalizations $F_O(a, x) = \delta_F(a, x)$, $\mathcal{P}_O(v, z) = \delta_{\mathcal{P}}(v, z)$. However, for reasons of continuity we will stay with Rudolph's version, corresponding to the normalization $F_O(a, x) = 1 = \mathcal{P}_O(v, z)$.

When $|L| = 1$ this reads

$$\delta_F(v^{-2}, z^2)F_L(v^{-2}, z^2) \equiv \delta_{\mathcal{P}}\mathcal{P}_{\partial A(L, f)}(v, z) - 1, \text{ mod } 2.$$

4.4 A lower bound for arc index from the Kauffman polynomial

In this section we discuss and prove a relationship between Kauffman's polynomial $F_L(a, x)$ and the arc index $\alpha(L)$. The proof draws together a number of results already presented in this thesis. In section 4.5 we make a conjecture, based on this bound and also on strong observational evidence, linking arc index and crossing number as an extension of theorem 2.5.2.

Define $G_L(a, x) = F_L(a, x) \text{ mod } 2$, *i.e.* Kauffman polynomial with coefficients reduced modulo 2. Note that Rudolph uses the notation G to denote something else in [Ru4].

Theorem 4.4.1 *Let K be a knot. Then $\alpha(K) \geq 2 + \text{spr}_a G_K(a, x)$.*

Proof. Let $G(K)$ be a grid diagram of K , based on an arc-presentation of K on $\alpha(K)$ arcs. From $G(K)$, we can construct, for some f^* , an embedded band diagram of $\partial A(K, f^*)$ on exactly $\alpha(K)$ braidstrings: we deduce that $b(\partial A(K, f^*)) \leq \alpha(K)$. By the MFW inequality (theorem 1.5.1(i)),

$$\alpha(K) \geq b(\partial A(K, f^*)) \geq 1 + \frac{1}{2}\text{spr}_v \left(\mathcal{P}_{\partial A(K, f^*)}(v, z) \right).$$

Notice that $2 + \text{spr}_v \left(\mathcal{P}_{\partial A(K, f^*)}(v, z) \right) = \text{spr}_v \left(\delta_{\mathcal{P}}\mathcal{P}_{\partial A(K, f^*)}(v, z) \right)$, since $\delta_{\mathcal{P}} = \frac{v^{-1}-v}{z}$. Therefore,

$$\alpha(K) \geq b(\partial A(K, f^*)) \geq \frac{1}{2}\text{spr}_v \left(\delta_{\mathcal{P}}\mathcal{P}_{\partial A(K, f^*)}(v, z) \right). \quad (4.1)$$

By proposition 4.3.1, we have $\delta_{\mathcal{P}}\mathcal{P}_{\partial A(K, 0)} - 1 = v^{2f} \left(\delta_{\mathcal{P}}\mathcal{P}_{\partial A(K, f)} - 1 \right)$ for all $f \in \mathbf{Z}$. In particular this is true when $f = m$, the 'least framing' of theorem

3.7.2. We write

$$\delta_{\mathcal{P}}\mathcal{P}_{\partial A(K,m)} = \sum_{i=d}^D Z_i(z)v^i,$$

where $Z_i(z) \in \mathbf{Z}[z^{\pm 1}]$ and $Z_d \neq 0 \neq Z_D$.

We show that $d = 0$, and also that $Z_d(z) \neq 1$, and hence

$$\text{spr}_v \left(\delta_{\mathcal{P}}\mathcal{P}_{\partial A(K,m)} - 1 \right) = \text{spr}_v \left(\delta_{\mathcal{P}}\mathcal{P}_{\partial A(K,m)} \right) = D - d.$$

Then we deduce, using proposition 4.3.1, that for all $f \in \mathbf{Z}$,

$$\text{spr}_v \left(\delta_{\mathcal{P}}\mathcal{P}_{\partial A(K,f)} - 1 \right) = D - d.$$

In particular, we deduce

$$\text{spr}_v \left(\delta_{\mathcal{P}}\mathcal{P}_{\partial A(K,0)} - 1 \right) = D - d. \quad (4.2)$$

By theorem 3.7.2, for all f , we have

$$\text{spr}_v \left(\delta_{\mathcal{P}}\mathcal{P}_{\partial A(K,f)} \right) \geq D - d, \quad (4.3)$$

and then it follows from equations 4.1, 4.3 and 4.2 respectively that

$$\begin{aligned} \alpha(K) &\geq \frac{1}{2} \text{spr}_v \left(\delta_{\mathcal{P}}\mathcal{P}_{\partial A(K,f^*)}(v, z) \right) \\ &\geq \frac{1}{2} (D - d) \\ &\geq \frac{1}{2} \text{spr}_v \left(\delta_{\mathcal{P}}\mathcal{P}_{\partial A(K,0)} - 1 \right). \end{aligned} \quad (4.4)$$

Using equation 4.4, and then the ‘mod 2’ congruence of proposition 4.3.2, we have

$$\begin{aligned} \alpha(K) &\geq \frac{1}{2} \text{spr}_v \left(\delta_{\mathcal{P}}\mathcal{P}_{\partial A(K,0)} - 1 \right) \\ &\geq \frac{1}{2} \text{spr}_v \left((\delta_{\mathcal{P}}\mathcal{P}_{\partial A(K,0)} - 1) \bmod 2 \right) \\ &= \frac{1}{2} \text{spr}_v \left(\delta_F G_K(v^{-2}, z^2) \right). \end{aligned}$$

The final step is to note that

$$\begin{aligned} \alpha(K) &\geq \frac{1}{2} \text{spr}_v \left(\delta_F G_K(v^{-2}, z^2) \right) = \frac{1}{2} \text{spr}_v \left(\frac{v^{-2} - z^2 + v^2}{z^2} G_K(v^{-2}, z^2) \right) \\ &= \text{spr}_a \left(\frac{a^{-1} - x + a}{x} G_K(a, x) \right) \\ &= 2 + \text{spr}_a \left(G_K(a, x) \right). \end{aligned}$$

It remains to show that, if $\delta_{\mathcal{P}}\mathcal{P}_{\partial A(K,m)} = \sum_{i=d}^D Z_i(z)v^i$, then (i) $d = 0$, and (ii) $Z_d(z) \neq 1$. The arguments for these run as follows.

To prove (ii), we assume that (i) is true, *i.e.* $d = 0$. From theorem 4.3.1, we have

$$\delta_{\mathcal{P}}\mathcal{P}_{\partial A(K,m)} - 1 = v^2\delta_{\mathcal{P}}\mathcal{P}_{\partial A(K,m+1)} - v^2,$$

and hence

$$\sum_{i=d}^D Z_i(z)v^i - 1 + v^2 = v^2\delta_{\mathcal{P}}\mathcal{P}_{\partial A(K,m+1)}.$$

Suppose, for a contradiction, that $Z_d(z) = 1$. Since $d = 0$, we can quickly deduce that the polynomial on the left has spread at most $D - d - 2$ in the v -variable, and hence the same is true of the polynomial on the right. That is,

$$\text{spr}_v \left(\delta_{\mathcal{P}}\mathcal{P}_{\partial A(K,m+1)} \right) \leq D - d - 2.$$

But by theorem 3.7.2, we know that for all $f \in \mathbf{Z}$,

$$\text{spr}_v \left(\delta_{\mathcal{P}}\mathcal{P}_{\partial A(K,f)} \right) \geq \text{spr}_v \left(\delta_{\mathcal{P}}\mathcal{P}_{\partial A(K,m)} \right) = D - d,$$

and so we have a contradiction.

To prove (i), we make some very careful observations of the restrictions on $\text{mindeg}_v \left(\delta_{\mathcal{P}}\mathcal{P}_{\partial A(K,f)} \right)$ and $\text{maxdeg}_v \left(\delta_{\mathcal{P}}\mathcal{P}_{\partial A(K,f)} \right)$, for $f = m - 1, m, m + 1$. From theorem 3.7.2 we know

$$\begin{aligned} \text{spr}_v \left(\delta_{\mathcal{P}}\mathcal{P}_{\partial A(K,m-1)} \right) &= D - d + 2, \\ \text{spr}_v \left(\delta_{\mathcal{P}}\mathcal{P}_{\partial A(K,m)} \right) &= D - d, \\ \text{spr}_v \left(\delta_{\mathcal{P}}\mathcal{P}_{\partial A(K,m+1)} \right) &= D - d \text{ or } D - d + 2. \end{aligned}$$

To compare the least and greatest powers of v in these polynomials, we write

$$\begin{aligned} \delta_{\mathcal{P}}\mathcal{P}_{\partial A(K,m-1)} &= v^2\delta_{\mathcal{P}}\mathcal{P}_{\partial A(K,m)} - v^2 + 1 \\ &= v^2 \sum_{i=d}^D Z_i(z)v^i - v^2 + 1 \\ &= \sum_{i=d}^D Z_i(z)v^{i+2} - v^2 + 1 \\ &= \sum_{j=e}^E Y_j(z)v^j, \text{ say,} \end{aligned} \tag{4.5}$$

and

$$\delta_{\mathcal{P}}\mathcal{P}_{\partial A(K,m+1)} = v^{-2}\delta_{\mathcal{P}}\mathcal{P}_{\partial A(K,m)} - v^{-2} + 1$$

$$\begin{aligned}
&= v^{-2} \sum_{i=d}^D Z_i(z)v^i - v^{-2} + 1 \\
&= \sum_{i=d}^D Z_i(z)v^{i-2} - v^{-2} + 1 \\
&= \sum_{j=g}^G X_j(z)v^j, \text{ say.}
\end{aligned} \tag{4.6}$$

By comparison of the last two lines of equation 4.5,

$$\begin{aligned}
E &\leq \max\{D + 2, 2, 0\} = \max\{D + 2, 2\} \\
e &\geq \min\{d + 2, 2, 0\} = \min\{d + 2, 0\}.
\end{aligned}$$

In fact, we have

$$\left. \begin{aligned}
E &= \max\{D + 2, 2\} \text{ or } D = 0, \\
e &= \min\{d + 2, 0\} \text{ or } d = -2.
\end{aligned} \right\} \tag{4.7}$$

A similar comparison in equation 4.6 gives

$$\begin{aligned}
G &\leq \max\{D - 2, -2, 0\} = \max\{D - 2, 0\} \\
g &\geq \min\{d - 2, -2, 0\} = \min\{d - 2, -2\}.
\end{aligned}$$

Again this simplifies to

$$\left. \begin{aligned}
G &= \max\{D - 2, 0\} \text{ or } D = 2, \\
g &= \min\{d - 2, -2\} \text{ or } d = 0.
\end{aligned} \right\} \tag{4.8}$$

We consider the four possible combinations for E and e in equations 4.7, for different values of d , generating contradictions. Some cases are excluded by further considering the four possible combinations for G and g in equations 4.8, as we will see.

Suppose firstly that $d > 0$. Therefore $d > -2$, and since $D > d$ we have $D > 0$. Referring to equations 4.7, there is only one case to consider: $E = \max\{D + 2, 2\}$, $e = \min\{d + 2, 0\}$. Now $D > 0$ implies $D + 2 > 2$, and $d > -2$ implies $d + 2 > 0$, and so

$$\begin{aligned}
E &= D + 2, \\
e &= 0.
\end{aligned}$$

Therefore $E - e = D + 2$. By theorem 3.7.2, we have $E - e = D - d + 2$, and equating these we have $D + 2 = D - d + 2$. This gives us $d = 0$, contradicting the assumption that d is strictly positive.

Now suppose that $d < 0$. The four cases of equations 4.7 are considered separately below.

1. $D = 0$ and $d = -2$. Therefore

$$\begin{aligned} E &\leq \max\{D + 2, 2\}, \\ e &\geq \min\{d + 2, 0\}. \end{aligned}$$

Therefore, $E - e \leq 2 - 0 = 2$, implying $D - d + 2 \leq 2$ and hence $D - d \leq 0$. But $D - d = 2 > 0$, so we have a contradiction.

2. $D = 0$ and $e = \min\{d + 2, 0\}$. Therefore, $E \leq 2$, so

$$D - d + 2 = E - e \leq 2 - \min\{d + 2, 0\}.$$

(i) If $e = 0$ then $D - d + 2 \leq 2$, so $D - d \leq 0$, so $D \leq d$. We know $D \geq d$, so we conclude $D = d = 0$, which is a contradiction since $d < 0$.

(ii) If $e = d + 2$ then $D - d + 2 \leq -d$, so $D \leq -2$ which contradicts $D = 0$.

3. $E = \max\{D + 2, 2\}$ and $d = -2$. Therefore, $e \geq 0$, so

$$D - d + 2 = E - e \leq \max\{D + 2, 2\}.$$

(i) If $E = D + 2$ then $D - d + 2 \leq D + 2$, so $d \geq 0$ which contradicts $d = -2$.

(ii) If $E = 2$ then $D - d + 2 \leq 2$, so $D - d \leq 0$, and so $D \leq d$. Again, we know $D \geq d$, so we conclude $D = d = -2$. In this case, recall equations 4.8. We deduce

$$G = \max\{D - 2, 0\} = 0, \quad g = \min\{d - 2, -2\} = -4.$$

We know $G - g \leq D - d + 2$. Therefore $D - d \geq G - g - 2 = 4 - 2 = 2$, which contradicts $D = d (= -2)$.

4. $E = \max\{D + 2, 2\}$ and $e = \min\{d + 2, 0\}$. There are four subcases here.

- $E - e = (D + 2) - 0 = D + 2 \Rightarrow D - d + 2 = D + 2 \Rightarrow d = 0$, which is a contradiction since $d < 0$.
- $E - e = (D + 2) - (d + 2) = D - d$ which is a contradiction, since $E - e = D - d + 2$.
- $E - e = 2 - (d + 2) = -d \Rightarrow D - d + 2 = -d \Rightarrow D = -2$. This gives us $D \neq 2$; also $d \leq D$, so $d \neq 0$. Recalling equations 4.8,

$$G = \max\{D - 2, 0\} = 0, \quad g = \min\{d - 2, -2\} = d - 2.$$

Therefore $G - g = -(d - 2)$; we know $G - g \leq D - d + 2$, and so we have $D - d + 2 \geq G - g = -d + 2 \Rightarrow D - d + 2 \geq -d + 2 \Rightarrow D \geq 0$, which contradicts $D = -2$.

- $E - e = 2 - 0 = 2 \Rightarrow D - d + 2 = 2 \Rightarrow D - d = 0 \Rightarrow D = d$. We have $d \geq -2$, $D \leq 0$, and therefore $d = -1$ or -2 . Recalling equations 4.8, we know $D \neq 2$, $d \neq 0$, and so
 - (i) $d = D = -2 \Rightarrow G = 0$, $g = -4 \Rightarrow G - g = 4$; or
 - (ii) $d = D = -1 \Rightarrow G = 0$, $g = -3 \Rightarrow G - g = 3$.
 In each case we have $G - g \leq D - d + 2$, so $D - d \geq G - g - 2 \geq 3 - 2 = 1$, which contradicts $D = d$.

Thus we conclude that $d = 0$, and the proof of theorem 4.4.1 is complete. \square

4.5 A conjecture for alternating knots

We see from the discussion so far that Rudolph's work fits quite neatly into the study of arc index. Theorem 4.4.1 adds to a list of similar results relating geometric properties of knots to features of polynomial invariants.

We can analyse the inequality of theorem 4.4.1, to see just how tight a bound it is. Calculation of $F_L(a, x)$ is possible via Ochiai's rather nice polynomials program [Oc]: from this it is possible to extract $\text{spr}_a(G_K(a, x))$ using a simple PASCAL procedure.

Having generated all knots of arc index at most 9 (see chapter 5), we test our inequality on this set. We discover that for all knots K with $\alpha(K) \leq 9$,

$$\text{spr}_a(G_K(a, x)) + 2 = \alpha(K) \Leftrightarrow K \text{ is an alternating knot.}$$

Also available [Th1] is a complete table of $F_K(a, x)$ for all knots K with $c(K) \leq 13$.¹² We recall theorem 2.5.2, which says that for certain knots K , $\alpha(K) \leq c(K) + 2$. Again we extract $\text{spr}_a(G_K(a, x))$, using another simple PASCAL procedure. We find that for K with $c(K) \leq 13$,

$$\text{spr}_a(G_K(a, x)) = c(K) \Leftrightarrow K \text{ is an alternating knot.}$$

So for knots satisfying the hypothesis of theorem 2.5.2, and with at most 13 crossings,

$$\text{spr}_a(G_K(a, x)) + 2 \geq \alpha(K) \Leftrightarrow K \text{ is an alternating knot,}$$

and hence theorem 4.4.1 yields equality for these alternating knots.

¹²Thanks are due to Morwen Thistlethwaite for making these tables available.

We can also make observations on the alternating knots which do not satisfy the hypothesis of theorem 2.5.2. The existence of such a knot K with $\text{spr}_a(G_K(a, x)) \neq c(K)$ would be quite revealing. On one hand,

$$\text{spr}_a(G_K(a, x)) > c(K) \Rightarrow \alpha(K) > c(K) + 2,$$

via theorem 4.4.1. Therefore, K would be a counter-example to the conjecture of [C-N], namely, that for all non-trivial links, $\alpha(L) \leq c(L) + 2$. On the other hand,

$$\text{spr}_a(G_K(a, x)) < c(K) \Rightarrow \text{spr}_a(G_K(a, x)) + 2 < c(K) + 2.$$

Then if we suppose that the inequality $\alpha(K) \geq \text{spr}_a(G_K(a, x)) + 2$ (theorem 4.4.1) yields equality for all alternating links, we would have $\alpha(K) < c(K) + 2$. There is no alternating knot for which this is known to be true, and indeed the opposite has been conjectured for alternating knots.

In view of the partial results found here, we make the following conjectures.

Conjecture 4.5.1 *Let K be a knot. Then*

$$\alpha(K) \geq \text{spr}_a(G_K(a, x)) + 2,$$

with equality if, and only if, K is an alternating knot.

This is an extension of theorem 4.4.1, and should be compared (on face value at least) with the following result, proved independently by Murasugi and by Thistlethwaite.

Theorem 4.5.2 [Mu, Th3] *Let K be a knot. Then*

$$c(K) \geq \text{spr}_t(V_K(t)),$$

with equality if, and only if, K is an alternating knot. □

The second conjecture is intended as a generalization of theorem 2.5.2.

Conjecture 4.5.3 *Let K be a knot. Then*

$$\alpha(K) \leq 2 + c(K),$$

with equality if, and only if, K is an alternating knot.

4.6 Proof of theorem 2.3.3

We are now in a position to prove theorem 2.3.3, which stated that, for a $(2, q)$ torus link L , $q \geq 2$, we have $\alpha(L) \geq 2 + q$.

Proof of theorem 2.3.3. Let L be the torus knot $T(2, q)$. We show that

$$\text{spr}_a(G_L(a, x)) = q;$$

then by theorem 4.4.1,

$$\alpha(L) \geq 2 + \text{spr}_a(G_L(a, x)) = 2 + q,$$

and the result follows.

So what follows is a proof that $\text{spr}_a(G_L(a, x)) = q$. We use an inductive technique, developed from application of the Kauffman skein relation (subsection 1.5.II). The relation quickly gives us, for $q \geq 2$,

$$\Lambda_{T(2,q)} = x \left(\Lambda_{T(2,q-1)} + a^{1-q} \right) - \Lambda_{T(2,q-2)},$$

and so

$$a^q F_{T(2,q)} = x \left(a^{q-1} F_{T(2,q-1)} + a^{1-q} \right) - a^{q-2} F_{T(2,q-2)},$$

which we simplify to

$$F_{T(2,q)} = x \left(a^{-1} F_{T(2,q-1)} + a^{1-2q} \right) - a^{-2} F_{T(2,q-2)}.$$

Now note that

$$\begin{aligned} F_{T(2,0)} &= F_{U_2} = \frac{a-x+a^{-1}}{x}, \\ F_{T(2,1)} &= F_{U_1} = 1, \end{aligned}$$

and so

$$\begin{aligned} F_{T(2,2)} &= a^{-1}(x - x^{-1}) + a^{-2} + a^{-3}(x - x^{-1}), \\ F_{T(2,3)} &= a^{-2}(x^2 - 2) + a^{-3}x + a^{-4}(x^2 - 1) + a^{-5}x, \\ F_{T(2,4)} &= a^{-3}(x^3 - 3x + x^{-1}) + a^{-4}(x^2 - 1) + a^{-5}(x^3 - 2x + x^{-1}) \\ &\quad + a^{-6}x^2 - a^{-7}x. \end{aligned}$$

First, we show that $\text{mindeg}_a(F_{T(2,q)}) = 1 - 2q$, $\text{maxdeg}_a(F_{T(2,q)}) = 1 - q$, and then we show that the coefficients of these extreme powers of a are non-zero when reduced modulo 2. We can then deduce that

$$\begin{aligned} \text{spr}_a(G_L(a, x)) &= \text{maxdeg}_a(F_{T(2,q)}) - \text{mindeg}_a(F_{T(2,q)}) \\ &= (1 - q) - (1 - 2q) \\ &= q. \end{aligned}$$

To see that $\text{mindeg}_a (F_{T(2,q)}) = 1 - 2q$, notice that this is true in the cases $q = 2, 3, 4$. For $q > 4$, we use the inductive relation:

$$\begin{aligned} F_{T(2,q)} &= x (a^{-1} F_{T(2,q-1)} + a^{1-2q}) && - a^{-2} F_{T(2,q-2)} \\ &= x (a^{2-2q} x + O(a^{3-2q})) + a^{1-2q} x && - a^{-2} (a^{5-2q} x + O(a^{6-2q})) \\ &= (a^{2-2q} x^2 + O(a^{3-2q})) + a^{1-2q} x && - (a^{3-2q} x + O(a^{4-2q})) \\ &= (a^{1-2q} x + O(a^{2-2q})). \end{aligned}$$

Further, the coefficient of a^{1-2q} in $F_{T(2,q)}$ is x , which is non-zero when reduced modulo 2.

We deduce that $\text{maxdeg}_a (F_{T(2,q)}) = 1 - q$, in a similar way. Notice that this is true in the cases $q = 2, 3, 4$, and accordingly for these cases we can write

$$F_{T(2,q)} = \sum_{i=1-2q}^{1-q} Z_i^q(x) a^i, \quad (4.9)$$

where $Z_i^q(x) \in \mathbf{Z}[x^{\pm 1}]$. For $q > 4$, the inductive relation gives

$$\begin{aligned} F_{T(2,q)} &= x (a^{-1} F_{T(2,q-1)} + a^{1-2q}) && - a^2 F_{T(2,q-2)} \\ &= x a^{-1} \left(\sum_{j=3-2q}^{2-q} Z_j^{q-1}(x) a^j \right) + x a^{1-2q} && - a^{-2} \left(\sum_{j=5-2q}^{3-q} Z_j^{q-2}(x) a^j \right) \\ &= x \left(\sum_{j=3-2q}^{2-q} Z_j^{q-1}(x) a^{j-1} \right) + x a^{1-2q} && - \left(\sum_{j=5-2q}^{3-q} Z_j^{q-2}(x) a^{j-2} \right). \end{aligned}$$

Then $\text{maxdeg}_a (F_{T(2,q)})$ is seen by observing that, on the right-hand side, the highest possible a -power with non-zero coefficient is a^{1-q} . Therefore, we can write $F_{T(2,q)} = \sum_{i=1-2q}^{1-q} Z_i^q(x) a^i$, for all $q \geq 2$; and further,

$$Z_{1-q}^q(x) = x Z_{2-q}^{q-1}(x) - Z_{3-q}^{q-2}(x).$$

Finally, we note that

$$\begin{aligned} Z_{-1}^2(x) &= x - x^{-1}, \\ Z_{-2}^3(x) &= x^2 - 2, \\ Z_{-3}^4(x) &= x^3 - 3x + x^{-1}. \end{aligned}$$

So, for $q = 2, 3, 4$, we have $Z_{1-q}^q(x) = x^{q-1} + \text{L.O.T.}$. For general q ,

$$\begin{aligned} Z_{1-q}^q(x) &= x Z_{2-q}^{q-1}(x) - Z_{3-q}^{q-2}(x) \\ &= x (x^{q-2} + \text{L.O.T.}) - (x^{q-3} + \text{L.O.T.}) \\ &= (x^{q-1} + \text{L.O.T.}) - (x^{q-3} + \text{L.O.T.}) \\ &= x^{q-1} + \text{L.O.T.}, \end{aligned}$$

which is non-zero when reduced modulo 2. □

Chapter 5

Extended computations for knots with small arc index

5.1 Introduction

Let α be a natural number. Recall, from section 2.2, that $\mathcal{K}(\alpha)$ denotes the set of knots K with arc index $\alpha(K) = \alpha$. By considering the construction of arc-presentations, it is easy to see that $|\mathcal{K}(\alpha)|$, the number of knots in $\mathcal{K}(\alpha)$, is finite; for there are only a finite number of ways of connecting a finite set of points pairwise by simple planar arcs, as our construction allows. When α is sufficiently small, we can apply computational techniques to help generate an exhaustive list of the elements of $\mathcal{K}(\alpha)$.

Recall that $\mathcal{D}_{\mathcal{K}}(\alpha)$ denotes the set of all α -arc diagrams of knots. As α grows we find

$$\alpha \ll |\mathcal{K}(\alpha)| \ll |\mathcal{D}_{\mathcal{K}}(\alpha)|.$$

We generate knots of arc index at most α by numerical representation of all possible diagrams. Due to the relative sizes of $|\mathcal{D}_{\mathcal{K}}(\alpha)|$ and α , the number of such diagrams under consideration soon gets very large. Since there are many diagrams generated which represent a given knot, we employ a number of *sieves* to detect some of this repetition, and remove redundant examples.

With the final ‘sieved’ list of diagrams, the following occurs. The diagrams have been represented in such a way that a representing braidword is easily computed. The braidword forms the input to a procedure (adapted from a program of Short, [M-S]) which calculates the Homfly polynomial invariant. These polynomials are sorted modulo mirror image, and listed in a well-defined order.

Each polynomial in turn can then be referred, by hand, to Thistlethwaite's tabulations of Homfly polynomials, [Th4] (subject to a change of variable which can be implemented with a simple MAPLE program¹³). The tabulations are restricted to knots of crossing number at most 13; our code includes a device to calculate an upper bound for crossing number for each knot, thus warning when a candidate knot may be too large for the tabulation.

Reference to [Th4] gives us a number of candidate knots for each polynomial. In the event of there being more than one candidate, observation of crossing number or other invariants will usually resolve the ambiguity.

Of the final list of knots, each one has arc index at most α . Comparison of this list with the results of experiments for smaller values of α will give the list of elements of $\mathcal{K}(\alpha)$.

5.2 Constructing the knot

First, we briefly recall that a link can be constructed from the union of a fixed number of simple arcs in a controlled way.

Let $A \cong S^1 \subset S^3$ be a binding circle in S^3 ; the complement $S^3 - A$ admits a fibration $H = \{H_\theta : 0 \leq \theta < 2\pi\}$ by open half-planes H_θ with $\partial H_\theta = A$. Choose half-planes $\{H_\theta : \theta = \frac{2(\alpha-k)\pi}{\alpha}, k = 0, \dots, \alpha-1\}$, and denote these $\{h_0, \dots, h_{\alpha-1}\}$. Note that for reasons of convenience in later definitions, the indices are ordered in the direction of *decreasing* θ .

Choose an orientation for A , and α distinct points $\{p_0, p_1, \dots, p_{\alpha-1}\}$ on A , which appear *in order of their indices* as we follow the orientation of A .

Now perform the following construction: join pairs of points $\{p_i\}$ by simple arcs $\{a_j\}$ in the $\{h_j\}$ such that

- (i) each h_j contains exactly one arc a_j ;
- (ii) each p_i is incident to exactly two arcs a_j .

The union $\bigcup_{j=0}^{\alpha-1} a_j$ is a knot or link, denoted L .

¹³MAPLE will also detect the incidence of polynomials that factorize, allowing us to identify possible connected sums.

5.3 Representing the knot

Write S_n for the set of permutations of n elements $\{0, 1, \dots, n-1\}$. Let $m \leq n$; an m -cycle $\rho \in S_n$ has the obvious definition, *i.e.* for all i , $\rho^k(i) = i \Leftrightarrow m|k$. We write an m -cycle in the form $\rho = (i_1, i_2, \dots, i_m)$, so that $\rho(i_j) = i_{j+1}$, $\rho(i_m) = i_1$. Suppose we have a diagram D of a link L which has the form of the construction described above. The diagram D can be reduced to a pair of permutations of S_α in the following way.

For some component L_r of L , choose an orientation. Choose one of the points of $L_r \cap A$: this is the starting point of a path round L_r . Let η_r be the cycle given by the subscripts of the h_j encountered as we follow the orientation of L_r . Let τ_r be the cycle of the subscripts of the p_i encountered as we follow the orientation of L_r . Perform this for each of the components of L in turn. Then define the permutations $\eta = \prod \eta_r$, $\tau = \prod \tau_r$. Note that the η_r are distinct, the τ_r are distinct, and $\eta, \tau \in S_\alpha$; also, for $i = 0, \dots, n-1$, $\eta(i) \neq i$ and $\tau(i) \neq i$.

In general, we write (η, τ) for the knot or link L constructed in this way.

Lemma 5.3.1 *Let L be an arc presentation of a link on α arcs. Then L is a knot (*i.e.* a 1-component link) $\Leftrightarrow \tau$ is an α -cycle $\Leftrightarrow \eta$ is an α -cycle.*

Proof. If L is a knot then each of the p_i is encountered exactly once as L is traversed, so that τ is a product of one cycle of length α . Conversely, if τ is an α -cycle then all the points p_i must lie on the same component of the link; since each component is composed of at least 2 arcs then there can be only one component.

A similar argument holds for η . □

Example. In figure 5.1, with starting point and orientation as indicated, one can easily verify that $\eta = (4, 0, 3, 1, 5, 2)$, $\tau = (0, 3, 1, 5, 2, 4)$.

Our classification is of knots (*i.e.* 1-component links). For a given α , the first task is to generate all relevant α -cycles; knot diagrams are then formed by taking pairs of α -cycles in an ordered way, and using the construction just described.

5.4 Preliminary sieves on the list of α -cycles

As mentioned at the beginning of the chapter, the number of possible diagrams grows very quickly with α , so a number of sieves are employed to keep the work

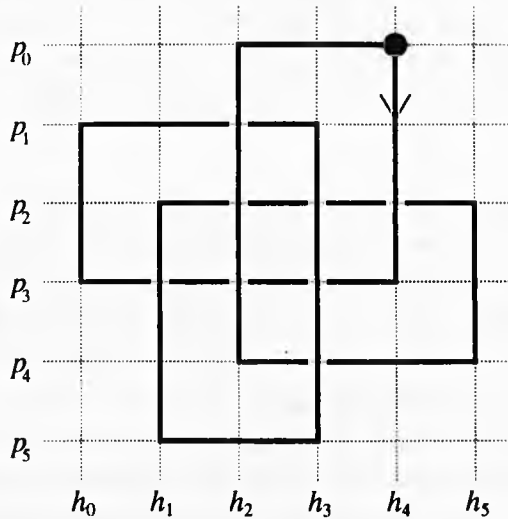


Figure 5.1: $\eta=(4, 0, 3, 1, 5, 2)$, $\tau=(0, 3, 1, 5, 2, 4)$

down to a minimum. We describe these in sections 5.4 and 5.5.

5.4.I Base points and arc-reducing moves

By the use of a couple of simple observations we can greatly reduce the number of α -cycles relevant to the experiment.

Proposition 5.4.1 *Let K be a knot, and $\eta, \tau \in S_\alpha$ the permutations giving K . If there is an $i \in [0, \alpha - 1]$ such that $|\eta(i) - i| \equiv 1 \pmod{\alpha}$ or $|\tau(i) - i| \equiv 1 \pmod{\alpha}$ then the arc index of K is strictly less than α .*

Proof. We use Cromwell's moves (section 2.3), which relate two arc-presentations of the same link. If $|\eta(i) - i| \equiv 1 \pmod{\alpha}$ then a pair of consecutive arcs are also adjacent, and an arc-reducing type IV move is applicable. If $|\tau(i) - i| \equiv 1 \pmod{\alpha}$ then a pair of consecutive points p_i, p_j are adjacent, and the diagram admits an arc-reducing type III move. \square

Let h_0 be the *base page* of the fibration H ; let p_0 be the *base point* of A . Collectively they are called the *base pair*, and they define the starting point of our path around K . We make the following observation.

Proposition 5.4.2 *A knot is independent of the choice of base page and base point.* \square

Consider the grid diagram G of K in \mathbf{R}^2 generated by (η, τ) , where the arcs are all drawn parallel to the y -axis, and the semiloops parallel to the x -axis. Suppose that G lies entirely in the half-plane $\{(x, y) : y < 0\}$. Let G' denote the image of G when reflected in the line $y = 0$; so G' is a diagram of \overline{K} . The reflection preserves the p_i , and so preserves τ ; it sends arc a_j to arc $a_{\alpha-1-j}$, and so sends η to a new α -cycle η' , where the i th entries of η and η' are additive inverses modulo $\alpha - 1$. We have $(\eta', \tau) = \overline{K}$. Now by proposition 5.4.2 we can change the labels of the h_j without altering the knot: we use the labels h'_j , where $h'_{(j+1) \bmod \alpha} = h_j$. This has the effect of adding 1 to each entry of η' modulo α , giving η'' . Hence, $(\eta'', \tau) = \overline{K}$. Now we have that the i th entries of η and η'' are additive inverses modulo α ; so $\eta'' = \overline{\eta}$. \square

By lemma 5.4.3, if $K = (\eta, \tau)$ then there are four pairs of α -cycles which are related by reflections, and represent either K or \overline{K} . They are (η, τ) , $(\overline{\eta}, \tau)$, $(\eta, \overline{\tau})$ and $(\overline{\eta}, \overline{\tau})$. They correspond to the four quadrants of \mathbf{R}^2 when dissected by the axes; figure 5.3 demonstrates this.

Up to mirror image, we need only consider one of these four diagrams. The following definition and proposition allow us to do that.

Let ρ be an α -cycle. We say that ρ is *proper* if $\rho(0) \leq \frac{\alpha}{2}$, with $\rho(\rho(0)) \leq \frac{\alpha}{2}$ if $\rho(0) = \frac{\alpha}{2}$.

Proposition 5.4.4 *If K can be represented by a pair (η, τ) of α -cycles, then it can be represented (modulo mirror image) by a pair of proper α -cycles.*

Proof. From the definition of $\overline{\rho}$, we have that ρ is proper $\Leftrightarrow \overline{\rho}$ is not proper. It follows that exactly one of the four diagrams (η, τ) , $(\overline{\eta}, \tau)$, $(\eta, \overline{\tau})$ and $(\overline{\eta}, \overline{\tau})$ has the property that both defining α -cycles are proper. \square

Since $\alpha(K) = \alpha(\overline{K})$, and we can easily establish the presence of K in a list by its Homfly polynomial or the Homfly polynomial of \overline{K} ,¹⁴ then we opt to search for knots modulo mirror image. We therefore employ a sieve to remove all non-proper α -cycles.

¹⁴This is because $\mathcal{P}_K(v, z) = \mathcal{P}_{\overline{K}}(v^{-1}, z)$.

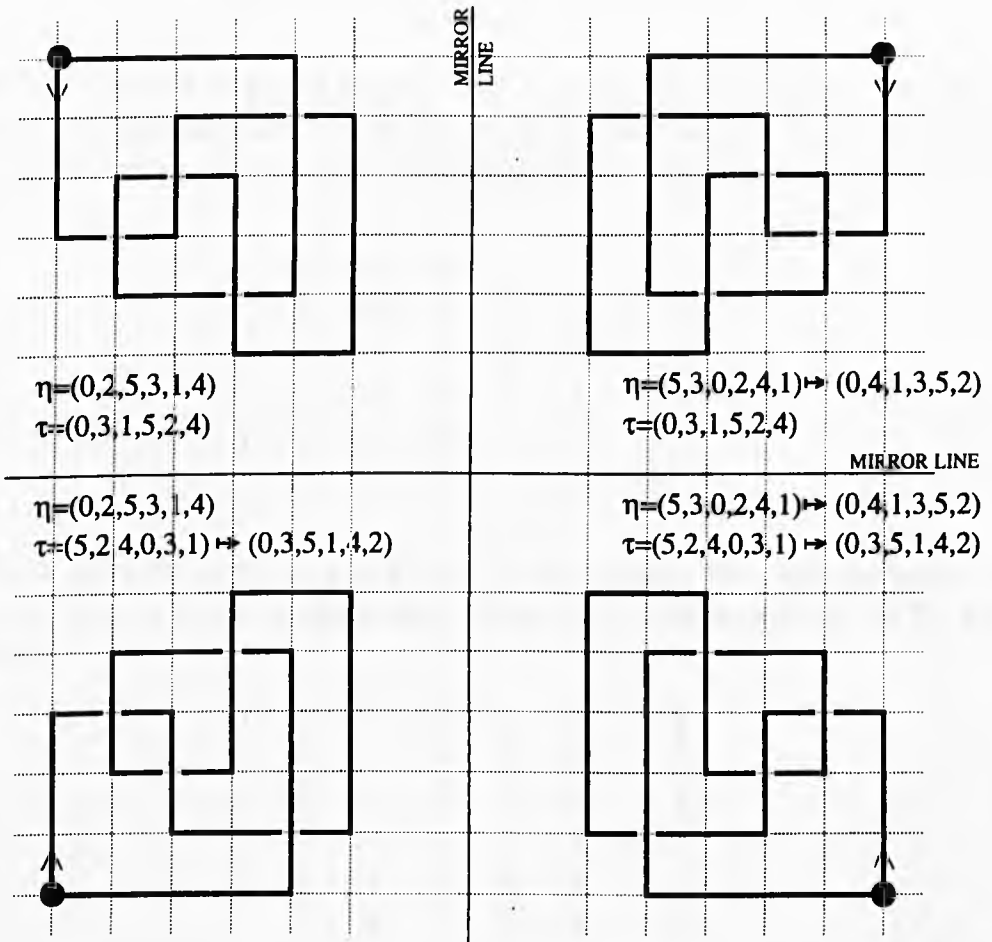


Figure 5.3: Four pairs of α -cycles generated by reflection

Example. Consider $K = (\eta, \tau)$ when $\eta = (0, 3, 5, 1, 4, 2)$, $\tau = (0, 4, 2, 5, 1, 3)$. In this case, $\alpha = 6$. The matrix M (as defined in section 2.2) is

$$\begin{pmatrix} 1 & 0 & -1 & 0 & 0 & 0 \\ 0 & -1 & 0 & 0 & 1 & 0 \\ 0 & 0 & 0 & -1 & 0 & 1 \\ 0 & 0 & 1 & 0 & -1 & 0 \\ -1 & 0 & 0 & 1 & 0 & 0 \\ 0 & 1 & 0 & 0 & 0 & -1 \end{pmatrix}.$$

Now, $\eta(0) = 3 = \frac{\alpha}{2}$ and $\eta(\eta(0)) = 5 > \frac{\alpha}{2}$, so η is not proper. We choose to replace η by its reflection, $\bar{\eta} = (0, 3, 1, 5, 2, 4)$. Now we have a new grid diagram of K , represented (up to mirror image) by $(\bar{\eta}, \tau)$, and the corresponding matrix M is

$$\begin{pmatrix} 1 & 0 & 0 & 0 & -1 & 0 \\ 0 & 0 & 1 & 0 & 0 & -1 \\ 0 & 1 & 0 & -1 & 0 & 0 \\ 0 & 0 & -1 & 0 & 1 & 0 \\ -1 & 0 & 0 & 1 & 0 & 0 \\ 0 & -1 & 0 & 0 & 0 & 1 \end{pmatrix}.$$

Next, note that $\tau(0) = 4 > \frac{\alpha}{2}$, so τ is not proper. We take the proper cycle $\bar{\tau} = (0, 2, 4, 1, 5, 3)$ in place of τ . Then K is represented by $(\bar{\eta}, \bar{\tau})$, and M becomes

$$\begin{pmatrix} 1 & 0 & 0 & 0 & -1 & 0 \\ 0 & -1 & 0 & 0 & 0 & 1 \\ -1 & 0 & 0 & 1 & 0 & 0 \\ 0 & 0 & -1 & 0 & 1 & 0 \\ 0 & 1 & 0 & -1 & 0 & 0 \\ 0 & 0 & 1 & 0 & 0 & -1 \end{pmatrix}.$$

5.4.III Rotating the grid diagram

In proposition 5.4.2 we stated that given an grid diagram G , the knot K thus presented is independent of the the choice of labels of the points $p_i \subset A$ and the half-planes h_j . We can rotate the indices, $i \mapsto i + s \pmod{\alpha}$, $j \mapsto j + t \pmod{\alpha}$ without affecting the resulting knot or link. In terms of the matrix M , these changes of base pair correspond to cyclic permutations of the rows and columns of M .

Consider such a matrix M , given by (η, τ) , with $M_{00} = 1$ and η, τ both proper cycles. We can, by such a cyclic permutation of rows and columns, generate a new matrix M' from M such that $M'_{00} = 1$. There are α matrices M' which can be generated in this way, one for each column (some of them may be equal). Consider one such M' , and let the defining α -cycles of M' be η', τ' ; they are not necessarily proper cycles.

We obtain η' from η by adding (modulo α) a *rotation index* x_η , say, to each entry of η , then cyclically rotating the entries until the first entry is 0. We obtain τ' from τ in a similar way: the rotation index is x_τ , say. The rotation indices x_η and x_τ are not necessarily equal. We denote η' by $\text{cyc}(\eta, x_\eta)$ and τ' by $\text{cyc}(\tau, x_\tau)$.

Given an α -cycle ρ , define its *class* $[\rho]$ to be the set

$$\{\text{cyc}(\rho, x) : x = 0, 1, \dots, \alpha - 1\}.$$

Lemma 5.4.5 *Let ρ, ρ' be α -cycles. Then $\rho' \in [\rho] \Leftrightarrow \rho \in [\rho']$.*

Proof. From the definition of $[\rho]$, we have that ρ' is obtained from ρ by adding a rotation index x_ρ to each entry of ρ , and then cycling the entries until the first entry is 0; that is, $\rho' = \text{cyc}(\rho, x_\rho)$. Now define the rotation index $x_{\rho'}$ as $x_{\rho'} = \alpha - x_\rho$. One can easily check that $\text{cyc}(\rho', x_{\rho'}) = \rho$. \square

Lemma 5.4.6 *Let K be a knot. Then*

$$K \in \{(\eta', \tau') : \eta' \in [\eta], \tau' \in [\tau]\} \Leftrightarrow K \in \{(\eta', \tau) : \eta' \in [\eta]\}.$$

Proof. ‘If’ is trivial. ‘Only if’: suppose $K = (\eta', \tau')$ with $\eta' \in [\eta], \tau' \in [\tau]$. Since $\tau' \in [\tau]$ then $\tau \in [\tau']$, so $(\eta', \tau') = (\eta'', \tau)$ for some $\eta'' \in [\eta']$, and hence $\eta'' \in [\eta]$ since it merely means adding the same integer to each entry and rotating. \square

This means that each knot obtainable by pairing a cycle of $[\eta]$ with a cycle of $[\tau]$ is also presentable by pairing a cycle of $[\eta]$ with τ itself.

The next step is to check that we can still assume that the defining cycles are proper. Given a cycle ρ , define its *bi-class* as the union of classes $[\rho] \cup [\bar{\rho}]$.

Lemma 5.4.7 *Let ρ, ρ' be α -cycles. Then $\rho' \in [\rho] \Leftrightarrow \bar{\rho}' \in [\bar{\rho}]$.*

Proof. We claim that for each x , there exists y such that $\overline{\text{cyc}(\rho, x)} = \text{cyc}(\bar{\rho}, y)$. For if we write $\rho = (\rho_0, \rho_1, \rho_2, \dots, \rho_{\alpha-2}, \rho_{\alpha-1})$, then

$$\begin{aligned} \text{cyc}(\rho, x) &= (0, \rho_{i+1} - \rho_i, \dots, \rho_{i-1} - \rho_i) \\ \Rightarrow \overline{\text{cyc}(\rho, x)} &= (0, \alpha - (\rho_{i+1} - \rho_i), \dots, \alpha - (\rho_{i-1} - \rho_i)) \\ &= (0, \alpha - \rho_{i+1} + \rho_i, \dots, \alpha - \rho_{i-1} + \rho_i) \end{aligned}$$

where $\rho_i + x \equiv 0 \pmod{\alpha}$, while

$$\begin{aligned} \bar{\rho} &= (0, \alpha - \rho_1, \dots, \alpha - \rho_{\alpha-1}) \\ \Rightarrow \text{cyc}(\bar{\rho}, y) &= (\alpha - \rho_i + y, \alpha - \rho_{i+1} + y, \dots, \alpha - \rho_{i-1} + y) \end{aligned}$$

where $y \equiv \rho_i \pmod{\alpha}$.

Then we deduce that for some x, y ,

$$\begin{aligned} \rho' \in [\rho] &\Rightarrow \rho' = \text{cyc}(\rho, x) \\ &\Rightarrow \bar{\rho}' = \overline{\text{cyc}(\rho, x)} \\ &\Rightarrow \bar{\rho}' = \text{cyc}(\bar{\rho}, y) \\ &\Rightarrow \bar{\rho}' \in [\bar{\rho}]. \end{aligned}$$

□

Proposition 5.4.8 *Let η, τ be proper α -cycles. Let K be a knot such that $K \in \{(\eta', \tau') : \eta' \in [\eta] \cup [\bar{\eta}], \tau' \in [\tau] \cup [\bar{\tau}]\}$. Then K can be represented, modulo mirror image, by (η'', τ) with $\eta'' \in [\eta] \cup [\bar{\eta}]$ and η'' proper.*

Proof. Write $K = (\eta', \tau')$, with $\eta' \in [\eta] \cup [\bar{\eta}], \tau' \in [\tau] \cup [\bar{\tau}]$. There are four cases to consider.

1. $\eta' \in [\eta], \tau' \in [\tau]$. By lemma 5.4.6, $K = (\eta'', \tau)$ for some $\eta'' \in [\eta]$. If η'' is proper then we have no more to prove. If η'' is not proper then $\bar{K} = (\bar{\eta}'', \tau)$; $\bar{\eta}''$ is proper by proposition 5.4.4, and $\bar{\eta}'' \in [\bar{\eta}]$ by lemma 5.4.7.
2. $\eta' \in [\eta], \tau' \notin [\tau]$. In this case $\bar{\tau}' \in [\tau]$; write $\bar{K} = (\eta', \bar{\tau}')$. By lemma 5.4.6, $\bar{K} = (\eta'', \tau)$ for some $\eta'' \in [\eta]$. If η'' is proper then there is no more to prove. If η'' is not proper write $K = (\bar{\eta}'', \tau)$, with $\bar{\eta}''$ proper by proposition 5.4.4, and $\bar{\eta}'' \in [\bar{\eta}]$ by lemma 5.4.7.
3. $\eta' \notin [\eta], \tau' \in [\tau]$. In this case $\bar{\eta}' \in [\eta]$; write $\bar{K} = (\bar{\eta}', \tau')$. By lemma 5.4.6, $\bar{K} = (\eta'', \tau)$ for some $\eta'' \in [\eta]$. If η'' is proper then there is no more to prove; else write $K = (\bar{\eta}'', \tau)$, with $\bar{\eta}''$ proper by proposition 5.4.4, and $\bar{\eta}'' \in [\bar{\eta}]$ by lemma 5.4.7.

4. $\eta' \notin [\eta]$, $\tau' \notin [\tau]$. In this case $\overline{\eta'} \in [\eta]$, $\overline{\tau'} \in [\tau]$; write $K = (\overline{\eta'}, \overline{\tau'})$. By lemma 5.4.6, $K = (\eta'', \tau)$ for some $\eta'' \in [\eta]$. If η'' is proper then there is no more to prove; else write $\overline{K} = (\overline{\eta''}, \tau)$, with $\overline{\eta''}$ proper by proposition 5.4.4, and $\overline{\eta''} \in [\overline{\eta}]$ by lemma 5.4.7.

□

Proposition 5.4.8 means that all knots that can be presented by a pair of proper α -cycles can also be presented by pairing a cycle from the list of proper cycles with a cycle from the list of proper bi-class representatives.

5.4.IV Initial discussion of the pseudocode

The algorithm is implemented in SUN PASCAL. This allows for ready use and adaptation of Short's package [M-S], which was written in the same language.

For the reasons of ordering, speed and storage space, we store the permutations as integers I_η and I_τ : in the example in subsection 5.4.I, $I_\eta = 403152$ and $I_\tau = 31524$.

This method of storage is convenient provided $\alpha \leq 10$. For larger experiments, we may write the permutation in 'base α ', and store as an integer base 10, recovering the permutation when necessary. As α grows, the size of the experiments (in terms of computer time and memory needed) may begin to outweigh the usefulness of the results, since Thistlethwaite's polynomial tabulations are necessarily finite.

A self-calling procedure `nextstep` generates α -cycles by building up a cycle one entry at a time. It runs lexicographically through all the possibilities, building up a list of α -cycles that are not sieved out by the sieves corresponding to propositions 5.4.1, 5.4.2 and 5.4.4. That is, ρ appears in the list if, and only if,

- (i) the first entry of ρ is 0 (proposition 5.4.2);
- (ii) for each $i = 0, \dots, \alpha - 1$, $|\rho(i) - i| > 1$ (proposition 5.4.1); and
- (iii) ρ is a proper α -cycle (proposition 5.4.4).

This list is denoted \mathcal{C}_α in the pseudocode.

We use the result of proposition 5.4.8 to compile a second list, \mathcal{SC}_α , which is a subset of \mathcal{C}_α . The list \mathcal{SC}_α contains exactly one proper representative ρ of each

bi-class; that is, for each bi-class we choose a proper element of the bi-class to represent it in \mathcal{SC}_α . Then proposition 5.4.8 can be interpreted as saying that

$$\begin{aligned} K &\in \{(\eta, \tau) : \eta \in \mathcal{C}_\alpha, \tau \in \mathcal{C}_\alpha\} \\ &\Leftrightarrow K \in \{(\eta, \tau) : \eta \in \mathcal{C}_\alpha, \tau \in \mathcal{SC}_\alpha\}. \end{aligned}$$

This is performed as follows: once a complete α -cycle ρ has been successfully generated, it is first added to the list \mathcal{C}_α . Then we use a function `isnewperm` to systematically check for the presence in \mathcal{SC}_α of the cycles $\text{cyc}(\rho, x_\rho)$ and their reflections as x_ρ passes through the values $0, \dots, \alpha - 1$. If such a cycle is found then `isnewperm` returns the negative: the bi-class is already represented in \mathcal{SC}_α . Otherwise ρ is the first element of its bi-class to be generated, and it is added to the list \mathcal{SC}_α .

5.5 More sieves on the list of diagrams

We will now cover details of other sieves used in our computations.

5.5.I The transpose of an arc-diagram

By this point, the sieves described in section 5.4 have been employed to produce the lists \mathcal{C}_α and \mathcal{SC}_α of α -cycles. A grid diagram G composed of $\eta \in \mathcal{C}_\alpha, \tau \in \mathcal{SC}_\alpha$ has α arcs, and so represents a knot K of arc index at most α .

We now begin to compile the list of such diagrams G ; they are stored in an array denoted \mathcal{G} . We examine each possible pair of α -cycles in turn. The following definition and propositions help us to detect reducibility of some diagrams.

Suppose ρ is an α -cycle. Let the *reverse* of ρ , denoted $\text{rev } \rho$, be given by reversing the entries of ρ , and cycling so that the first entry is 0: so $\rho^i(j) = (\text{rev } \rho)^{-i}(j)$. For example, if $\rho = (0, 2, 5, 3, 1, 4)$ then $\text{rev } \rho = (0, 4, 1, 3, 5, 2)$.

Proposition 5.5.1 *Let $K = (\eta, \tau)$. Then $(\text{rev } \tau, \text{rev } \eta)$ also represents K .*

Proof. Let G be the diagram of K obtained from the cycle-pair (η, τ) . We assume that it lies in the plane $z = 0$ in \mathbf{R}^3 and is viewed from the positive end of the z -axis. Recall that the arcs lie parallel to the y -axis, and the semi-loops parallel to the x -axis.

Let G^T be the ‘transpose’¹⁵ of G obtained by rotating the plane $z = 0$ through 180° about the line $x + y = 0 = z$, and reversing the orientation. It is a fairly easy exercise to check that if this diagram is given by (η', τ') then, traversing the knot from the same starting point, the order of the planes encountered in G^T is the opposite to the order of the points encountered when traversing G ; *i.e.*, $\tau' = \text{rev } \eta$. By a similar observation, $\eta' = \text{rev } \tau$. \square

It should be noted at this point that given a pair of α -cycles η, τ , the knots

$$(\eta, \tau), (\eta, \text{rev } \tau), (\tau, \eta)$$

may be inequivalent knots. For example consider $\eta = (0, 4, 2, 5, 7, 1, 3, 6)$, $\tau = (0, 2, 5, 3, 7, 1, 4, 6)$, and hence $\text{rev } \tau = (0, 6, 4, 1, 7, 3, 5, 2)$. Then these cycle-pairs represent the knots 6_2 , 3_1 and U_1 respectively, as seen in figure 5.4.

We can define a natural total ordering on the set of α -cycles, by a lexicographical method. Given two α -cycles ρ_1, ρ_2 , we write $\rho_1 > \rho_2$ if there exists an m such that

$$\begin{aligned} \rho_1^i(0) &= \rho_2^i(0) & \text{for } i < m, \\ \rho_1^m(0) &> \rho_2^m(0). \end{aligned}$$

For example, it is easy to see that $(0, 3, 5, 1, 4, 2) > (0, 3, 1, 5, 2, 4)$.

The following lemma allows us to deduce proposition 5.5.3. This gives us another simple sieve, which is discussed in the opening paragraph of subsection 5.5.II.

Lemma 5.5.2 *The operations of reverse and reflection on an α -cycle ρ are commutative. That is,*

$$\overline{\text{rev } \rho} = \text{rev } (\bar{\rho}).$$

Proof. Write $\rho = (\rho_0, \rho_1, \rho_2, \dots, \rho_{\alpha-2}, \rho_{\alpha-1})$. Then by definition,

$$\begin{aligned} \text{rev } \rho &= (\rho_0, \rho_{\alpha-1}, \rho_{\alpha-2}, \dots, \rho_2, \rho_1) \\ \Rightarrow \overline{\text{rev } \rho} &= (\rho_0, \alpha - \rho_{\alpha-1}, \alpha - \rho_{\alpha-2}, \dots, \alpha - \rho_2, \alpha - \rho_1) \\ \Rightarrow \text{rev } (\overline{\text{rev } \rho}) &= (\rho_0, \alpha - \rho_1, \alpha - \rho_2, \dots, \alpha - \rho_{\alpha-2}, \alpha - \rho_{\alpha-1}). \end{aligned}$$

Now note that $\bar{\rho} = (\rho_0, \alpha - \rho_1, \alpha - \rho_2, \dots, \alpha - \rho_{\alpha-2}, \alpha - \rho_{\alpha-1})$. \square

¹⁵This is so-called because the matrices M and M^T corresponding to G and G^T are mutually transpose.

Proposition 5.5.3 *Let K be a knot. We have*

$$\begin{aligned} K &\in \{(\eta, \tau) : \eta \in \mathcal{C}_\alpha, \tau \in \mathcal{SC}_\alpha, \text{rev } \eta \in \mathcal{SC}_\alpha\}. \\ &\Rightarrow K \in \{(\eta, \tau) : \eta \in \mathcal{C}_\alpha, \tau \in \mathcal{SC}_\alpha, \tau \leq \text{rev } \eta\}. \end{aligned}$$

Proof. If K is written (η, τ) with $\tau \leq \text{rev } \eta$ then no work needs to be done. So suppose that K is written as the pair (η, τ) with $\tau > \text{rev } \eta$. We need to find an explicit pair η', τ' such that $(\eta', \tau') = K$, $\eta' \in \mathcal{C}_\alpha$, $\tau' \in \mathcal{SC}_\alpha$ and $\tau' \leq \text{rev } \eta'$.

By proposition 5.5.1, we know that $K = (\text{rev } \tau, \text{rev } \eta)$. It may be that $\text{rev } \tau \notin \mathcal{C}_\alpha$. We consider two distinct cases.

1. $\text{rev } \tau \in \mathcal{C}_\alpha$. Write $\eta' = \text{rev } \tau$, $\tau' = \text{rev } \eta$, and $K = (\eta', \tau')$. Now we have

$$\text{rev } \eta < \tau \Leftrightarrow \text{rev } \eta < \text{rev } (\text{rev } \tau) \Leftrightarrow \tau' < \text{rev } \eta',$$

as required.

2. $\text{rev } \tau \notin \mathcal{C}_\alpha$. We replace $\text{rev } \tau$ by its reflection $\overline{\text{rev } \tau}$; so $\eta' = \overline{\text{rev } \tau}$, $\tau' = \text{rev } \eta$ and $\overline{K} = (\eta', \tau')$. Now notice that $\tau < \overline{\text{rev } \tau}$ because τ is proper. Therefore, we have

$$\text{rev } \eta < \tau \Rightarrow \text{rev } \eta < \overline{\text{rev } \tau} \stackrel{\text{lemma 5.5.2}}{\Leftrightarrow} \text{rev } \eta < \text{rev } (\overline{\text{rev } \tau}) \Leftrightarrow \tau' < \text{rev } \eta'.$$

□

5.5.II Further discussion of the pseudocode

By proposition 5.5.3, if $K = (\eta, \tau)$ with $\text{rev } \eta \in \mathcal{SC}_\alpha$ and $\tau > \text{rev } \eta$, then we can write $K = (\eta', \tau')$ or $\overline{K} = (\eta', \tau')$ with $\tau' \leq \text{rev } \eta'$. Therefore, if $\text{rev } \eta \in \mathcal{SC}_\alpha$, we only need to check those pairs (η, τ) with $\tau \leq \text{rev } \eta$. This sieve is manifested in the lines

```

for  $\forall \rho \in \mathcal{C}_\alpha$  do begin
   $\eta := \rho$ ;
  if  $\min(\text{rev } \eta, \overline{\text{rev } \eta}) \notin \mathcal{SC}_\alpha$  then
     $\mathcal{VSC}_\alpha(\eta) := \{\gamma \in \mathcal{SC}_\alpha : \gamma \leq \min(\text{rev } \eta, \overline{\text{rev } \eta})\}$ 
  else
     $\mathcal{VSC}_\alpha(\eta) := \mathcal{SC}_\alpha$ ;
  for  $\forall \gamma \in \mathcal{VSC}_\alpha(\eta)$  do begin...

```

at lines 6–12 of the pseudocode. The set $\mathcal{VSC}_\alpha(\eta)$ is defined, for each η , according to whether the proper cycle $\text{rev } \rho$ (or $\overline{\text{rev } \rho}$) is contained in \mathcal{SC}_α . Then we look at knots composed of the pair (η, τ) where $\eta \in \mathcal{C}_\alpha$, $\tau \in \mathcal{VSC}_\alpha(\eta)$.

First, the loop looks for ways of reducing the number of arcs in the diagram. Recall that two arcs of a knot which are joined by a point of the binding circle are called *consecutive*; and two arcs which lie on half-planes h_i, h_j with $|i - j| \equiv 1 \pmod{\alpha}$ are called *adjacent*.

A function `canbeignored` takes each pair of consecutive arcs in the diagram and judges whether type II moves can be applied to arrange the arcs to be adjacent: if so an arc-reducing type IV move can be applied, and the knot has arc index strictly less than α . If such a reduction is discovered then the pair is discarded and the next pair is called. This is evident in lines 16–27 of the pseudocode.

Note that the procedure is performed twice: we can attempt to apply type I moves in order to find a diagram which allows a type III move. In fact, we do this by applying the function `canbeignored` to the pair $(\text{rev } \tau, \text{rev } \eta)$. This is seen in lines 28–39 of the pseudocode.

If a pair (η, τ) does not fall through this sieve then it is stored in an array \mathcal{G} . For each $\eta \in \mathcal{C}_\alpha$, when the pairs $\{(\eta, \tau) : \tau \in \mathcal{SC}_\alpha\}$ have been checked by `canbeignored`, a procedure `findduplicates` applies type II moves to the diagram (η, τ) , searching for pairs $(\eta, \tau'), (\eta, \tau'')$ which represent the same knot. It takes τ' and applies type II moves, updating τ' as it goes; then if $\tau' = \tau''$ at any point, one of the representative pairs is deleted, for only one is needed. This is shown in lines 44–52.

The result is a list of pairs of cycles (η, τ) . A final sieve compares knots $(\eta', \tau), (\eta'', \tau)$ by applying type I moves and updating η' , deleting one of the pairs if $\eta' = \eta''$. In practical terms this is done by compiling a second list $\mathcal{G}^T = \{(\text{rev } \tau, \text{rev } \eta) : (\eta, \tau) \in \mathcal{G}\}$, and applying `canbeignored` to that list (lines 59–71). The resulting list of pairs of cycles (η, τ) is no bigger than before, and will usually be considerably smaller.

A procedure `braidword` takes a pair of cycles, and generates a braidword in the braid group

$$B_\tau = \left\langle \sigma_1, \dots, \sigma_6 : \begin{array}{l} \sigma_i \sigma_j \sigma_i = \sigma_j \sigma_i \sigma_j, \quad |i - j| = 1; \\ \sigma_i \sigma_j = \sigma_j \sigma_i, \quad |i - j| \geq 2. \end{array} \right\rangle,$$

which closes to the knot $K = (\eta, \tau)$. By proposition 2.5.1, we can assume that the number of braidstrings is bounded above by $\frac{1}{2}\alpha$. The method for obtaining a braid presentation from an arc presentation is described in section 2.2, and also

covered independently in [Cr]. The resulting braidword is fed into the procedure `polys`, which is adapted from a program of Short [M-S] to produce the Homfly polynomial of a closed braid and some of its specializations from a braid input. Our version delivers only the Homfly polynomial. The resulting polynomials $\mathcal{P}_K(v, z)$ are sorted and stored in an array $\text{Polys}(\alpha)$, and are eventually printed.

Knots can be identified from a combination of the Homfly polynomial (referring to Thistlethwaite's tables of polynomial invariants [Th4]), and bounds on crossing number.

5.6 Size of output

The following table gives an indication of the size of storage required to execute the program.

α	$ \mathcal{C}_\alpha $	$ \mathcal{SC}_\alpha $	$ \mathcal{G} $ (largest)	$ \mathcal{G} $ (final)	$ \text{Polys}(\alpha) $
5	1	1	1	1	1
6	3	1	1	1	1
7	23	5	15	11	3
8	177	27	292	196	13
9	1553	175	6594	4046	44
10	14963	1533			

For the case $\alpha = 10$, the number of cycle-pairs generated exceeds the available storage space. For this reason, we split the entire set of cycle-pairs into smaller batches, by partitioning \mathcal{G} into a number of smaller lists at the stage where we begin to search for duplicates of knots. A number of cycle-pairs which would normally be excluded as duplicating another cycle-pair then are included; more importantly, no knots are lost.

The pseudocode for this program is listed in appendix A.

5.7 Results

For arc index up to 9, we can completely classify all knots. For arc index 10, it is possible to list all Homfly polynomials of knots, but since the Thistlethwaite tables are limited to knots of 13 crossings or less, a complete classification of knots is harder. There are, however, some positive results. For example, we can

deduce that both the Conway and Kinoshita-Terasaka knots have arc index 11 (see corollary 5.8.4).

The classification is included below: complete for $\alpha \leq 9$, partial for $\alpha = 10$. The key to reading the tables is as follows. The integers represent the coefficients, and are bracketed into like powers of z . The least powers of v are indicated in small numbers before each bracket. For example,

$$2 \quad (0 \ 2 \ 0 \ -1)(1 \ 2 \ 1 \ 0) = v^2 \left((v^2 - v^6) + z^2(1 + 2v^2 + v^4) \right).$$

Knots are sorted first into groups of like arc index, so knots appear in exactly one set $\mathcal{K}(\alpha)$. Within these sets, the polynomials are ordered, first by the breadth of the polynomial (*i.e.* the difference between least and greatest powers of v), then in order of coefficients themselves, starting with the least, in lexicographic order. Since we are working up to mirror image, and we know $\mathcal{P}_K(v, z) = \mathcal{P}_{\overline{K}}(v^{-1}, z)$, the polynomials have been listed so that powers of v are positively biased. The notation for the knots themselves comes from Thistlethwaite's listing [Th4], and the Rolfsen [Ro] notation is also given where applicable.

Remark. Table 5.3 contains $\mathcal{P}_K(v, z)$ for all K with $\alpha(K) \leq 10$. Some of the polynomials also appear in tables 5.1 and 5.2. The knots indicated in brackets in table 5.3 are known to have arc index 10: however, they are not necessarily the only knots of arc index 10 to have the given polynomial.

5.8 Comments

We can make the following observations.

Corollary 5.8.1 *If K is an alternating knot with $c(K) = 8$, then $\alpha(K) = 10$. \square*

Corollary 5.8.2 *If K is an alternating knot with $c(K) = 9$, then $\alpha(K) = 11$.*

Proof. By corollary 2.5.8, we have $\alpha(K) \leq 11$ for all these knots. Since for each K , $\mathcal{P}_K(v, z)$ is not listed in tables 5.1, 5.2 or 5.3 then we deduce $\alpha(K) \geq 11$. \square

Corollary 5.8.3 *Let $K = 5.2$ and $K' = 10.136$. Then we have*

$$\begin{aligned} \mathcal{P}_K(v, z) &= \mathcal{P}_{K'}(v, z), \\ \alpha(K) &= 7 \neq 9 = \alpha(K'). \end{aligned}$$

\square

Remark. The knots 5.2 and 10.136 are the smallest pair of knots to be distinguishable by arc index, but not by Homfly polynomial. Compare with corollary 2.5.12.

Corollary 5.8.4 *The Conway and Kinoshita-Terasaka knots, denoted as 11.403 and 11.411 respectively, each have arc index 11, and so can be distinguished neither by Homfly polynomial nor by arc index.*

Proof. It is well known (for example, [L-M] p.111) that these two knots, which are mutants, have identical Homfly polynomial, namely

$$v^{-2} ((-2 + 7v^2 - 6v^4 + 2v^6) + z^2(-3 + 11v^2 - 11v^4 + 3v^6) + z^4(-1 + 6v^2 - 6v^4 + v^6) + z^6(v^2 - v^4)).$$

Note that this polynomial does not appear in tables 5.1, 5.2 or 5.3, so we conclude that each knot has arc index at least 11. Figures 5.5 and 5.6 give presentations of each knot on 11 arcs, so we conclude that the arc index of each knot is exactly 11. □

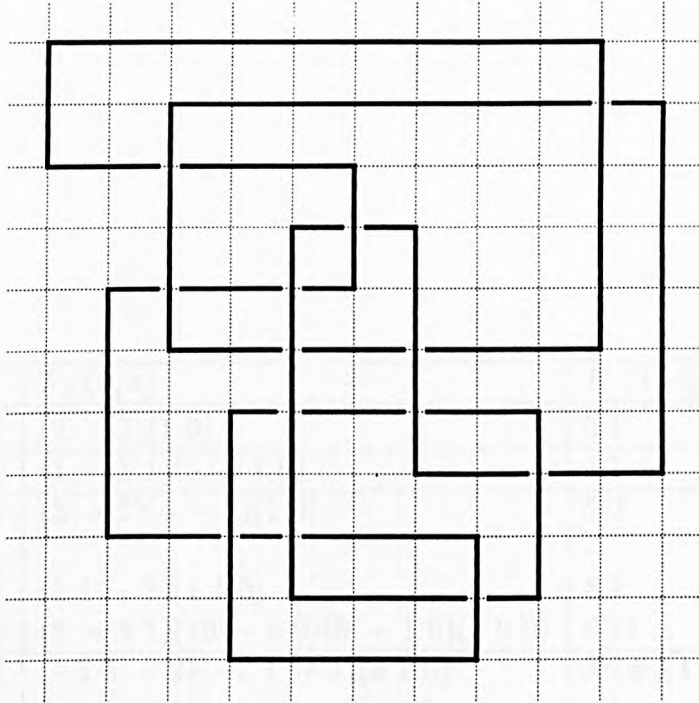


Figure 5.5: An 11-arc presentation of the Conway knot 11.403

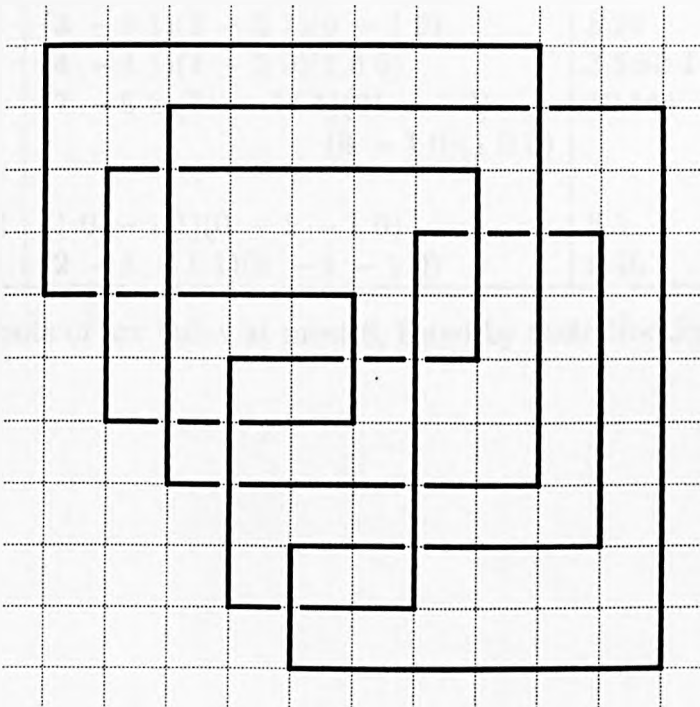


Figure 5.6: An 11-arc presentation of the Kinoshita-Terasaka knot 11.411

$\alpha(K)$	v^r	$\mathcal{P}_K(v, z)$	K [Th4]	K [Ro]
5	2	(2 -1)(1 0)	3.1	3 ₁
6	-2	(1 -1 1)(0 -1 0)	4.1	4 ₁
7	4	(3 -2)(4 -1)(1 0)	5.2	5 ₁
	2	(1 1 -1)(1 1 0)	5.1	5 ₂
	6	(5 -5 1)(10 -5 0)(6 -1 0)(1 0 0)	8.21	8 ₁₉
8	-2	(-2 5 -2)(-1 4 -1)(0 1 0)	3.1#3.1	3 ₁ #3 ₁
	-2	(-1 3 -1)(-1 3 -1)(0 1 0)	6.1	6 ₃
	0	(-1 4 -2)(-1 4 -1)(0 1 0)	8.19	8 ₂₀
	-2	(2 -3 2)(1 -4 1)(0 -1 0)	9.45	9 ₄₂
	0	(2 -2 1)(1 -3 1)(0 -1 0)	6.2	6 ₂
	2	(3 -3 1)(2 -3 1)(0 -1 0)	8.20	8 ₂₁
	4	(4 -4 1)(4 -2 0)(1 0 0)	3.1#3.1	3 ₁ #3 ₁
	8	(7 -8 2)(21 -14 1)(21 -7 0) (8 -1 0)(1 0 0)	10.144	10 ₁₂₄
	-2	(1 0 -1 1)(0 -1 -1 0)	6.3	6 ₁
	0	(2 -1 -1 1)(0 -1 -1 0)	9.46	9 ₄₆

Table 5.1: Knots of arc index at most 8, listed by their Homfly polynomials

$\alpha(K)$	v^r	$\mathcal{P}_K(v, z)$	K [Th4]	K [Ro]
9	4	(3 - 2)(4 - 1)(1 0)	10.136	10 ₁₃₂
	6	(4 - 3)(10 - 4)(6 - 1)(1 0)	7.7	7 ₁
	4	(0 4 - 3)(2 6 - 2)(1 2 0)	9.49	9 ₄₉
	4	(1 2 - 2)(3 3 - 1)(1 1 0)	7.5	7 ₃
	4	(2 0 - 1)(3 2 - 1)(1 1 0)	7.3	7 ₅
	6	(3 - 1 - 1)(9 - 1 - 1)(6 0 0)(1 0 0)	10.155	10 ₁₆₁
	8	(6 - 6 1)(21 - 13 1)(21 - 7 0)(8 - 1 0)(1 0 0)	10.150	10 ₁₃₉
	10	(9 - 11 3)(39 - 31 4)(57 - 27 1) (36 - 9 0)(10 - 1 0)(1 0 0)	12.1530	
	0	(0 0 3 - 2)(1 - 1 3 0)(0 - 1 0 0)	9.47	9 ₄₈
	-2	(0 2 - 2 1)(-1 2 - 2 0)(0 1 0 0)	7.1	7 ₇
	2	(0 2 0 - 1)(1 2 1 0)	7.6	7 ₄
	-2	(1 - 2 3 - 1)(0 - 2 3 - 1)(0 0 1 0)	9.42	9 ₄₄
	-2	(1 - 2 3 - 1)(1 - 3 2 0)(0 - 1 0 0)	10.126	10 ₁₃₆
	0	(1 - 2 4 - 2)(0 - 1 4 - 1)(0 0 1 0)	10.152	10 ₁₄₀
	0	(1 - 1 2 - 1)(1 - 2 2 0)(0 - 1 0 0)	7.2	7 ₆
	2	(1 0 1 - 1)(1 1 1 0)	7.4	7 ₂
	2	(1 0 1 - 1)(3 - 3 3 0)(1 - 4 1 0)(0 - 1 0 0)	10.154	10 ₁₆₀
	-2	(1 1 - 3 2)(0 0 - 4 1)(0 0 - 1 0)	11.405	
	0	(1 1 - 2 1)(-2 4 - 3 0)(-1 4 - 1 0)(0 1 0 0)	9.48	9 ₄₇
	6	(1 4 - 5 1)(6 7 - 5 0)(5 5 - 1 0)(1 1 0 0)	10.151	10 ₁₄₂
	0	(2 - 3 3 - 1)(1 - 3 2 0)(0 - 1 0 0)	3.1#4.1	3 ₁ #4 ₁
	2	(2 - 2 2 - 1)(2 - 2 2 0)(0 - 1 0 0)	9.43	9 ₄₅
	4	(2 - 1 1 - 1)(4 0 1 0)(1 0 0 0)	10.137	10 ₁₄₅
	6	(2 2 - 4 1)(6 6 - 5 0)(5 5 - 1 0)(1 1 0 0)	10.145	10 ₁₂₈
	0	(3 - 5 4 - 1)(4 - 10 5 0)(1 - 6 1 0)(0 - 1 0 0)	11.386	
	2	(3 - 4 3 - 1)(4 - 7 4 0)(1 - 5 1 0)(0 - 1 0 0)	9.44	9 ₄₃
	4	(3 - 3 2 - 1)(6 - 5 3 0)(2 - 4 1 0)(0 - 1 0 0)	11.461	
	4	(4 - 5 3 - 1)(7 - 8 4 0)(2 - 5 1 0)(0 - 1 0 0)	11.486	
	8	(4 - 1 - 3 1)(17 - 3 - 4 0)(20 - 1 - 1 0) (8 0 0 0)(1 0 0 0)	12.1879	
	12	(14 - 21 9 - 1)(70 - 70 15 0)(133 - 84 7 0) (121 - 45 1 0)(55 - 11 0 0) (12 - 1 0 0)(1 0 0 0)	$T(4, 5)$	

Table 5.2: Knots of arc index 9, listed by their Homfly polynomials

$\text{spr}_v \mathcal{P}_K(v, z)$	v^r	$\mathcal{P}_K(v, z)$	$(K \text{ [Ro]})$
1	0	(1)	
2	2	(2 - 1)(1 0)	
	4	(3 - 2)(4 - 1)(1 0)	
	6	(4 - 3)(10 - 4)(6 - 1)(1 0)	
3	-2	(-5 11 - 5)(-7 19 - 7)(-2 11 - 2)(0 2 0)	(10 ₁₂₅)
	-2	(-3 7 - 3)(-4 11 - 4)(-1 6 - 1)(0 1 0)	
	0	(-3 8 - 4)(-6 16 - 6)(-2 10 - 2)(0 2 0)	(3 ₁ #5 ₁)
	0	(-3 8 - 4)(-4 12 - 4)(-1 6 - 1)(0 1 0)	
	2	(-3 9 - 5)(-5 17 - 6)(-2 10 - 2)(0 2 0)	
	-2	(-2 5 - 2)(-3 8 - 3)(-1 5 - 1)(0 1 0)	
	-2	(-2 5 - 2)(-1 4 - 1)(0 1 0)	
	0	(-2 6 - 3)(-5 13 - 5)(-2 9 - 2)(0 2 0)	(8 ₁₀)
	0	(-2 6 - 3)(-3 9 - 3)(-1 5 - 1)(0 1 0)	(10 ₁₂₆)
	2	(-2 7 - 4)(-3 12 - 4)(-1 6 - 1)(0 1 0)	
	-2	(-1 3 - 1)(-3 7 - 3)(-1 5 - 1)(0 1 0)	
	-2	(-1 3 - 1)(-1 3 - 1)(0 1 0)	
	-2	(-1 3 - 1)(1 - 1 1)(1 - 3 1)(0 - 1 0)	8 ₁₈
	0	(-1 4 - 2)(-3 8 - 3)(-1 5 - 1)(0 1 0)	(8 ₇)
	0	(-1 4 - 2)(-1 4 - 1)(0 1 0)	
	2	(-1 5 - 3)(-4 13 - 5)(-2 9 - 2)(0 2 0)	
	2	(-1 5 - 3)(-2 9 - 3)(-1 5 - 1)(0 1 0)	(10 ₁₄₈)
	0	(0 2 - 1)(-2 5 - 2)(-1 4 - 1)(0 1 0)	(10 ₁₅₆ , 8 ₁₆)
	2	(0 3 - 2)(-2 8 - 3)(-1 5 - 1)(0 1 0)	(10 ₁₄₃)
	4	(0 4 - 3)(2 6 - 2)(1 2 0)	
	-2	(1 - 1 1)(0 - 1 0)	
	-2	(1 - 1 1)(2 - 5 2)(1 - 4 1)(0 - 1 0)	(8 ₁₇)
	0	(1 0 0)(2 - 4 2)(1 - 4 1)(0 - 1 0)	
	2	(1 1 - 1)(-1 5 - 2)(-1 4 - 1)(0 1 0)	(10 ₁₅₉)
	2	(1 1 - 1)(1 1 0)	
	4	(1 2 - 2)(3 3 - 1)(1 1 0)	
-2	(2 - 3 2)(1 - 4 1)(0 - 1 0)		
-2	(2 - 3 2)(3 - 8 3)(1 - 5 1)(0 - 1 0)	(8 ₉)	
0	(2 - 2 1)(1 - 3 1)(0 - 1 0)		
0	(2 - 2 1)(3 - 7 3)(1 - 5 1)(0 - 1 0)	(10 ₁₄₁)	
2	(2 - 1 0)(3 - 4 2)(1 - 4 1)(0 - 1 0)	(10 ₁₅₀)	
4	(2 0 - 1)(3 2 - 1)(1 1 0)		
4	(2 0 - 1)(5 - 2 1)(2 - 3 1)(0 - 1 0)	(10 ₁₅₇)	

Table 5.3: Table of $\mathcal{P}_K(v, z)$ for all knots K of arc index at most 10; (i)

$\text{spr}_v \mathcal{P}_K(v, z)$	v^T	$\mathcal{P}_K(v, z)$	$(K \text{ [Ro]})$	
3	0	$(3 - 4 2)(3 - 8 3)(1 - 5 1)(0 - 1 0)$	(10_{155})	
	2	$(3 - 3 1)(2 - 3 1)(0 - 1 0)$		
	2	$(3 - 3 1)(4 - 7 3)(1 - 5 1)(0 - 1 0)$	(8_2)	
	4	$(3 - 2 0)(6 - 5 2)(2 - 4 1)(0 - 1 0)$		
	6	$(3 - 1 - 1)(9 - 1 - 1)(6 0 0)(1 0 0)$		
	-2	$(4 - 7 4)(4 - 12 4)(1 - 6 1)(0 - 1 0)$		
	0	$(4 - 6 3)(4 - 11 4)(1 - 6 1)(0 - 1 0)$		
	2	$(4 - 5 2)(4 - 8 3)(1 - 5 1)(0 - 1 0)$	(8_5)	
	2	$(4 - 5 2)(6 - 12 5)(2 - 9 2)(0 - 2 0)$		
	4	$(4 - 4 1)(4 - 2 0)(1 0 0)$		
	4	$(4 - 4 1)(6 - 6 2)(2 - 4 1)(0 - 1 0)$	(10_{149})	
	4	$(4 - 4 1)(8 - 10 4)(3 - 8 2)(0 - 2 0)$		
	2	$(5 - 7 3)(7 - 15 6)(2 - 10 2)(0 - 2 0)$		
	4	$(5 - 6 2)(7 - 9 3)(2 - 5 1)(0 - 1 0)$	(10_{127})	
	6	$(5 - 5 1)(10 - 5 0)(6 - 1 0)(1 0 0)$		
	6	$(5 - 5 1)(12 - 9 2)(7 - 5 1)(1 - 1 0)$		
	2	$(6 - 9 4)(7 - 16 6)(2 - 10 2)(0 - 2 0)$		
	4	$(6 - 8 3)(9 - 14 5)(3 - 9 2)(0 - 2 0)$		
	6	$(6 - 7 2)(11 - 8 1)(6 - 2 0)(1 0 0)$	$(3_1 \# 5_1)$	
	6	$(6 - 7 2)(13 - 12 3)(7 - 6 1)(1 - 1 0)$		
	8	$(6 - 6 1)(21 - 13 1)(21 - 7 0)$		
			$(8 - 1 0)(1 0 0)$	
	4	$(7 - 10 4)(10 - 17 6)(3 - 10 2)(0 - 2 0)$		
	6	$(7 - 9 3)(13 - 13 3)(7 - 6 1)(1 - 1 0)$		
	8	$(7 - 8 2)(21 - 14 1)(21 - 7 0)$		
			$(8 - 1 0)(1 0 0)$	
	6	$(8 - 11 4)(16 - 20 6)(8 - 11 2)(1 - 2 0)$		
	8	$(8 - 10 3)(22 - 17 2)(21 - 8 0)$	(10_{152})	
			$(8 - 1 0)(1 0 0)$	
	10	$(9 - 11 3)(39 - 31 4)(57 - 27 1)$		
		$(36 - 9 0)(10 - 1 0)(1 0 0)$		
10	$(10 - 13 4)(39 - 32 4)(57 - 27 1)$			
		$(36 - 9 0)(10 - 1 0)(1 0 0)$		
10	$(11 - 15 5)(40 - 35 5)(57 - 28 1)$			
		$(36 - 9 0)(10 - 1 0)(1 0 0)$		
12	$(12 - 16 5)(66 - 60 10)(132 - 78 6)$			
		$(121 - 44 1)(55 - 11 0)(12 - 1 0)(1 0 0)$		

Table 5.3: (ii)

$\text{spr}_v \mathcal{P}_K(v, z)$	v^r	$\mathcal{P}_K(v, z)$	$(K \text{ [Ro]})$
4	-2	$(-5 \ 11 \ -5 \ 0)(-10 \ 26 \ -12 \ 1)(-6 \ 22 \ -7 \ 0)$ $(-1 \ 8 \ -1 \ 0)(0 \ 1 \ 0 \ 0)$	(10 ₁₅₃)
	-2	$(-5 \ 12 \ -7 \ 1)(-10 \ 26 \ -13 \ 1)(-6 \ 22 \ -7 \ 0)$ $(-1 \ 8 \ -1 \ 0)(0 \ 1 \ 0 \ 0)$	
	0	$(-5 \ 13 \ -8 \ 1)(-10 \ 27 \ -13 \ 1)(-6 \ 22 \ -7 \ 0)$ $(-1 \ 8 \ -1 \ 0)(0 \ 1 \ 0 \ 0)$	
	2	$(-5 \ 14 \ -9 \ 1)(-10 \ 30 \ -14 \ 1)(-6 \ 23 \ -7 \ 0)$ $(-1 \ 8 \ -1 \ 0)(0 \ 1 \ 0 \ 0)$	
	2	$(-5 \ 15 \ -11 \ 2)(-10 \ 30 \ -15 \ 1)(-6 \ 23 \ -7 \ 0)$ $(-1 \ 8 \ -1 \ 0)(0 \ 1 \ 0 \ 0)$	
	-2	$(-4 \ 9 \ -4 \ 0)(-7 \ 17 \ -5 \ -1)(-2 \ 11 \ -1 \ 0)$ $(0 \ 2 \ 0 \ 0)$	
	0	$(-4 \ 9 \ -3 \ -1)(-7 \ 18 \ -4 \ -1)(-2 \ 11 \ -1 \ 0)$ $(0 \ 2 \ 0 \ 0)$	
	0	$(-4 \ 10 \ -5 \ 0)(-9 \ 24 \ -11 \ 1)(-6 \ 21 \ -7 \ 0)$ $(-1 \ 8 \ -1 \ 0)(0 \ 1 \ 0 \ 0)$	
	2	$(-4 \ 12 \ -8 \ 1)(-9 \ 27 \ -13 \ 1)(-6 \ 22 \ -7 \ 0)$ $(-1 \ 8 \ -1 \ 0)(0 \ 1 \ 0 \ 0)$	
	4	$(-4 \ 14 \ -11 \ 2)(-8 \ 31 \ -16 \ 1)(-5 \ 24 \ -7 \ 0)$ $(-1 \ 8 \ -1 \ 0)(0 \ 1 \ 0 \ 0)$	
	-2	$(-3 \ 6 \ -1 \ -1)(-4 \ 10 \ -1 \ -1)(-1 \ 6 \ 0 \ 0)(0 \ 1 \ 0 \ 0)$	
	0	$(-3 \ 7 \ -2 \ -1)(-5 \ 14 \ -4 \ 0)(-2 \ 9 \ -2 \ 0)(0 \ 2 \ 0 \ 0)$	
	0	$(-3 \ 7 \ -2 \ -1)(-4 \ 11 \ -1 \ -1)(-1 \ 6 \ 0 \ 0)(0 \ 1 \ 0 \ 0)$	
	0	$(-3 \ 9 \ -6 \ 1)(-9 \ 23 \ -12 \ 1)(-6 \ 21 \ -7 \ 0)$ $(-1 \ 8 \ -1 \ 0)(0 \ 1 \ 0 \ 0)$	
	2	$(-3 \ 10 \ -7 \ 1)(-9 \ 26 \ -13 \ 1)(-6 \ 22 \ -7 \ 0)$ $(-1 \ 8 \ -1 \ 0)(0 \ 1 \ 0 \ 0)$	
	2	$(-3 \ 10 \ -7 \ 1)(-7 \ 22 \ -11 \ 1)(-5 \ 18 \ -6 \ 0)$ $(-1 \ 7 \ -1 \ 0)(0 \ 1 \ 0 \ 0)$	
	4	$(-3 \ 12 \ -10 \ 2)(-7 \ 28 \ -15 \ 1)(-5 \ 23 \ -7 \ 0)$ $(-1 \ 8 \ -1 \ 0)(0 \ 1 \ 0 \ 0)$	
	-2	$(-2 \ 2 \ 4 \ -3)(-3 \ 5 \ 6 \ -3)(0 \ 3 \ 3 \ 0)$	
	-2	$(-2 \ 2 \ 4 \ -3)(-2 \ 2 \ 9 \ -4)(0 \ 1 \ 6 \ -1)(0 \ 0 \ 1 \ 0)$	
	-2	$(-2 \ 3 \ 2 \ -2)(-4 \ 8 \ 2 \ -2)(-1 \ 6 \ 1 \ 0)(0 \ 1 \ 0 \ 0)$	
	-2	$(-2 \ 3 \ 2 \ -2)(-2 \ 4 \ 4 \ -2)(0 \ 2 \ 2 \ 0)$	
	-2	$(-2 \ 4 \ 0 \ -1)(-3 \ 8 \ -2 \ 0)(-1 \ 5 \ -1 \ 0)(0 \ 1 \ 0 \ 0)$	
	-2	$(-2 \ 4 \ 0 \ -1)(-2 \ 5 \ 1 \ -1)(0 \ 2 \ 1 \ 0)$	
	-2	$(-2 \ 5 \ -2 \ 0)(-4 \ 9 \ -2 \ -1)(-1 \ 6 \ 0 \ 0)(0 \ 1 \ 0 \ 0)$	
	0	$(-2 \ 5 \ -1 \ -1)(-4 \ 10 \ -1 \ -1)(-1 \ 6 \ 0 \ 0)(0 \ 1 \ 0 \ 0)$	
	0	$(-2 \ 5 \ -1 \ -1)(-3 \ 9 \ -2 \ 0)(-1 \ 5 \ -1 \ 0)(0 \ 1 \ 0 \ 0)$	
	0	$(-2 \ 5 \ -1 \ -1)(-2 \ 6 \ 1 \ -1)(0 \ 2 \ 1 \ 0)$	

Table 5.3: (iii)

$\text{spr}_v \mathcal{P}_K(v, z)$	v^r	$\mathcal{P}_K(v, z)$	$(K \text{ [Ro]})$
4	2	$(-2\ 7\ -4\ 0)(-4\ 15\ -7\ 1)(-4\ 13\ -5\ 0)$ $(-1\ 6\ -1\ 0)(0\ 1\ 0\ 0)$	
	2	$(-2\ 8\ -6\ 1)(-6\ 19\ -10\ 1)(-5\ 17\ -6\ 0)$ $(-1\ 7\ -1\ 0)(0\ 1\ 0\ 0)$	
	4	$(-2\ 9\ -7\ 1)(-4\ 21\ -11\ 1)(-4\ 18\ -6\ 0)$ $(-1\ 7\ -1\ 0)(0\ 1\ 0\ 0)$	
	-2	$(-1\ 0\ 5\ -3)(-1\ -1\ 10\ -4)(0\ 0\ 6\ -1)(0\ 0\ 1\ 0)$	
	-2	$(-1\ 0\ 5\ -3)(-1\ 1\ 6\ -2)(0\ 1\ 2\ 0)$	
	-2	$(-1\ 1\ 3\ -2)(-2\ 3\ 4\ -2)(0\ 2\ 2\ 0)$	
	-2	$(-1\ 1\ 3\ -2)(-1\ 2\ 3\ -1)(0\ 1\ 1\ 0)$	$(3_1 \# \overline{5}_2)$
	-2	$(-1\ 2\ 1\ -1)(-3\ 6\ 0\ -1)(-1\ 5\ 0\ 0)(0\ 1\ 0\ 0)$	
	-2	$(-1\ 2\ 1\ -1)(-1\ 2\ 2\ -1)(0\ 1\ 1\ 0)$	$(10_{129}, 8_8)$
	0	$(-1\ 2\ 2\ -2)(-1\ 3\ 3\ -1)(0\ 1\ 1\ 0)$	(10_{130})
	-2	$(-1\ 3\ -1\ 0)(-2\ 4\ 0\ -1)(0\ 2\ 1\ 0)$	(10_{165})
	0	$(-1\ 3\ 0\ -1)(-3\ 7\ 0\ -1)(-1\ 5\ 0\ 0)(0\ 1\ 0\ 0)$	
	0	$(-1\ 3\ 0\ -1)(-2\ 6\ -1\ 0)(-1\ 4\ -1\ 0)(0\ 1\ 0\ 0)$	(10_{151})
	-2	$(-1\ 4\ -3\ 1)(-3\ 7\ -4\ 0)(-1\ 5\ -1\ 0)(0\ 1\ 0\ 0)$	
	2	$(-1\ 4\ -1\ -1)(-2\ 9\ -2\ 0)(-1\ 5\ -1\ 0)(0\ 1\ 0\ 0)$	
	2	$(-1\ 6\ -5\ 1)(-6\ 18\ -10\ 1)(-5\ 17\ -6\ 0)$ $(-1\ 7\ -1\ 0)(0\ 1\ 0\ 0)$	
	4	$(-1\ 7\ -6\ 1)(-4\ 20\ -11\ 1)(-4\ 18\ -6\ 0)$ $(-1\ 7\ -1\ 0)(0\ 1\ 0\ 0)$	
	6	$(-1\ 9\ -9\ 2)(-1\ 24\ -15\ 1)(0\ 22\ -7\ 0)$ $(0\ 8\ -1\ 0)(0\ 1\ 0\ 0)$	
	-2	$(0\ -2\ 6\ -3)(-1\ -2\ 10\ -4)(0\ 0\ 6\ -1)(0\ 0\ 1\ 0)$	
	-2	$(0\ -1\ 4\ -2)(-1\ 0\ 5\ -2)(0\ 1\ 2\ 0)$	
	0	$(0\ -1\ 5\ -3)(-1\ 1\ 6\ -2)(0\ 1\ 2\ 0)$	
	-2	$(0\ 0\ 2\ -1)(-1\ 1\ 2\ -1)(0\ 1\ 1\ 0)$	(8_{13})
	0	$(0\ 0\ 3\ -2)(1\ -1\ 3\ 0)(0\ -1\ 0\ 0)$	
	-2	$(0\ 1\ 0\ 0)(-1\ 1\ 1\ -1)(0\ 1\ 1\ 0)$	(10_{146})
	0	$(0\ 1\ 1\ -1)(-1\ 2\ 2\ -1)(0\ 1\ 1\ 0)$	
	-2	$(0\ 2\ -2\ 1)(-1\ 2\ -2\ 0)(0\ 1\ 0\ 0)$	
	2	$(0\ 2\ 0\ -1)(-1\ 6\ -1\ 0)(-1\ 4\ -1\ 0)(0\ 1\ 0\ 0)$	
	2	$(0\ 2\ 0\ -1)(1\ 2\ 1\ 0)$	
	2	$(0\ 3\ -2\ 0)(-3\ 11\ -6\ 1)(-4\ 12\ -5\ 0)$ $(-1\ 6\ -1\ 0)(0\ 1\ 0\ 0)$	
	4	$(0\ 5\ -5\ 1)(-3\ 17\ -10\ 1)(-4\ 17\ -6\ 0)$ $(-1\ 7\ -1\ 0)(0\ 1\ 0\ 0)$	
	-2	$(1\ -4\ 7\ -3)(0\ -5\ 11\ -4)(0\ -1\ 6\ -1)(0\ 0\ 1\ 0)$	

Table 5.3: (iv)

$\text{spr}_v \mathcal{P}_K(v, z)$	v^r	$\mathcal{P}_K(v, z)$	$(K \text{ [Ro]})$
4	-2	(1 - 2 3 - 1)(0 - 2 3 - 1)(0 0 1 0)	
	-2	(1 - 2 3 - 1)(1 - 3 2 0)(0 - 1 0 0)	
	0	(1 - 2 4 - 2)(0 - 1 4 - 1)(0 0 1 0)	
	0	(1 - 2 4 - 2)(3 - 6 5 0)(1 - 5 1 0)(0 - 1 0 0)	
	-2	(1 - 1 1 0)(1 - 2 - 1 1)(0 - 1 - 1 0)	(10 ₁₄₇)
	0	(1 - 1 2 - 1)(-1 2 0 0)(-1 3 - 1 0)(0 1 0 0)	(10 ₁₆₄)
	0	(1 - 1 2 - 1)(0 - 1 3 - 1)(0 0 1 0)	
	0	(1 - 1 2 - 1)(1 - 2 2 0)(0 - 1 0 0)	
	2	(1 - 1 3 - 2)(1 0 4 - 1)(0 0 1 0)	
	-2	(1 0 - 1 1)(0 - 1 - 1 0)	
	-2	(1 0 - 1 1)(0 1 - 5 2)(0 1 - 4 1)(0 0 - 1 0)	
	-2	(1 0 - 1 1)(1 - 2 - 2 1)(0 - 1 - 1 0)	
	-2	(1 0 - 1 1)(1 0 - 6 3)(0 0 - 5 1)(0 0 - 1 0)	
	0	(1 0 0 0)(1 - 1 - 1 1)(0 - 1 - 1 0)	(8 ₁₄)
	2	(1 0 1 - 1)(1 1 1 0)	
	2	(1 0 1 - 1)(3 - 3 3 0)(1 - 4 1 0)(0 - 1 0 0)	
	-2	(1 1 - 3 2)(0 0 - 4 1)(0 0 - 1 0)	
	-2	(1 1 - 3 2)(0 2 - 8 3)(0 1 - 5 1)(0 0 - 1 0)	
	-2	(1 1 - 3 2)(1 - 1 - 5 2)(0 - 1 - 2 0)	
	0	(1 1 - 2 1)(-2 4 - 3 0)(-1 4 - 1 0)(0 1 0 0)	
	0	(1 1 - 2 1)(1 - 1 - 2 1)(0 - 1 - 1 0)	(8 ₁₁)
	0	(1 1 - 2 1)(1 1 - 6 3)(0 0 - 5 1)(0 0 - 1 0)	
	2	(1 1 - 1 0)(-2 8 - 5 1)(-4 11 - 5 0)	
		(-1 6 - 1 0)(0 1 0 0)	
	2	(1 1 - 1 0)(2 0 - 1 1)(0 - 1 - 1 0)	(10 ₁₆₆)
	-2	(1 2 - 5 3)(1 1 - 10 4)(0 0 - 6 1)(0 0 - 1 0)	
	0	(1 2 - 4 2)(0 3 - 8 3)(0 1 - 5 1)(0 0 - 1 0)	
	0	(1 2 - 4 2)(1 2 - 9 4)(0 0 - 6 1)(0 0 - 1 0)	
	2	(1 2 - 3 1)(1 2 - 3 1)(0 0 - 1 0)	(10 ₁₃₃)
	2	(1 2 - 3 1)(2 - 1 0 0)(1 - 3 1 0)(0 - 1 0 0)	
	2	(1 3 - 5 2)(2 3 - 9 4)(0 0 - 6 1)(0 0 - 1 0)	
	4	(1 3 - 4 1)(2 5 - 3 0)(1 2 0 0)	(8 ₁₅)
	6	(1 4 - 5 1)(6 7 - 5 0)(5 5 - 1 0)(1 1 0 0)	
	6	(1 5 - 7 2)(3 13 - 9 0)(4 10 - 2 0)(1 2 0 0)	
	0	(2 - 3 3 - 1)(1 - 3 2 0)(0 - 1 0 0)	
	-2	(2 - 2 0 1)(1 - 3 - 2 1)(0 - 1 - 1 0)	(8 ₄)
	-2	(2 - 2 0 1)(2 - 6 1 0)(1 - 4 1 0)(0 - 1 0 0)	(10 ₁₅₈)
	-2	(2 - 2 0 1)(3 - 7 0 1)(1 - 5 0 0)(0 - 1 0 0)	
	0	(2 - 2 1 0)(2 - 4 0 1)(0 - 2 - 1 0)	
	2	(2 - 2 2 - 1)(2 - 2 2 0)(0 - 1 0 0)	

Table 5.3: (v)

$\text{spr}_v \mathcal{P}_K(v, z)$	v^r	$\mathcal{P}_K(v, z)$	$(K \text{ [Ro]})$	
4	-2	(2 -1 -2 2)(1 -3 -3 1)(0 -1 -1 0)	(8 ₆)	
	0	(2 -1 -1 1)(0 -1 -1 0)		
	0	(2 -1 -1 1)(1 -2 -2 1)(0 -1 -1 0)		
	0	(2 -1 -1 1)(2 -3 -3 2)(0 -2 -2 0)		
	2	(2 -1 0 0)(2 -1 -1 1)(0 -1 -1 0)	(10 ₁₃₁)	
	4	(2 -1 1 -1)(4 0 1 0)(1 0 0 0)		
	2	(2 0 -2 1)(2 -1 -2 1)(0 -1 -1 0)		
	4	(2 0 -1 0)(6 -5 4 -1)(5 -10 5 0) (1 -6 1 0)(0 -1 0 0)		
	4	(2 1 -3 1)(3 2 -2 0)(1 1 0 0)	(3 ₁ #5 ₂)	
	4	(2 1 -3 1)(4 1 -3 1)(1 0 -1 0)		
	6	(2 2 -4 1)(6 6 -5 0)(5 5 -1 0)(1 1 0 0)		
	6	(2 2 -4 1)(8 2 -3 0)(6 1 0 0)(1 0 0 0)		
	8	(2 4 -7 2)(11 12 -13 1)(15 15 -7 0) (7 7 -1 0)(1 1 0 0)		
	-2	(3 -5 3 0)(4 -10 2 1)(1 -6 0 0)(0 -1 0 0)		
	0	(3 -5 4 -1)(4 -10 5 0)(1 -6 1 0)(0 -1 0 0)		
	-2	(3 -4 1 1)(2 -6 -1 1)(0 -2 -1 0)		
	-2	(3 -4 1 1)(3 -9 2 0)(1 -5 1 0)(0 -1 0 0)		(10 ₁₄₄)
	0	(3 -4 2 0)(2 -5 0 1)(0 -2 -1 0)		
	0	(3 -4 2 0)(4 -9 2 1)(1 -6 0 0)(0 -1 0 0)		
	2	(3 -4 3 -1)(4 -7 4 0)(1 -5 1 0)(0 -1 0 0)		
	0	(3 -3 0 1)(2 -5 -1 1)(0 -2 -1 0)		(10 ₁₆₃)
	0	(3 -3 0 1)(4 -9 1 1)(1 -6 0 0)(0 -1 0 0)		
	2	(3 -3 1 0)(3 -4 0 1)(0 -2 -1 0)		
	4	(3 -3 2 -1)(6 -5 3 0)(2 -4 1 0)(0 -1 0 0)		
	0	(3 -2 -2 2)(2 -4 -4 2)(0 -2 -2 0)		(10 ₁₃₄)
	2	(3 -2 -1 1)(2 -2 -2 1)(0 -1 -1 0)		
	2	(3 -2 -1 1)(4 -6 0 1)(1 -5 0 0)(0 -1 0 0)		
	4	(3 -1 -2 1)(4 0 -3 1)(1 0 -1 0)		
	4	(3 -1 -2 1)(5 -3 0 0)(2 -3 1 0)(0 -1 0 0)		
	6	(3 0 -3 1)(7 3 -4 0)(5 4 -1 0)(1 1 0 0)		
	6	(3 1 -5 2)(9 0 -5 1)(6 0 -1 0)(1 0 0 0)		
	8	(3 2 -6 2)(11 11 -13 1)(15 15 -7 0) (7 7 -1 0)(1 1 0 0)		
	2	(4 -7 6 -2)(10 -21 13 -1)(6 -21 7 0) (1 -8 1 0)(0 -1 0 0)		
	0	(4 -5 1 1)(3 -7 -2 2)(0 -3 -2 0)		

Table 5.3: (vi)

$\text{spr}_v \mathcal{P}_K(v, z)$	v^r	$\mathcal{P}_K(v, z)$	$(K \text{ [Ro]})$
4	2	$(4 - 5 2 0)(5 - 9 2 1)(1 - 6 0 0)(0 - 1 0 0)$	(10 ₁₅₄)
	4	$(4 - 5 3 - 1)(7 - 8 4 0)(2 - 5 1 0)(0 - 1 0 0)$	
	4	$(4 - 5 3 - 1)(10 - 15 9 - 1)(6 - 16 6 0)$ $(1 - 7 1 0)(0 - 1 0 0)$	
	0	$(4 - 4 - 1 2)(2 - 6 - 2 1)(0 - 2 - 1 0)$	
	2	$(4 - 4 0 1)(3 - 5 - 1 1)(0 - 2 - 1 0)$	
	2	$(4 - 4 0 1)(4 - 6 - 2 2)(0 - 3 - 2 0)$	
	4	$(4 - 3 - 1 1)(5 - 3 - 2 1)(1 - 1 - 1 0)$	
	4	$(4 - 3 - 1 1)(7 - 7 0 1)(2 - 5 0 0)(0 - 1 0 0)$	
	6	$(4 - 2 - 2 1)(9 - 2 - 2 0)(6 0 0 0)(1 0 0 0)$	
	8	$(4 - 1 - 3 1)(17 - 3 - 4 0)(20 - 1 - 1 0)$ $(8 0 0 0)(1 0 0 0)$	
	0	$(5 - 10 8 - 2)(10 - 25 14 - 1)(6 - 22 7 0)$ $(1 - 8 1 0)(0 - 1 0 0)$	
	2	$(5 - 8 5 - 1)(7 - 15 7 0)(2 - 10 2 0)(0 - 2 0 0)$	
	2	$(5 - 8 5 - 1)(10 - 22 12 - 1)(6 - 21 7 0)$ $(1 - 8 1 0)(0 - 1 0 0)$	
	4	$(5 - 7 4 - 1)(9 - 13 6 0)(3 - 9 2 0)(0 - 2 0 0)$	
	4	$(5 - 7 4 - 1)(10 - 16 9 - 1)(6 - 16 6 0)$ $(1 - 7 1 0)(0 - 1 0 0)$	
	2	$(5 - 6 1 1)(5 - 10 1 1)(1 - 6 0 0)(0 - 1 0 0)$	
	4	$(5 - 6 2 0)(10 - 16 8 - 1)(6 - 16 6 0)$ $(1 - 7 1 0)(0 - 1 0 0)$	
	4	$(5 - 5 0 1)(7 - 8 0 1)(2 - 5 0 0)(0 - 1 0 0)$	
	6	$(5 - 5 1 0)(13 - 12 5 - 1)(10 - 12 5 0)$ $(2 - 6 1 0)(0 - 1 0 0)$	
	8	$(5 - 3 - 2 1)(18 - 6 - 3 0)(20 - 2 - 1 0)$ $(8 0 0 0)(1 0 0 0)$	
	10	$(5 - 1 - 5 2)(29 - 6 - 10 1)(51 - 5 - 6 0)$ $(35 - 1 - 1 0)(10 0 0 0)(1 0 0 0)$	
	4	$(6 - 9 5 - 1)(10 - 16 7 0)(3 - 10 2 0)(0 - 2 0 0)$	
	4	$(6 - 9 5 - 1)(11 - 19 10 - 1)(6 - 17 6 0)$ $(1 - 7 1 0)(0 - 1 0 0)$	
	6	$(6 - 8 4 - 1)(16 - 19 9 - 1)(11 - 17 6 0)$ $(2 - 7 1 0)(0 - 1 0 0)$	
	6	$(6 - 7 2 0)(14 - 15 6 - 1)(10 - 13 5 0)$ $(2 - 6 1 0)(0 - 1 0 0)$	

Table 5.3: (vii)

$\text{spr}_v \mathcal{P}_K(v, z)$	v^r	$\mathcal{P}_K(v, z)$	$(K \text{ [Ro]})$
4	8	(6 - 5 - 1 1)(18 - 7 - 3 0)(20 - 2 - 1 0) (8 0 0 0)(1 0 0 0)	
	4	(7 - 11 6 - 1)(13 - 24 12 - 1)(7 - 21 7 0) (1 - 8 1 0)(0 - 1 0 0)	
	6	(7 - 10 5 - 1)(17 - 22 10 - 1)(11 - 18 6 0) (2 - 7 1 0)(0 - 1 0 0)	
	6	(7 - 9 3 0)(16 - 20 8 - 1)(11 - 17 6 0) (2 - 7 1 0)(0 - 1 0 0)	
	8	(7 - 7 0 1)(21 - 14 0 0)(21 - 7 0 0) (8 - 1 0 0)(1 0 0 0)	
	4	(8 - 13 7 - 1)(12 - 23 11 - 1)(6 - 18 6 0) (1 - 7 1 0)(0 - 1 0 0)	
	6	(8 - 12 6 - 1)(17 - 23 10 - 1)(11 - 18 6 0) (2 - 7 1 0)(0 - 1 0 0)	
	10	(8 - 8 0 1)(33 - 17 - 5 1)(52 - 11 - 5 0) (35 - 2 - 1 0)(10 0 0 0)(1 0 0 0)	
	6	(9 - 14 7 - 1)(18 - 26 11 - 1)(11 - 19 6 0) (2 - 7 1 0)(0 - 1 0 0)	
	8	(9 - 13 6 - 1)(28 - 31 11 - 1)(26 - 24 6 0) (9 - 8 1 0)(1 - 1 0 0)	
	8	(10 - 15 7 - 1)(25 - 25 6 0)(22 - 13 1 0) (8 - 2 0 0)(1 0 0 0)	
	8	(10 - 15 7 - 1)(28 - 32 11 - 1)(26 - 24 6 0) (9 - 8 1 0)(1 - 1 0 0)	
	8	(11 - 17 8 - 1)(29 - 35 12 - 1)(26 - 25 6 0) (9 - 8 1 0)(1 - 1 0 0)	
	10	(12 - 18 8 - 1)(43 - 42 9 0)(58 - 33 2 0) (36 - 10 0 0)(10 - 1 0 0)(1 0 0 0)	
	12	(14 - 21 9 - 1)(70 - 70 15 0)(133 - 84 7 0) (121 - 45 1 0)(55 - 11 0 0)(12 - 1 0 0)(1 0 0 0)	
	12	(15 - 23 10 - 1)(70 - 71 15 0)(133 - 84 7 0) (121 - 45 1 0)(55 - 11 0 0)(12 - 1 0 0)(1 0 0 0)	
	14	(19 - 31 15 - 2)(115 - 130 35 - 1)(279 - 211 28 0) (339 - 165 9 0)(221 - 66 1 0)(78 - 13 0 0) (14 - 1 0 0)(1 0 0 0)	

Table 5.3: (viii)

$\text{spr}_v \mathcal{P}_K(v, z)$	v^r	$\mathcal{P}_K(v, z)$	$(K \text{ [Ro]})$
5	-4	$(1 - 2 3 - 2 1)(0 - 2 2 - 2 0)(0 0 1 0 0)$	$(4_1 \# 4_1)$
	-4	$(1 - 2 6 - 8 4)(0 - 4 10 - 15 4)$ $(0 - 1 6 - 7 1)(0 0 1 - 1 0)$	
	-4	$(1 - 1 1 - 1 1)(0 - 2 1 - 2 0)(0 0 1 0 0)$	(8_{12})
	-4	$(1 - 1 1 - 1 1)(0 0 - 3 0 0)(0 1 - 3 1 0)$ $(0 0 - 1 0 0)$	
	-4	$(1 - 1 2 - 3 2)(0 - 1 0 - 4 1)(0 0 0 - 1 0)$	(10_{137})
	-2	$(1 - 1 2 - 2 1)(0 - 2 2 - 2 0)(0 0 1 0 0)$	
	-4	$(1 0 - 1 0 1)(0 - 1 - 2 - 1 0)$	(8_3)
	-4	$(1 0 0 - 2 2)(0 - 1 - 1 - 4 1)(0 0 0 - 1 0)$	(8_1)
	-2	$(1 0 0 - 1 1)(0 - 1 - 1 - 1 0)$	
	-2	$(1 0 1 - 3 2)(0 - 1 0 - 4 1)(0 0 0 - 1 0)$	(10_{137})
	-4	$(1 1 - 3 1 1)(0 1 - 7 1 0)(0 1 - 4 1 0)(0 0 - 1 0 0)$	
	-2	$(1 1 - 2 0 1)(0 1 - 6 1 0)(0 1 - 4 1 0)(0 0 - 1 0 0)$	(8_1)
	0	$(1 1 - 1 - 1 1)(0 0 - 1 - 1 0)$	
	0	$(1 1 0 - 3 2)(0 0 0 - 4 1)(0 0 0 - 1 0)$	(8_1)
	-4	$(2 - 4 5 - 4 2)(1 - 8 10 - 8 1)$ $(0 - 5 12 - 5 0)(0 - 1 6 - 1 0)(0 0 1 0 0)$	
	-4	$(2 - 3 2 - 1 1)(1 - 4 0 - 1 0)(0 - 1 0 0 0)$	(10_{138})
	-4	$(2 - 3 3 - 3 2)(1 - 6 5 - 6 1)$ $(0 - 4 8 - 4 0)(0 - 1 5 - 1 0)(0 0 1 0 0)$	
	-2	$(2 - 3 3 - 2 1)(1 - 6 5 - 3 0)(0 - 2 4 - 1 0)$ $(0 0 1 0 0)$	(10_{138})
	-4	$(2 - 2 0 0 1)(1 - 4 - 1 - 1 0)(0 - 1 0 0 0)$	
	-4	$(2 - 2 1 - 2 2)(0 - 3 0 - 3 0)(0 0 1 0 0)$	(10_{138})
	-2	$(2 - 2 1 - 1 1)(0 - 3 1 - 2 0)(0 0 1 0 0)$	
	-2	$(2 - 2 1 - 1 1)(1 - 4 0 - 1 0)(0 - 1 0 0 0)$	(10_{138})
	0	$(2 - 2 2 - 2 1)(0 - 2 2 - 2 0)(0 0 1 0 0)$	
	0	$(2 - 2 2 - 2 1)(1 - 5 5 - 3 0)(0 - 2 4 - 1 0)$ $(0 0 1 0 0)$	(10_{138})
	-4	$(2 - 1 - 1 - 1 2)(0 - 3 - 1 - 3 0)(0 0 1 0 0)$	
	-2	$(2 - 1 - 1 0 1)(0 - 2 - 2 - 1 0)$	(10_{138})
	0	$(2 - 1 0 - 1 1)(1 - 3 0 - 1 0)(0 - 1 0 0 0)$	
	2	$(2 0 - 1 - 1 1)(1 0 - 1 - 1 0)$	

Table 5.3: (ix)

$\text{spr}_v \mathcal{P}_K(v, z)$	v^r	$\mathcal{P}_K(v, z)$	$(K [\text{Ro}])$
5	-2	$(3 - 4 2 - 1 1)(2 - 8 3 - 2 0)(0 - 3 3 - 1 0)$ $(0 0 1 0 0)$	
	0	$(3 - 4 3 - 2 1)(2 - 8 6 - 3 0)(0 - 3 4 - 1 0)$ $(0 0 1 0 0)$	
	-2	$(3 - 3 0 0 1)(1 - 5 - 1 - 1 0)(0 - 1 0 0 0)$	
	0	$(3 - 3 1 - 1 1)(1 - 4 0 - 1 0)(0 - 1 0 0 0)$	
	2	$(3 - 2 0 - 1 1)(2 - 3 0 - 1 0)(0 - 1 0 0 0)$	
	-4	$(4 - 8 6 - 2 1)(4 - 15 10 - 4 0)(1 - 7 6 - 1 0)$ $(0 - 1 1 0 0)$	
	-2	$(4 - 7 5 - 2 1)(4 - 14 8 - 3 0)(1 - 7 5 - 1 0)$ $(0 - 1 1 0 0)$	
	0	$(4 - 6 4 - 2 1)(4 - 13 8 - 3 0)(1 - 7 5 - 1 0)$ $(0 - 1 1 0 0)$	
	2	$(4 - 5 3 - 2 1)(3 - 8 6 - 3 0)(0 - 3 4 - 1 0)$ $(0 0 1 0 0)$	
	0	$(5 - 8 5 - 2 1)(5 - 16 9 - 3 0)(1 - 8 5 - 1 0)$ $(0 - 1 1 0 0)$	
	2	$(5 - 7 4 - 2 1)(5 - 13 8 - 3 0)(1 - 7 5 - 1 0)$ $(0 - 1 1 0 0)$	
	4	$(6 - 8 4 - 2 1)(8 - 14 8 - 3 0)(2 - 7 5 - 1 0)$ $(0 - 1 1 0 0)$	

Table 5.3: (x)

Appendix A

Pseudocode

In this pseudocode, there is certain notation, which is also used in chapter 5. Let \mathcal{C}_α denote the set of α -cycles

$$\mathcal{C}_\alpha = \left\{ \rho : \begin{array}{l} \rho^k(i) = i \Leftrightarrow \alpha|k; \\ |\rho(i) - i| \neq 1. \end{array} \right\}$$

The set \mathcal{SC}_α is the set of proper bi-class representatives of elements of \mathcal{C}_α . The set $\mathcal{VSC}_\alpha(\rho)$, for each $\rho \in \mathcal{C}_\alpha$, is a subset of \mathcal{SC}_α , defined within the code. The set \mathcal{G} is defined as a set $\{(\eta, \tau)\}$ of pairs of α -cycles, and is updated as new pairs of α -cycles are found. The set $\text{Polys}(\alpha)$ is the set of Homfly polynomials generated by the code.

It should be noted that the pseudocode is representative of a real computer algorithm: as such, the variables used (including those defined above) have a value at any given time during the execution of the algorithm, which is completely determined by all the preceding steps in the algorithm.

```
begin  
  readln( $\alpha$ );  
  if  $\alpha = 10$  then readln(subcase)1;  
  <initializations>;  
  <generate sets  $\mathcal{C}_\alpha$  and  $\mathcal{SC}_\alpha$ >2;  
  for  $\forall \rho \in \mathcal{C}_\alpha$  do begin3  
     $\eta := \rho$ ;
```

¹See section 5.6.

²See section 5.4.

³Goes through elements of \mathcal{C}_α in a well-defined order.

if $\min(\text{rev}\eta, \overline{\text{rev}\eta}) \notin SC_\alpha$ **then**⁴
 $\mathcal{V}SC_\alpha(\eta) := \{\gamma \in SC_\alpha : \gamma \leq \min(\text{rev}\eta, \overline{\text{rev}\eta})\}$ ⁵
else
 $\mathcal{V}SC_\alpha(\eta) := SC_\alpha$;
for $\forall \gamma \in \mathcal{V}SC_\alpha(\eta)$ **do begin**⁶
 $\tau := \gamma$;
 <count number of crossings $c((\eta, \tau))$ of grid diagram (η, τ) >;
if $c((\eta, \tau)) < \alpha - 2$ **then** <move to next $\gamma \in \mathcal{V}SC_\alpha(\eta)$ >;
for $i := 1$ **to** α **do begin**
 while <we can move arc a_i to the right by a type II move>⁷ **do**
 <type II move on a_i >;
 while <we can move arc $a_{\tau(i)}$ to the left by a type II move> **do**
 <type II move on $a_{\tau(i)}$ >;
 if $\langle a_i$ or $a_{\tau(i)}$ is adjacent to a consecutive arc> **then goto** 100⁸;
 while <we can move arc a_i to the left by a type II move> **do**
 <type II move on a_i >;
 while <we can move arc $a_{\tau(i)}$ to the right by a type II move> **do**
 <type II move on $a_{\tau(i)}$ >;
 if $\langle a_i$ or $a_{\tau(i)}$ is adjacent to a consecutive arc> **then goto** 100⁸;
 end; {next i }
 for $i := 1$ **to** α **do begin**
 while <we can move point x_i upwards by a type I move> **do**
 <type I move on x_i >;
 while <we can move point $x_{\eta(i)}$ downwards by a type I move> **do**
 <type I move on $x_{\eta(i)}$ >;
 if $\langle x_i$ or $x_{\eta(i)}$ is adjacent to a consecutive point> **then goto** 100⁹;
 while <we can move point x_i downwards by a type I move> **do**
 <type I move on x_i >;
 while <we can move point $x_{\eta(i)}$ upwards by a type I move> **do**
 <type I move on $x_{\eta(i)}$ >;
 if $\langle x_i$ or $x_{\eta(i)}$ is adjacent to a consecutive point> **then goto** 100⁹;
 end; {next i }
 $\mathcal{G} := \mathcal{G} \cup \{(\eta, \tau)\}$;
 100: **end; {next $\gamma \in \mathcal{V}SC_\alpha(\eta)$ }**

⁴Note that $\min(\text{rev}\eta, \overline{\text{rev}\eta})$ is necessarily proper.

⁵See proposition 5.5.3.

⁶Goes through elements of $\mathcal{V}SC_\alpha(\eta)$ in a well-defined order.

⁷Recall the type I–IV moves of section 2.3.

⁸If two arcs are both consecutive and adjacent then an arc-reducing type IV move is applicable.

⁹If two points are both consecutive and adjacent then an arc-reducing type III move is applicable.

```

 $\mathcal{G}_\eta := \{(\eta, \gamma) \in \mathcal{G} : \gamma \in \mathcal{VSC}_\alpha(\eta)\};$ 
for  $(\eta, \tau) \in \mathcal{G}_\eta$  do begin10
  while <we can move arc  $a_i$  to the right by a type II move> do begin
    <move  $a_i$  to the right by type II move>;
    <recalculate  $\tau$ >;
    while <we can move arc  $a_{\tau(i)}$  to the left by a type II move> do begin
      <move  $a_{\tau(i)}$  to the left by type II move>;
      <recalculate  $\tau$ >;
      if  $(\eta, \tau) \in \mathcal{G}_\eta$  then  $\mathcal{G}_\eta := \mathcal{G}_\eta - \{(\eta, \tau)\};$ 
    end; {while}
  end; {while}
end; {next  $(\eta, \tau)$ }
end; {next  $\rho$ }
 $\mathcal{G} := \bigcup_{\eta \in \mathcal{C}_\alpha} \{\mathcal{G}\};$ 
 $\mathcal{G}^T := \{(\rho, \gamma) : (\text{rev } \gamma, \text{rev } \rho) \in \mathcal{G}\};$ 
 $\mathcal{G}_\eta^T := \{(\rho, \gamma) \in \mathcal{G}^T : \rho = \eta\};$ 
for <each  $\mathcal{G}_\eta^T$ > do begin
  for  $(\eta, \tau) \in \mathcal{G}_\eta^T$  do begin
    for  $i := 1$  to  $\alpha$  do begin
      while <we can move arc  $a_i$  to the right by a type II move> do begin
        <move  $a_i$  to the right by type II move>;
        <recalculate  $\tau$ >;
        while <we can move arc  $a_{\tau(i)}$  to the left by a type II move> do begin
          <move  $a_{\tau(i)}$  to the left by type II move>;
          <recalculate  $\tau$ >;
          if  $(\eta, \tau) \in \mathcal{G}_\eta^T$  then  $\mathcal{G}_\eta^T := \mathcal{G}_\eta^T - \{(\eta, \tau)\};$ 
        end; {while}
      end; {while}
    end; {next  $i$ }
  end; {next  $(\eta, \tau) \in \mathcal{G}_\eta^T$ }
end; {next  $\mathcal{G}_\eta^T$ }
 $\mathcal{G}^T := \bigcup_{\eta: \text{rev}\eta \in \mathcal{SC}_\alpha} \{\mathcal{G}_\eta^T\};$ 

```

¹⁰Goes through elements of \mathcal{G}_η in a well-defined order.

```

for  $(\eta, \tau) \in \mathcal{G}^T$  do begin11
  <calculate braidword for  $(\eta, \tau)$  from grid diagram>;
  <calculate  $\mathcal{P}_K(v, z)$  using [M-S]>;
  <possibly replace  $\mathcal{P}_K(v, z)$  with  $\mathcal{P}_{\bar{K}}(v, z)$ >12;
  if  $\mathcal{P}_K(v, z) \notin \text{Polys}(\alpha)$  then  $\text{Polys}(\alpha) := \text{Polys}(\alpha) \cup \mathcal{P}_K(v, z)$  ;
end; {next  $(\eta, \tau) \in \mathcal{G}^T$ }
for  $\mathcal{P}_K(v, z) \in \text{Polys}(\alpha)$  do13 write( $\mathcal{P}_K(v, z)$ );
end.

```

¹¹Goes through elements of \mathcal{G}^T in a well-defined order.

¹²We work up to mirror image. See section 5.4.

¹³Goes through elements of $\text{Polys}(\alpha)$ in a well-defined order.

References

- [Al] Alexander, J.W.: *A lemma on systems of knotted curves*, Proc. Nat. Acad. Sci. USA **9** (1923) 93–95
- [Ar] Artin, E.: *Theorie der Zöpfe*, Abh. Math. Sem. Univ. Hamburg **4** (1925) 47–72
- [B-J] Barnette, D. and Jukovič, E.: *Hamiltonian circuits on 3-polytopes*, J. Combinatorial Theory **2** (1970) 54–59
- [B-M1] Birman, J.S. and Menasco, W.W.: *Studying links via closed braids I: A finiteness theorem*, Pacific J. Math. **154** No. 1 (1992) 17–36
- [B-M2] Birman, J.S. and Menasco, W.W.: *Studying links via closed braids II: On a theorem of Bennequin*, Topology Appl. **40** (1991) 71–82
- [B-M3] Birman, J.S. and Menasco, W.W.: *Studying links via closed braids III: Classifying links which are closed 3-braids*, Pacific J. Math. **161** No. 1 (1993) 25–113
- [B-M4] Birman, J.S. and Menasco, W.W.: *Studying links via closed braids IV: Split and composite links*, Invent. Math. **102** (1990) 115–139
- [B-M5] Birman, J.S. and Menasco, W.W.: *Studying links via closed braids V: The unlink*, Trans. Amer. Math. Soc. **329** (1992) 585–606
- [B-M6] Birman, J.S. and Menasco, W.W.: *Studying links via closed braids VI: A non-finiteness theorem*, Pacific J. Math. **156** No. 2 (1992) 265–285
- [B-M7] Birman, J.S. and Menasco, W.W.: *Special positions for essential tori in link complements*, Topology **33** No. 3 (1994) 525–556
- [B-Z] Burde, G. and Ziechang, H.: *Knots*, de Gruyter Studies in Mathematics **5** (1985)
- [Bi] Birman, J.S.: *Braids, links and mapping class groups*, Annals of Math. Studies **82** (1974)
- [Br] Brunn, H.: *Über verknötete Kurven*, Mathematiker-Kongresses Zurich 1897, Leipzig (1898) 256–259

- [C-N] Cromwell, P.R. and Nutt, I.J.: *Embedding knots and links in an open book II: Bounds on arc index*, to appear in *Math. Proc. Camb. Phil. Soc.* (1995)
- [Cr] Cromwell, P.R.: *Embedding knots and links in an open book I: basic properties*, to appear in *Topology and its Applications* (1995)
- [F-W] Franks, J. and Williams, R.F.: *Braids and the Jones-Conway polynomial*, *Trans. Amer. Math. Soc.* **303** (1987) 97–108
- [F-Y-H-L-M-O] Freyd, P., Yetter, D., Hoste, J., Lickorish, W.B.R., Millett, K.C., Ocneanu, A.: *A new polynomial invariant of knots and links*, *Bull. Amer. Math. Soc.* **12** (1985) 239–246
- [Ha] Hansen, V.L.: *Braids and coverings*, *London Math. Soc. Student Texts* **18** (1989)
- [Kan] Kanenobu, T.: *Infinitely many knots with the same polynomial invariant*, *Proc. Amer. Math. Soc.* **97** No. 1 (1986) 158–162
- [Kau1] Kauffman, L.H.: *An invariant of regular isotopy*, *Trans. Amer. Math. Soc.* **318** (1990) 417–471
- [Kau2] Kauffman, L.H.: *State models and the Jones polynomial*, *Topology* **26** No. 3 (1987) 395–407
- [L-M] Lickorish, W.B.R. and Millett, K.C.: *A polynomial invariant for knots and links*, *Topology* **26** No. 1 (1987) 107–141
- [M-S] Morton, H.R. and Short, H.B.: *Calculating the 2-variable polynomial for knots presented as closed braids*, *J. Algorithms* **11** (1990) 117–131
- [Ma] Markov, A.A.: *Über die freie Äquivalenz geschlossener Zöpfe*, *Recueil Mathématique Moscou* **1** (1935) 73–78
- [Mo1] Morton, H.R.: *Invariants of links and 3-manifolds from skein theory and from quantum groups*, in ‘Topics in knot theory’, the Proceedings of the NATO Summer Institute in Erzurum 1992, NATO ASI Series C 399, ed. M. Bozhüyük, Kluwer (1993) 107–156
- [Mo2] Morton, H.R.: *Seifert circles and knot polynomials*, *Math. Proc. Camb. Phil. Soc.* **99** (1986) 107–109
- [Mo3] Morton, H.R.: *Threading knot diagrams*, *Math. Proc. Camb. Phil. Soc.* **99** (1986) 247–260
- [Mu] Murasugi, K.: *Jones polynomials and classical conjectures in knot theory*, *Topology* **26** No. 2 (1987) 187–194

- [Oc] Ochiai, M.: *NKNOTTHEORY*, Polynomial calculation program available by anonymous ftp at ics.nara-wu.ac.jp/ochiai
- [P-T] Przytycki, J.H. and Traczyk, P.: *Invariants of links of Conway type*, Kobe J. Math. **4** (1987) 169–188
- [Re] Reidemeister, K.: *Knottentheorie*, *Ergebn. Math. Grenzgeb. Bd. 1* Berlin. Springer-Verlag (1932)
- [Ro] Rolfsen, D.: *Knots and links*, Publish or Perish Inc. (1976)
- [Ru1] Rudolph, L.: *Constructions of quasipositive knots and links, I*, in *Nœuds, Tresses et Singularités (L'Ens. Math. Mono. 31)* ed. C. Weber, Kundig, Geneva (1983) 233–245
- [Ru2] Rudolph, L.: *Constructions of quasipositive knots and links, II*, *Contemp. Math.* **35** (1984) 485–491
- [Ru3] Rudolph, L.: *A characterization of quasipositive Seifert surfaces (Constructions of quasipositive knots and links, III)*, *Topology* **31** No. 2 (1992) 231–237
- [Ru4] Rudolph, L.: *Quasipositive annuli (Constructions of quasipositive knots and links, IV)*, *J. Knot Theory and its Ramifications* **1** No. 4 (1992) 451–466
- [Ru5] Rudolph, L.: *A congruence between link polynomials*, *Math. Proc. Camb. Phil. Soc.* **107** (1990) 319–327
- [Ta] Tait, P.G.: *On knots I, II, III*, *Scientific Papers, I 1877–1885* London: Camb. Univ. Press (1898) 273–437
- [Th1] Thistlethwaite, M.B.: *Tabulation of Kauffman polynomials of knots to 13 crossings*, University of Tennessee
- [Th2] Thistlethwaite, M.B.: *Kauffman polynomial and alternating links*, *Topology* **27** No. 3 (1988) 311–318
- [Th3] Thistlethwaite, M.B.: *A spanning tree expansion of the Jones polynomial*, *Topology* **26** No. 3 (1987) 297–309
- [Th4] Thistlethwaite, M.B.: *Tabulation of Homfly polynomials of knots to 13 crossings*, computer printouts, Polytechnic of the South Bank (1986)
- [Tr] Traczyk, P.: *A new proof of Markov's theorem*, preprint (1992)
- [Tu] Tutte, W.T.: *A theorem on planar graphs*, *Trans. Amer. Math. Soc.* **82** (1956) 99–116

